Université de Montréal

Role of the homeodomain transcription factor Hoxa13 in embryonic development and formation of extra-embryonic structures.

par

Martina Scotti

Programmes de Biologie Moléculaire

Faculté de Médecine

Thèse présentée à la Faculté de Médecine

en vue de l'obtention du grade de *Philosophiae Doctor* (Ph.D)

en Biologie Moléculaire

Décembre, 2011

Université de Montréal

Faculté de Médecine

Cette thèse intitulée:

Role of the homeodomain transcription factor Hoxa13 in embryonic development and formation of extra-embryonic structures

présentée par:

Martina Scotti

a été évaluée par un jury composé des personnes suivantes :

Dr Jean-Philippe Gratton, président-rapporteur

Dre Marie Kmita, directrice de recherche

Dr Hans Larsson, membre du jury

Dre Jacqueline Deschamps, examinatrice externe

Dr François Dubé, représentant de la Doyenne

Résumé

La famille des gènes Hox code pour des facteurs de transcription connus pour leur contribution essentielle à l'élaboration de l'architecture du corps et ce, au sein de tout le règne animal. Au cours de l'évolution chez les vertébrés, les gènes Hox ont été redéfinis pour générer toute une variété de nouveaux tissus/organes. Souvent, cette diversification s'est effectuée via des changements quant au contrôle transcriptionnel des gènes *Hox*.

Chez les mammifères, la fonction de *Hoxa13* n'est pas restreinte qu'à l'embryon même, mais s'avère également essentielle pour le développement de la vascularisation fœtale au sein du labyrinthe placentaire, suggérant ainsi que sa fonction au sein de cette structure aurait accompagné l'émergence des espèces placentaires.

Au chapitre 2, nous mettons en lumière le recrutement de deux autres gènes *Hoxa*, soient *Hoxa10* et *Hoxa11*, au compartiment extra-embryonnaire. Nous démontrons que l'expression de *Hoxa10*, *Hoxa11* et *Hoxa13* est requise au sein de l'allantoïde, précurseur du cordon ombilical et du système vasculaire fœtal au sein du labyrinthe placentaire. De façon intéressante, nous avons découvert que l'expression des gènes *Hoxa10-13* dans l'allantoïde n'est pas restreinte qu'aux mammifères placentaires, mais est également présente chez un vertébré non-placentaire, indiquant que le recrutement des ces gènes dans l'allantoïde précède fort probablement l'émergence des espèces placentaires. Nous avons généré des réarrangements génétiques et utilisé des essais transgéniques pour étudier les mécanismes régulant l'expression des gènes *Hoxa* dans l'allantoïde. Nous avons identifié

un fragment intergénique de 50 kb capable d'induire l'expression d'un gène rapporteur dans l'allantoïde. Cependant, nous avons trouvé que le mécanisme de régulation contrôlant l'expression du gène *Hoxa* au sein du compartiment extra-embryonnaire est fort complexe et repose sur plus qu'un seul élément cis-régulateur.

Au chapitre 3, nous avons utilisé la cartographie génétique du destin cellulaire pour évaluer la contribution globale des cellules exprimant *Hoxa13* aux différentes structures embryonnaires. Plus particulièrement, nous avons examiné plus en détail l'analyse de la cartographie du destin cellulaire de *Hoxa13* dans les pattes antérieures en développement. Nous avons pu déterminer que, dans le squelette du membre, tous les éléments squelettiques de l'autopode (main), à l'exception de quelques cellules dans les éléments carpiens les plus proximaux, proviennent des cellules exprimant *Hoxa13*. En contraste, nous avons découvert que, au sein du compartiment musculaire, les cellules exprimant *Hoxa13* et leurs descendantes (Hoxa13lin+) s'étendent à des domaines plus proximaux du membre, où ils contribuent à générer la plupart des masses musculaires de l'avant-bras et, en partie, du triceps. De façon intéressante, nous avons découvert que les cellules exprimant *Hoxa13* et leurs descendantes ne sont pas distribuées uniformément parmi les différents muscles. Au sein d'une même masse musculaire, les fibres avec une contribution Hoxa13lin+ différente peuvent être identifiées et les fibres avec une contribution semblable sont souvent regroupées ensemble. Ce résultat évoque la possibilité que *Hoxa13* soit impliqué dans la mise en place de caractéristiques spécifiques des groupes musculaires, ou la mise en place de connections nerf-muscle.

Prises dans leur ensemble, les données ici présentées permettent de mieux comprendre le rôle de *Hoxa13* au sein des compartiments embryonnaires et extra-embryonnaires. Par ailleurs, nos résultats seront d'une importance primordiale pour soutenir les futures études visant à expliquer les mécanismes transcriptionnels soutenant la régulation des gènes *Hoxa* dans les tissus extra-embryonnaires.

Mots-clés : gènes *Hox*, allantoïde, placenta, muscles, régulation transcriptionnelle.

Abstract

The Hox family of transcription factors is well known for its key contribution in the establishment of the body architecture in all the animal kingdom. During vertebrate evolution, *Hox* genes have been co-opted to pattern a variety of novel tissues/organs. Often, this diversification has been achieved by changes in *Hox* transcriptional control.

In mammals, *Hoxa13* function is not restricted to the embryo proper, but is also essential for the proper development of the fetal vasculature within the placental labyrinth, suggesting that its function in this structure accompanied the emergence of placental species.

In chapter 2, we report on the recruitment of two other *Hoxa* genes, namely *Hoxa10* and *Hoxa11*, in the extra embryonic compartment. We show that *Hoxa10, Hoxa11* and *Hoxa13* expression is required in the allantois, the precursor of the umbilical cord and fetal vasculature within the placental labyrinth. Interestingly, we found that *Hoxa10-13* gene expression in the allantois is not restricted to placental mammals, but is also present in a non-placental vertebrate, indicating that the recruitment of these genes in the allantois most likely predates the emergence of placental species. We generated genetic rearrangements and used transgenic assays to investigate the regulatory mechanisms underlying *Hoxa* gene expression in the allantois. We identified a 50 kb intergenic fragment able to drive reporter gene expression in the allantois. However, we found that the regulatory mechanism

controlling *Hoxa* gene expression in the extra-embryonic compartment is very complex and relies on more than one *cis*-regulatory element.

In chapter 3, we used genetic fate mapping to assess the overall contribution of *Hoxa13* expressing cells to the different embryonic structures. In particular, we focused on *Hoxa13* fate-mapping analysis in the developing forelimbs. We could determine that, in the limb skeleton, all autopod (hand) skeletal elements, with the exception of a few cells in the most proximal carpal elements, originate from *Hoxa13* expressing cells. In contrast, we found that, in the muscle compartment, *Hoxa13* expressing cells and their descendants extend to more proximal limb domains, where they contribute to most of the muscle masses of the forearm and, in part, to the triceps. Interestingly we found that *Hoxa13* expressing cells and their descendants are not identically distributed among different muscles. Within the same muscular mass, fibres with different *Hoxa13*lin+ contribution can be identified, and fibers with similar contribution are often clustered together. This result raises the possibility that *Hoxa13* might be involved in establishing specific features of muscle groups, or in establishing nerve-muscle connectivity.

Altogether, the data presented herein provide a better understanding of the role of *Hoxa13* in both the embryonic and extra-embryonic compartment. Moreover, our results will be of key importance for further investigations aimed at unravelling transcriptional mechanisms underlying *Hoxa* gene regulation in extra embryonic tissues.

Keywords: *Hox* genes, allantois, placenta, muscles, transcriptional regulation.

Table of contents

List of figures and tables

Alla mia mamma.

Acknowledgments

I wish to thank my supervisor, Dr. Marie Kmita, for giving me the opportunity to work in her lab. During all these six years, I greatly appreciated her support, help and encouragement, both from the professional and personal point of view. I also wish to thank Prof. Denis Duboule of the University of Geneva and the Swiss Ph.D program NCCR "Frontiers in Genetics" for giving me the privilege of joining their doctoral school and for their financial support at the beginning of my Ph.D in Geneva and during the first year here in Canada.

I am also honored and pleased that Dr. Jacqueline Deschamps, Dr. Hans Larrson and Dr. Jean-Philippe Gratton accepted to be members of my thesis jury.

I also want to thank the members of my Ph.D committee for their help and advice over these years: Dr. Jean-Francois Coté, Dr. Jean Vacher, Dr. Jean-Philippe Gratton, Dr. Maxime Bouchard and Dr. Michel Cayouette.

All these years wouldn't have been the same without the Kmita lab members. It has been a privilege to work with such great people. Many of you are and have been my family and friends over the last six years. A special thank you to Damien Gregoire, Gemma de Martino, Mark Cwajna and Tong Yu Wang. I miss you very much and it was very hard to finish this Ph.D without your daily presence. Thank you also to the current members, especially Rushikesh Sheth, for his advice and discussion, which I really appreciated in this

last phase of my studies, and Jessica Pham, for her good mood and energy. Moreover, I greatly appreciated Jessica's help with the French translation of the abstract of this thesis.

I want also to thank many scientist and friends here at the IRCM, for exchanging ideas and coffees: Elena, Wendy, Manishha, Amel, Chris, Mat, Christine, Vas, Jimmy, Dom&Shuofei.

This thesis wouldn't exist without Luisa. Thanks for your daily encouragement and help during these last months and for being such a good friend! Thanks also to Elena, Luisa's mother, for adopting me and for being so generous and kind.

Finally I wish to thank my father Maurizio and his wife Tiziana for their constant support, and Nasr, whose presence over the last year has been extremely precious for my equilibrium.

Chapter 1: Introduction

1.1 The *Hox* genes.

1.1.1 Key features of *Hox* genes.

Members of the *Hox* gene family play a pivotal role in axial patterning of animals with bilateral symmetry, among which they are surprisingly conserved (Carroll, 1995; Duboule, 1992; Krumlauf, 1994). *Hox* genes were first identified in the fruit fly *Drosophila melanogaster*, in which they confer segment identity along the primary anterior-posterior (AP) body axis (Lewis, 1978). When mutated in the fly, loss of *Hox* genes cause dramatic homeotic phenotypes, conditions in which one body segment is transformed into the identity of another one. It was subsequently discovered that *Hox* genes code for transcription factors sharing a sequence of 60 amino acids DNA-binding domain, referred to as the homeodomain (Scott and Weiner, 1984), related to the helix-turn-helix motif of prokaryotic DNA-binding proteins (Kissinger et al., 1990; Otting et al., 1990). Despite their key function during embryogenesis, relatively little is known about the molecular events that these transcription factors trigger. Hox proteins bind DNA with little specificity, recognizing a core sequence composed by only four nucleotides. Moreover, due to the high conservation of the homeodomain, most Hox proteins bind in vitro to simple sequences with the same affinity (Ekker et al., 1994; Hoey and Levine, 1988). This suggests that the specificity achieved by these transcription factors *in vivo* is most likely due to the additional presence of cofactors on target genes promoters. Different Hox co-factors have been identified, including members of the Pbx and Meis TALE homoedomain transcription

factors (reviewed for example in (Mann and Affolter, 1998; Moens and Selleri, 2006)). Multiprotein complexes composed by Hox and cofactors bind DNA sequences, acting both as activators or repressors of transcription.

In most vertebrates 39 *Hox* genes have been identified. These genes are clustered on four genomic loci spanning over 100 to 150 kilobase pairs (kb), referred to as *HoxA, B, C* and *D* clusters. Each *Hox* cluster contains a series of nine to eleven contiguous genes transcribed from the same DNA strand, thus defining a 5' to 3' polarity to the cluster. Genes are referred to paralogous groups 1 to 13 based on their sequence similarity with genes located on the other clusters. Even if some paralogous group are missing in each cluster, the gene order is always maintained, such that group 1 genes are always located at the 3' end of the complex, and group 13 at the 5' (Krumlauf, 1992; Scott, 1992) (Fig. 1.1).

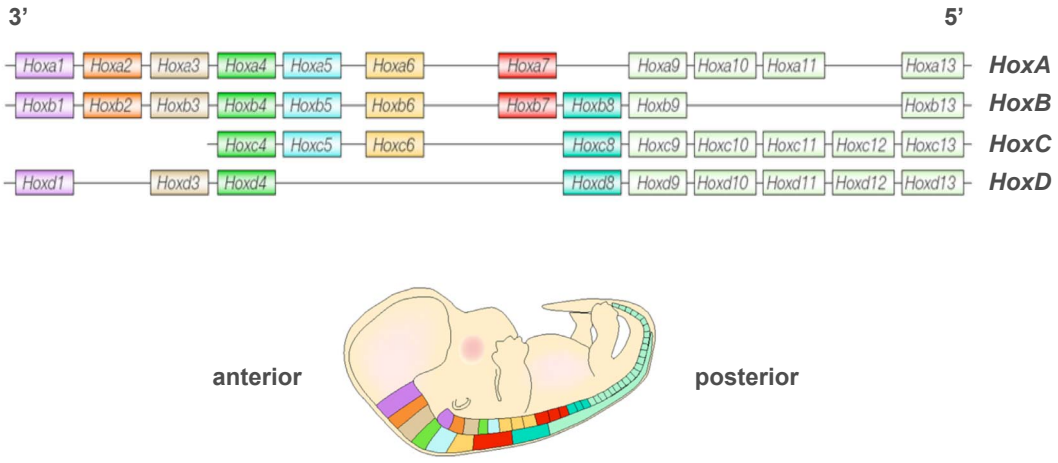

Figure 1.1 *Hox* gene clusters in the mouse.
In the mouse, as in most vertebrates, 39 *Hox* genes have been identified. These genes are clustered on four genomic loci, referred to as *HoxA, B, C* and *D* clusters. Each *Hox* cluster contains nine to eleven contigous genes transcribed from the same DNA strand, conferring a 5' to 3' polarity of the cluster. *Hox* genes are expressed in overlapping domains during embryogenesis, such that their anterior limit of expression is collinear with the gene positions along the complex. Accordingly, genes located at the 3' of each *Hox* clusters are expressed in more anterior structures of the developing embryo, while more 5' *Hox* gene transcripts are restricted to more posterior domains of the body.
(modified from *Pearson et. al 2005*)

1.1.2 Evolution of *Hox* gene clusters.

Importantly, the function of *Hox* genes in patterning the AP axis is conserved among all species, and changes in the body plan organization among different species are generally associated with changes in *Hox* gene number, pattern or boundary of expression (Burke et al., 1995; Cohn and Tickle, 1999). *Hox* genes have been identified in all bilaterian animals investigated so far (de Rosa et al., 1999), and, in most cases, they show a clustered organization, with the exception of the platyhelminth *Schistosoma mansoni* and the urochordate *Oikopleura dioica*, in which *Hox* genes are found scattered in the genome, with little if any linkage (Pierce et al., 2005; Seo et al., 2004). Despite its evolutionary and developmental significance, the origin of the *Hox* gene clusters remains obscure. However, the highly conserved organization described in most bilaterian *Hox* clusters indicates that the common bilaterian ancestor had a set of clustered *Hox* genes. It has been proposed that during early evolution, an ancestral *ProtoHox* cluster has emerged by tandem gene duplication in *cis* of a single ancestral *ProtoHox* gene (Garcia-Fernandez, 2005). This early gene amplification would also explain the clustered organization of *Hox* genes that is found already in cnidarians (animals with a radial symmetry) (Chourrout et al., 2006; Ryan et al., 2007). Subsequently, whole cluster duplication and split of the resulting sister clusters generated the *Hox* and *ParaHox* clusters (Brooke et al., 1998). From this putative ground state, a wide variety of *Hox* gene organizations have evolved. In all invertebrates investigated so far, including the insect *Drosophila melanogaster*, only one single *Hox*

cluster has been identified. The *Drosophila Hox* cluster (HOM-C) contains eight genes: *Labial (lb), Proboscipedia (Pb), Deformed (Dfd), Sex comb reduced (Scr), Antennapedia (Antp), Ultrabihtorax (Ubx), Abdominal-A (Abd-A)* and *Abdominal-B (Abd-B)*. This single cluster was split into two sub-clusters, the Antennapedia (ANT-C) containing the first five genes, and the Bithorax (BX-C) containing the last three (Kaufman et al., 1980). The consensus view is that a single *Hox* cluster was at the origin of vertebrate evolution, a situation potentially reflected today by the single cluster of the cephalochordate *Amphioxus* (Garcia-Fernandez and Holland, 1994). The number of *Hox* genes within the cluster increased during evolution, as exemplified by the expansion of the *Abd-B*-related gene repertoire in *Amphioxus*, leading to a cluster of 14 *Hox* genes in this organism (Ferrier et al., 2000). This single ancestral Hox cluster was subsequently amplified in the vertebrate lineage, possibly following successive whole genome duplications near the origin of vertebrates. For example, the lamprey, a jawless primitive vertebrate, has three (possibly four *Hox* clusters) (Force et al., 2002; Irvine et al., 2002). In higher vertebrates, like mammals, two rounds of whole genome duplications most likely originated a total of four paralogous clusters, referred to as *HoxA* to *HoxD*. Members of each cluster can be classified in paralogy groups, from 1 to 13. Paralogy groups 1 to 8 are homologous to the *Drosophila* genes *Labial, Proboscipedia, Deformed, Sex comb reduced, Antennapedia, Ultrabitorax,* and *Abdominal-A,* while the paralogy group 9 to 13 are related to the *Abdominal-B* gene (Krumlauf, 1994). In teleost fishes, an additional round of genome

duplication occurred, generating seven *Hox* clusters in zebrafish, one of the *HoxD* clusters being lost (Amores et al., 1998; Woltering and Durston, 2006). Interestingly however, the total number of genes in zebrafish is not much higher than in other species with only four clusters, most of the duplicated genes being lost.

It was proposed that the expansion of *Hox* clusters resulted in looser evolutionary constraints on Hox genes, allowing them to acquire novel functions (Holland and Garcia-Fernandez, 1996). Accordingly, the duplication of *Hox* clusters in higher vertebrates was accompanied by gene loss: as a result, none of the four *Hox* clusters displays all 13 paralogy groups. Comparing vertebrate *Hox* gene clusters with their invertebrate counterparts reveals that the firsts show the higher degree of organization (reviewed in (Duboule, 2007)). In fact, in vertebrates, Hox clusters are considerably more compact than in other species, and no non-Hox genes are found interspersed in the complexes, as it is the case for *Drosophila* and the sea urchin. Furthermore, in most vertebrates, repetitive sequences are excluded from the *Hox* clusters, arguing for a strong selective pressure to exclude the invasion by mobile genetic elements at the base of vertebrate evolution (Amemiya et al., 2008; Fried et al., 2004). An exception to repetitive elements exclusion within *Hox* complexes in vertebrates has been recently reported in both squamates (like lizards and snakes) and caecilieans (snake-like amphibians) (Di-Poi et al., 2009; Mannaert et al., 2010). Interestingly these organisms display a divergent body plan organization from the other vertebrates. Changes in *Hox* genes expression, possibly deriving from this altered

Hox cluster organization, have been proposed as a possible explanation for this striking morphological diversity (Di-Poi et al., 2010b). Two scenarios can account for the increased organization of vertebrate Hox genes. Either the tightly structured organization found nowadays in vertebrates represents the evolutionary ground state that eventually deteriorated during the evolution of other lineages, or, alternatively, a disorganized Hox complex underwent a "consolidation" and compaction process in the case of vertebrates (Duboule, 2007). To support this latter hypothesis, an increased regulatory complexity at vertebrate loci has been proposed as a potential evolutionary constraint for Hox cluster compaction, including both newly acquired expression specificity, as well as ancient collinear transcription mechanisms.

1.1.3 Collinearity.

One of the most fascinating features of *Hox* genes is the phenomenon of collinearity, which stands for the correspondence between gene order within each *Hox* cluster and the distribution of gene transcripts along the main body axis (reviewed in (Kmita and Duboule, 2003)). This property was first described in *Drosophila*, where the distributions of *Hox* transcripts, as well as their domain of action along the AP axis of the embryo, are collinear to the *Hox* gene location along the chromosome (Lewis, 1978). Subsequently, the same kind of "spatial collinearity" was found to occur also in vertebrates, where genes of all four clusters show expression territories along the AP axis according to

the relative position they occupy within their respective complexes (Duboule and Dolle, 1989; Gaunt, 1988; Graham et al., 1989). *Hox* genes in vertebrates are expressed in overlapping domains during embryogenesis, such that their anterior limit of expression is collinear with the gene positions along the complex. Accordingly, genes located at the 3' of each *Hox* clusters are expressed in more anterior structures of the developing embryo, while more 5' *Hox* gene transcripts are restricted to more posterior domains of the body (Duboule and Dolle, 1989; Graham et al., 1989). This "spatial collinearity", analogous to the one described in *Drosophila*, is observed in a variety of tissues along the main body axis, such as the neural tube and the paraxial mesoderm, but also in the gastrointestinal tract and urogenital system (Gaunt, 1988; Yokouchi et al., 1995) (Graham et al., 1989). Additionally, similar links between gene order and nested expression domains are found in secondary body axis, such as the external genitalia and limbs (Dolle and Duboule, 1989; Dolle et al., 1991; Haack and Gruss, 1993; Nelson et al., 1996).

"Spatial collinearity" has been reported in all bilaterian organisms investigated so far, independently from the strict clustered organization of the *Hox* complex (as reported in *C. elegans* (Wang et al., 1993)). Strikingly, even organisms with a completely fragmented *Hox* gene organization present such a "trans-collinearity", and *Hox* genes are still expressed in the body axis accordingly to groups of paralogy (Duboule, 2007; Seo et al., 2004). This apparent lack of interdependence between clustering and "spatial collinearity" challenges the claim that this phenomenon might represent a major constraint on maintaining *Hox*

genes clustered together. Furthermore, in the mouse, randomly integrated transgenes carrying single *Hox* genes with relatively reduced neighboring sequence could reproduce major aspects of the endogenous gene's spatial transcript distribution (Puschel et al., 1991; Whiting et al., 1991).

However, a *Hox* transgene randomly inserted into the genome shows some differences in the temporal dynamics of activation as compared to the endogenous gene, raising the possibility that the clustering of *Hox* genes is required for the fine-tuning during *Hox* gene activation process. In fact, unlike *Drosophila* genes, vertebrate *Hox* genes display an additional degree of complexity, resulting in the link between the onset of their expression during development and their position inside the complexes. This phenomenon is referred to as "temporal collinearity" and is observed in all vertebrates, in both the primary and secondary axes of the developing embryo ((Dolle and Duboule, 1989); reviewed in (Deschamps and van Nes, 2005)). In the vertebrate primary body axis, *Hox* genes start to be expressed during early gastrulation, following a subsequent activation from the 3' end to 5' end of the clusters. This process is completed by late tail bud stage, around embryonic day 9 (e9) (Dolle et al., 1989; Izpisua-Belmonte et al., 1991). Genes activated early on are expressed in more anterior structures of the embryo, while genes activated later on are progressively restricted to more posterior embryonic compartments.

1.2 *Hox* gene function.

1.2.1 Homeotic transformations.

Genetic analysis in *Drosophila* has shown that mutations in *Hox* genes give rise to transformation of a specific part of the body of the fly into a completely different one: this phenomenon is called homeotic transformation. For example, in the *Antennapedia* mutation, the fly develops an extra pair of legs in place of the antenna, while the *Bithorax* mutation leads to the growth of an extra pair of wings (Lewis, 1978). It was shown that loss of function mutation in *Hox* genes usually lead to anteriorizing homeotic transformations, i.e., the transformation of a body segment into a more anterior one. Vice-versa, gain of function of a specific *Hox* gene anterior to the position in which it is normally expressed imposes a posterior identity to the segment where the *Hox* gene is ectopically expressed (Akam, 1987; Lewis, 1978; McGinnis and Krumlauf, 1992). Results obtained over the last three decades have demonstrated that the function of *Drosophila Hox* genes in specifying the identity of the different body segments along the AP axis is largely conserved in vertebrates. Each of the 39 *Hox* genes, as well as entire *Hox* clusters, has been genetically inactivated in the mouse. In parallel, classical transgenesis in the mouse was used to investigate the phenotypic outcomes of misexpressing a specific Hox gene in an embryonic domain in which it is not normally expressed.

Altogether, these studies have provided much support to the idea that vertebrate *Hox* genes, as well as their *Drosophila* counterparts, can specify morphological identity of metameric structures in the body plan. This view is also supported by evidence in other animal model organisms, like *Xenopus* and *Zebrafish*, in which mRNA injections or antisense approach experiments have been performed (Cho et al., 1991; McClintock et al., 2002).

1.2.2 *Hox* gene function in the primary vertebrate body axis.

During vertebrate embryogenesis the extension of the body along the AP axis is coupled with the process of somitogenesis. The segmented structure of the vertebrate body plan is mostly apparent at the level of somatic mesoderm derivatives, such as the vertebrae, but also at the level of the central nervous system, where, for example, the hindbrain is subdivided into eight rhombomeres. Consistently, alteration of *Hox* expression mainly affects the morphology of these segmented structures (reviewed in (Burke, 2000; Lumsden and Krumlauf, 1996; Trainor and Krumlauf, 2001)).

"Hox code" and posterior prevalence:

In vertebrates, *Hox* expression patterns in the trunk, unlike in *Drosophila*, is characterized by large domains of expression, partially overlapping in the posterior region

of the main body axis. This led to the hypothesis that the identity of segments at different axial levels of the embryo relies on a different combination of Hox proteins, referred to as the "Hox code" (Kessel and Gruss, 1991). However, loss-of-function experiments in the mouse usually lead to morphological changes confined to the most rostral segments in which a given *Hox* gene is normally expressed. These observations indicate that a functional hierarchy exists among *Hox* genes, and that the most posterior *Hox* gene that is expressed in a determined segment imposes its function over more anterior *Hox* genes. This model is referred to as "posterior prevalence" (Duboule and Morata, 1994). In this view, nested and overlapping expression domains are only a way to confer discrete identities to the undifferentiated extending body axis. Notably, the phenomenon of "posterior prevalence" is not limited to the main body axis, but occurs also in secondary axis, like the limbs (see e.g. (Herault et al., 1997; Kmita et al., 2002a; Peichel et al., 1997; van der Hoeven et al., 1996)). "Posterior prevalence" is related to the phenomenon of "phenotypic suppression" described in *Drosophila*. Unlike in vertebrates, the distribution of *Hox* transcripts along the body axis in *Drosophila* is characterized by largely non-overlapping patterns. Posterior Hox proteins were shown to down-regulate the expression of more anterior *Hox* genes. Ectopic expression of *Hox* genes in Drosophila, however, demonstrated that this effect does not involve transcriptional repression, but rather acts at the post-transcriptional level (Duboule and Morata, 1994).

Loss-of-function phenotypes:

As mentioned earlier, loss-of-function mutations induce anteriorization mainly confined to the region corresponding to the anterior limit of expression of a given *Hox* gene. For example, the inactivation of *Hoxa1*, which is normally expressed up to rombobere 4 (r4) in the hindbrain, produces abnormalities only in r4 to r8 and their derivatives, leaving more anterior or posterior structures of the body unaffected (Carpenter et al., 1993; Chisaka et al., 1992; Lufkin et al., 1991). The inactivation of *Hoxa2* leads to anterior homeotic transformation of the cranial neural crest derivatives from the second branchial arch to a first branchial arch identity (Gendron-Maguire et al., 1993; Rijli et al., 1993).

In the axial skeleton, inactivation of *Hox* genes leads to anterior transformation of vertebrae. For example, *Hoxa4* mutants show partial transformation of the third cervical vertebra (C3) towards a C2 identity (Kostic and Capecchi, 1994). Inactivation of *Hoxb4* or *Hoxd4* leads to partial transformation of C2 into C1 (Horan et al., 1995a; Ramirez-Solis et al., 1993). In more posterior domains of the trunk, homeosis of thoracic vertebrae is observed in many mutants. For example, *Hoxc4* inactivation leads to anterior transformation of the third thoracic vertebra (T3) (Saegusa et al., 1996). *Hoxc8* mutants show anterior transformation of T8 to T7 and of the fist lumbar vertebrae (L1) to T13 (Le Mouellic et al., 1992). Finally, several examples of inactivations of *Abd-B*- related genes illustrate the requirement for these genes in conferring proper lumbo-sacral vertebral

identity. Following inactivation of *Hoxa9*, anterior homeosis of the first five lumbar vertebrae is observed (Fromental-Ramain et al., 1996a). Inactivation of the paralogous *Hoxd9* leads to anterior transformations from L3 to the first caudal vertebra, which assumes a sacral identity (Fromental-Ramain et al., 1996a). Similarly, upon *Hoxd11* inactivation, the sacral region displays anterior transformation, resulting in a posterior shift of the sacrum (Davis and Capecchi, 1994; Favier et al., 1995).

Gain-of-function phenotypes:

In many cases, ectopic *Hox* expression leads to posterior transformations, mainly restricted to regions of the body that are rostral to the normal limit of expression of the gene. For example, ectopic widespread expression of *Hoxa1* leads to rhombomere transformation, resulting in change of r2 and r3 towards r4 identity (Zhang et al., 1994). Ectopic expression of *Hoxa7* under the control of the ubiquitous β-actin promoter leads to the appearance of an additional first cervical vertebra and other severe cranio-facial defects (Kessel et al., 1990). The expression of *Hoxd4* under the control of the *Hoxa1* promoter leads to transformation of the occipital bones into structures resembling cervical vertebrae, since neural arches are induced (Lufkin et al., 1992). *Hoxb8* expression under the retinoic acid receptor (RAR) β2 promoter leads to cervical vertebrae adopting a more posterior identity (Charite et al., 1995).

Unexpected phenotypes:

In some cases, *Hox* gene inactivation results in posterior, rather than anterior transformations, or in a complex combination of both. These results may, however, reflect technical limitations of gene-targeting technology as it was originally developed. For instance, mice lacking *Hoxb2* present partial transformation of C2 in C1 and splitting of the sternum into two longitudinal structures (Barrow and Capecchi, 1996). This sternal defect is reminiscent of *Hoxb4* inactivation, and consistently, *Hoxb4* expression is decreased or suppressed in these mutants. In parallel, *Hoxb2* mutant mice display facial paralysis, as do mice with *Hoxb1* inactivation (Goddard et al., 1996). Accordingly, *Hoxb1* expression in neural crest cells is abrogated in these mutants (Barrow and Capecchi, 1996). *Hoxa11* inactivation leads to posterior homeotic transformation probably linked to *Hoxa10* misexpression (Branford et al., 2000; Small and Potter, 1993).

Targeting constructs employed to generate gene inactivation typically include a selection cassette, to allow selection of integration events in ES cell clones. The presence of strong promoters in the selection cassettes, such as the phosphoglycerate kinase promoter (PGK), can perturb the regulation of neighboring genes, competing for enhancer activity, or, alternatively, the targeting of the cassette can disrupt regulatory elements, ultimately leading to loss or gain-of-expression of one or several genes (Beckers and Duboule, 1998; Rijli et al., 1994; Zakany et al., 1997b). More recently, the Cre-loxP recombinase approach has been used to ultimately remove the selection cassette. However, most *Hox* gene

inactivations were produced before the advent of this technique, and still include the selection cassette. Thus, the resulting phenotypes should be interpreted with caution.

Conversely, *Hox* gene gain of function can also induce unexpected anterior vertebral transformations. For example, transgenic mice carrying over 40 copies of a human *Hoxc6* transgene present anterior transformation of thoracic and lumbar vertebrae. However, this doesn't happen when a lower copy number of the transgene is integrated, suggesting that a quantitative effect is responsible for the former phenotype (Jegalian and De Robertis, 1992). More recently, to circumvent this problem, single-copy integration of a transgene can be achieved using retroviruses and transposons (Ding et al., 2005; Lois et al., 2002; Mates et al., 2009).

Functional redundancy:

In some cases, the inactivation of a single *Hox* gene does not result in any obvious phenotype. This is the case for instance with *Hoxa7* and *Hoxd8* mutation (Chen et al., 1998; van den Akker et al., 2001). In general, compared to the drastic effect of homeotic transformation in *Drosophila*, loss-of-function mutations in mice result in relatively mild effects.

For example, inactivation of the *Hox4* paralogs (*Hoxa4, Hoxb4* and *Hoxd4*) results in dose dependent increase in the severity of the resulting phenotype, leading to an increment in the number of cervical vertebrae adopting a C1 identity, compared to what is

observed in single mutants (Horan et al., 1995a; Horan et al., 1995b). Inactivation of *Hox9* paralogs (*Hoxa9, Hoxb9, Hoxc9* and *Hoxd9*) leads to transformation of posterior thoracic and anterior lumbar vertebrae into a more anterior thoracic morphology (McIntyre et al., 2007). Surprisingly, the presence of a single wild-type allele out of eight was sufficient to drastically reduce the severity of all these observed phenotypes. The inactivation of *Hox10* paralogs (*Hoxa10, Hoxc10* and *Hoxd10*) results in mice with transformation of all lumbar vertebrae into rib-bearing structures, similar to thoracic vertebrae. Moreover, inactivation of *Hox11* paralogs (*Hoxa11, Hoxc11* and Hoxd11) causes transformation of sacral vertebrae to a lumbar phenotype (Wellik and Capecchi, 2003). Also in these cases, the presence of a single wild-type allele out of eight could drastically reduce the severity of the phenotypes observed in *Hox* triple mutants (Fig. 1.2).

Thus, the duplication of the ancestral *Hox* cluster in the vertebrate lineage, and the resulting generation of different members for the same paralogy group, is likely to account for this effect. This suggests that *Hox* genes of the same paralogy group, if not others, can have partially redundant functions.

In other cases, genetic interactions among paralogs are more complex. For example, *Hoxa3* and *Hoxd3* single mutants do not display overlapping phenotypes, even if they are expressed in the same structures. However, double gene inactivation causes exacerbation of both individual phenotypes revealing an unexpected synergism (Chisaka and Capecchi, 1991; Condie and Capecchi, 1993). Another interesting result is obtained by combined

gene inactivation of *Hoxb8, Hoxc8* and *Hoxd8*. Single mutants display some distinct phenotypes (Le Mouellic et al., 1992; Tiret et al., 1993; van den Akker et al., 1999). Nevertheless, compound inactivation reveal synergistic interaction in the patterning along the AP axis, yet some phenotypes observed in *Hoxc8*/*Hoxd8* double mutants are rescued by *Hoxb8* inactivation, suggesting that qualitative differences among *Hox8* paralogous proteins may exist (van den Akker et al., 2001).

Even though *Hox* paralogous genes show closer sequence similarity than neighboring genes of the same cluster, there are several examples of functional redundancy among non-paralogous genes located in *trans* or even in *cis*. If we look at *Hoxa10* and *Hoxd11* compound mutants, animals display up to eight lumbar vertebrae with concomitant shift of the sacrum, a phenotype reminiscent of *Hoxa11*/*Hoxd11* compound mutants, but distinct from single mutants involving *Hoxa10, Hoxa11* or *Hoxd11* inactivation (Favier et al., 1996). In some other cases, functional redundancy was even reported between neighboring genes in *cis*. *Hoxb5*/*Hoxb6* trans-heterozygous mutants show the same phenotype as both homozygous, carrying C6 to C5 and T1 in C7 anterior transformations (Rancourt et al., 1995).

Many other examples of functional redundancy have been reported in other tissues, such as the limbs (see for example (Fromental-Ramain et al., 1996a; Fromental-Ramain et al., 1996b; Wellik and Capecchi, 2003)) or the kidney (Davis et al., 1995).

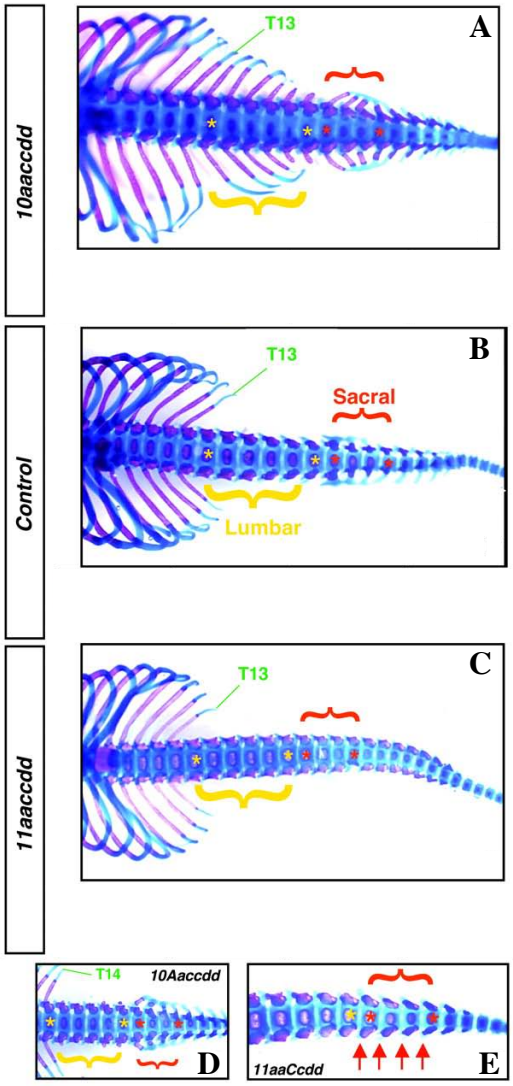

Figure 1.2 Homeotic transformations and functional redundancy among paralogous *Hox* genes.
Representation of a wild-type skeleton (B).The inactivation of *Hox10* paralogs (*Hoxa10, Hoxc10* and *Hoxd10*) results in mice with transformation of all lumbar vertebrae (yellow) into rib-bearing structures, similar to thoracic vertebrae (A). Inactivation of *Hox11* paralogs (*Hoxa11, Hoxc11* and *Hoxd11*) causes transformation of sacral vertebrae (red) to a lumbar phenotype (C). Surprisingly, the presence of a single wild-type allele out of eight is sufficient to reduce drastically the observed phenotype (D, E).
(modified from *Wellik and Capecchi, 2003*)

1.2.3 *Hox* genes and evolutionary novelties.

In the course of vertebrate evolution, besides their ancestral function in patterning the main body axis, *Hox* genes have been recurrently co-opted to pattern novel structures of the body. Due to two rounds of whole-genome duplications, higher vertebrates present four *Hox* clusters and thus up to four paralogous genes for each paralogy group. The presence of up to four paralogous genes allowed the allocation of different functions to different genes, often through the acquisition of new expression specificities. In this section, I will review some examples relevant for this thesis and subsequently discuss the specific functions of *Hoxa13* in embryonic and extra-embryonic structures.

Hox gene functions in the limbs:

The vertebrate limb is one of the most important morphological adaptations that enabled the transition from aquatic to the terrestrial environment in the course of vertebrate evolution. Work from different laboratories has demonstrated that *Hox* genes have been recruited to pattern this secondary body axis. Gain and loss-of-function experiments have demonstrated that 5' members of the *HoxA* and *HoxD* clusters are essential for the proper patterning and growth of limb skeleton. Genes of these two clusters are expressed in complex and dynamic patterns during forelimb and hindlimb development, characterized by two different waves of expression (reviewed in (Zakany and Duboule, 2007)). In the early limb bud, 5' *Hoxa* and *Hoxd* genes are sequentially activated in time and space,

reminiscent of the spatial and temporal collinearity occurring in the trunk and their expression patterns are progressively restricted towards the posterior margin of the bud (Dolle et al., 1989; Haack and Gruss, 1993). Later in development, during the second wave of expression, genes of the *HoxA* and *HoxD* clusters show a quite distinct and more complex expression profile. In fact, while *Hoxd* gene expression still show an anterior-posterior polarity, *Hoxa* genes rapidly loose this posterior restriction, but are progressively confined to the distal limb domain (proximo-distal polarity). This observation suggests that the regulatory mechanisms underlying *Hoxa* and *Hoxd* gene expression in this second phase of expression may have evolved separately, after cluster duplication occurred (Zakany and Duboule, 2007).

It was proposed that the appearance of the second wave of *Hox* genes expression in the developing limb accompanied the evolution of the most distal limb structures, the digits, from an ancestral fin-like appendage (described as the "fin to limb" transition) (Sordino et al., 1995). However, this view was recently challenged by the discovery that two waves of *Hox* gene expression are also present in different fishes (Ahn and Ho, 2008; Davis et al., 2007; Freitas et al., 2007; Johanson et al., 2007). Only the analysis of regulatory elements in fishes, and the comparison with the ones already identified in the mouse, will help to understand whether tetrapod digits are an adaptation of pre-existing structures or are a functional novelty that has evolved together with specific new regulatory elements (Woltering and Duboule, 2010).

Patterning defects along the proximo-distal (PD) axis of the limb, caused by *Hox* gene inactivation, are collinear with the gene position in the complex. Mutation in *Hoxa9* and *Hoxd9* paralogs leads to mild growth defects in the most proximal domain of the limb, the stylopod, group 11 gene inactivation affects the intermediate region of the limb, the zeugopod, *Hoxa13* and *Hoxd13* mutants display defects in the digits and carpal/tarsal bones (Davis and Capecchi, 1994; Fromental-Ramain et al., 1996b; Small and Potter, 1993). Compound *Hoxa* and *Hoxd* paralogous gene inactivation usually results in much more severe phenotypes than single gene inactivation (Davis et al., 1995; Fromental-Ramain et al., 1996b). Finally, the complete deletions of the *HoxA* and *HoxD* clusters in the limbs result in early developmental arrest, leading to a truncated limb at the proximal level of the humerus (Kmita et al., 2005).

Hox genes functions in external genitalia and reproductive tract:

Interestingly, group 9 to group 13 genes of the *HoxA* and *HoxD* clusters are also expressed in the genital bud, the structure that will give rise to external genitalia. Deletion of group 13 paralogous genes results in a similar dose-dependent reduction of both penian bone and digits (Kondo et al., 1997; Zakany et al., 1997a). Both external genitals and digits develop in a similar way and share a number of common signalling pathways (Yamada et al., 2006). Most recently, similar regulatory mechanisms have been identified for both structures. Enhancer sequences for both limb and genitals reside on the centromeric side of the *HoxD* cluster (Spitz et al., 2001; Spitz et al., 2005). Moreover, the *Ulnaless* inversion,

in which *Hoxd* genes are moved away from regulatory sequences located on the centromeric side of the cluster, results in down-regulation of *Hoxd* genes in both digits and genitals (Spitz et al., 2003). Transgenic assays also demonstrated that enhancer elements able to drive reporter gene expressing in the limbs are also active in the genitals (Gonzalez et al., 2007). Finally, *Hoxd* genes are expressed in a quantitative collinear manner in both structures (Montavon et al., 2008). Altogether, this suggests that the acquisition of new *Hox* expression specificities has been instrumental for the emergence of both digits and external genitalia during evolution, these structures being a combined adaptation to terrestrial life, allowing for both effective locomotion and internal fertilization.

Placental mammals present essential innovations compared to other animals, such as the differentiation of the oviducts into uterus and upper vagina, the presence of a highly specialized epithelium, referred to as the endometrium, and the placenta, a specialized organ that mediates the feto-maternal exchanges (Wagner and Lynch, 2005). 5' *Hoxa* genes are expressed in a collinear manner in the female reproductive tract, such that *Hoxa9* transcript is detected in the oviduct, *Hoxa10* in the developing uterus, *Hoxa11* in the uterus and cervix and *Hoxa13* in the upper vagina (Taylor et al., 1997; Warot et al., 1997). *Hoxa10* is expressed in the uterine epithelium and is up-regulated during implantation, when the uterine stroma is transformed into decidua. *Hoxa10* inactivation leads to anterior homeotic transformation of the uterus in oviduct and homozygous mutant females are partially infertile, as a result of implantation defects (Benson et al., 1996; Satokata et al.,

1995). Similarly, females lacking *Hoxa11* present with a small uterus and implantation defects (Gendron et al., 1997; Hsieh-Li et al., 1995). The combined inactivation of *Hoxa11* and *Hoxd11* results in anterior homeotic transformation of the male reproductive tract, while *Hoxd11* loss-of-function confers male sterility (Davis et al., 1995).

1.2.4 *Hoxa13* functions in the embryo proper.

Preliminary insights into *Hoxa13* gene function came from the discovery that the mouse spontaneous mutant "*Hypodactyly*" (*Hd*) carries a deletion of 50 base pairs (bp) in the *Hoxa13* coding sequence (Mortlock et al., 1996). The *Hd* mutation was first described in 1970 (Hummel, 1970) as a semidominant mutation leading to digit defects and shortening of digit I in heterozygous animals, while the majority of *Hd*/*Hd* embryos die *in utero*. Rare homozygous survivors are infertile and display severe autopod defects, characterized by the presence of only one digit and defects in carpal and tarsal elements (Hummel, 1970; Mortlock et al., 1996). Subsequently, two loss-of-function alleles have been generated in mice. The first engineered inactivation of *Hoxa13* (referred to as *Hoxa13*-/-) disrupts the homeobox in the second exon (Fromental-Ramain et al., 1996b) and the second *Hoxa13* loss-of-function allele was generated by targeting of a green fluorescent protein (GFP) into exon 2 (hereafter referred to as $Hoxa13^{GFP}$) (Stadler et al., 2001). Interestingly, the limb phenotype of these *Hoxa13* mutants is much less severe than

the *Hd*/*Hd* one. In fact, it was found that the *Hd* mutation leads to the production of a dominant negative Hoxa13 protein, in which the first wild-type 25 amino acids are followed by 275 new residues, resulting from the frame-shift caused by the 50 bp deletion in the gene sequence (Post et al., 2000). In the limb bud of these mutants the expression of other *Hox* genes is impaired and massive cell-death is detected (Post and Innis, 1999).

Many spontaneous mutations in different regions of the *Hoxa13* gene have been described in humans, causing the Hand-Foot-Genital syndrome (HFGS) (Frisen et al., 2003; Goodman et al., 2000; Jorgensen et al., 2010; Mortlock and Innis, 1997; Utsch et al., 2007). HFGS is a rare, dominantly inherited condition in which affected individuals present a phenotype very similar to the one of heterozygous *Hd* mutants, including digit 1 hypoplasia (short digit 1), brachydactyly (shortening) of the other digits and brachydactyly and clinodactyly (curvature) of digit 5. HFGS is also accompanied by lower genito-urinary tract malformations, such as hypospadias in males and Mullerian duct fusion defects in females, leading in the most severe cases to the presence of a "duplicated uterus" together with ectopic ureteric orifices (Poznanski et al., 1975; Stern et al., 1970) (Donnenfeld et al., 1992; Halal, 1988).

Hoxa13 **functions in the limb.**

In the mouse, *Hoxa13* starts to be expressed in the posterior and distal part of the limb bud around e10. At e12.5 its expression is detected in the entire presumptive autopod,

both in digit condensations and interdigital tissue and later, at e13.5-e14.5, *Hoxa13* transcript is restricted to peridigital tissue and interarticular condensations (Haack and Gruss, 1993; Stadler et al., 2001).

Hoxa13-/- adults are not viable due to mid-gestation embryonic lethality. *Hoxa13* homozygous mutant embryos can be analyzed up to e15 and display limb abnormalities in the autopod of both forelimb and hindlimbs, characterized by lack of digit 1 chondrogenic condensation, variable syndactyly and barachydactyly of other digits, loss of the second phalangeal cartilage, and delayed or absent pre-cartilaginous condensation for carpal and tarsal elements. Rare homozygous mutants have been recently recovered after birth, allowing for the analysis of skeletal defects in adult mutants that confirmed previous conclusions (Perez et al., 2010). Heterozygous animals are fully viable and fertile and display only mild limb abnormalities, such as fusion of digits 2 and 3 at the level of the soft tissues and alteration of the claw of digit 1 (Fromental-Ramain et al., 1996b). *Hoxa13/Hoxd13* compound mutants display a much more severe phenotype compared to the one observed in single loss-of-function inactivation and the severity increases progressively with the number of alleles inactivated (Dolle et al., 1993; Fromental-Ramain et al., 1996b). In fact, the most compromised autopod is observed in *Hoxa13-/-; Hoxd13-/-* embryos, which display almost complete digit loss and absence of carpal/tarsal condensations, demonstrating the fundamental importance of these paralogous genes in digit formation. *Hoxa13* mutants show a more severe phenotype in limb domains where

Hoxa13 function cannot be completely compensated by its paralog *Hoxd13*, including the forming digit 1 and carpal/tarsal elements of the limb (Haack and Gruss, 1993)

Subsequent studies have aimed to understand the molecular pathways regulated by *Hoxa13*. Studies using avian embryos suggested that *Hoxa13* expression is important to confer cell-cell adhesiveness properties and that *Hoxa13* expressing cells are able to selectively associate and form aggregates *in vitro* (Yokouchi et al., 1995). Further analysis demonstrated that *Hoxa13* directly activates the expression of the tyrosine kinase receptor *ephrin A7* (*EphA7*) in limb mesenchymal condensations, and that this activation is required for proper mesenchymal condensation in the limb autopod (Salsi and Zappavigna, 2006; Stadler et al., 2001). Moreover, *Hoxa13* activates the expression of *bone morphogenetic protein* 2 and 7 (*Bmp2* and *Bmp7*) in the autopod by binding to upstream sequences of these genes. In the developing limb, *Bmp2* and *Bmp7* are key regulators of chondrogenesis as well as interdigital programmed cell death (IPCD) required for proper digit separation (Macias et al., 1997; Merino et al., 1998; Yokouchi et al., 1996; Zou et al., 1997; Zou and Niswander, 1996; Zuzarte-Luis and Hurle, 2002). Decreased expression of *Bmp2* and *Bmp7* thus underlies loss of IPCD in *Hoxa13* homozygous mutants, leading to fused digits (Knosp et al., 2004).

In addition to its function in skeletal pattering, *Hoxa13* is also activated in myogenic progenitors of the limb, derived from the hypaxial dermomyotome of the somites. After these cells have entered the limb bud territory, some of them start expressing *Hoxa13,* and

Hoxa13 expression is maintained in limb the musculature at least until e13.5 (Yamamoto et al., 1998; Yamamoto and Kuroiwa, 2003). However, the functional relevance of *Hoxa13* expression in limb muscles remains unclear, and the phenotype of *Hoxa13*-/- mouse embryos has not been characterized for the presence of patterning or functional defects in the muscular tissues. Studies in chick showed that *Hoxa13* expression in myogenic progenitors of the limb is not under the control of signals derived from the apical ectodermal ridge (AER), unlike *Hoxa13* expression in mesenchymal cells, but is controlled by signals from the zone of polarizing activity (ZPA), via *Bmp2* regulation (Hashimoto et al., 1999). One study has linked *Hoxa13* function to the regulation of the transcription factor *MyoD,* which is involved in the process of muscular differentiation (reviewed in (Tajbakhsh and Buckingham, 2000)). Electroporation experiments in the chick and *in vitro* studies using myoblast cells showed that forced expression of *Hoxa13* inhibits expression of *MyoD* and the expression of *MyoD* is consistently enhanced in *Hoxa13*-/- mutants (Yamamoto and Kuroiwa, 2003). However, the functional relevance of this regulation is not clear and further studies in this direction have not yet been performed, leaving the potential function of *Hoxa13* expression in the limb musculature still largely unexplored.

Hoxa13 function in the urogenital system and gastrointestinal tract.

Hoxa13 and *Hoxd13* are co-expressed in the mesenchyme of the genital bud and urogenital sinus and, at lower levels, in the urogenital sinus epithelium (Oefelein et al., 1996; Podlasek et al., 1997; Warot et al., 1997). In particular, *Hoxa13* is expressed in the

caudal portion of the Mullerian ducts, caudal portion of the ureters, in the developing bladder, in male prostate and seminal vesicles, in female cervix and vagina and in the epithelium of hindgut and rectum (Warot et al., 1997).

Inactivation experiments have revealed an essential function for *Hoxa13* and *Hoxd13* in the development of urogenital system and gastrointestinal tract. *Hoxa13*-/- mutants display agenesis of the caudal part of the Mullerian ducts, abnormal location of ureter extremities, absence of developing bladder and, in general, hypoplasia of the entire urogenital sinus. In the genital bud, programmed cell death and cell proliferation are necessary for tissue remodelling and for proper growth and closure of the penile urethra. *Hoxa13* function in this structure is essential for normal *Bmp* and *Fgf* signalling. Downregulation of *Bmp7* and *Fgf8* levels in *Hoxa13*-/- mutants reduces apoptosis and cell proliferation in the genital bud, causing hypospadia, a defect in urethral closure (Morgan et al., 2003). *Hoxa13* inactivation also affects the vasculature within the distal part of the genital bud, which is characterized by abnormally dilated capillaries (Morgan et al., 2003). In the vascular endothelium of the genital bud, Hoxa13 directly binds discrete regions of the *EphA6* and *EphA7* promoters. *Hoxa13* inactivation leads to *EphA6* and *EphA7* down-regulation, making a possible link between reduced expression of these cell adhesion molecules and the abnormally dilated vessels within the genital bud (Shaut et al., 2007).

In contrast, in the development of the gastrointestinal tract, simple inactivation of *Hoxa13* does not cause overt abnormalities (Warot et al., 1997). As for the limbs,

Hoxa13/Hoxd13 compound mutants display a more severe phenotype, demonstrated by the complete absence of genital bud and fusion of hindgut and urogenital sinus into a cloaca-like structure (Warot et al., 1997). Moreover, *Hoxa13+/-; Hoxd13-/-* mutants display gastrointestinal abnormalities more severe than in simple *Hoxd13* loss-of-function, such as dilatation of the rectum with absence of rectal glands, together with defects of both the epithelial and the smooth muscle layers, the latter being detached from the mucosa and occasionally interrupted (Kondo et al., 1996; Warot et al., 1997). Altogether *Hoxa13* and *Hoxd13* expression in the posterior extremities of digestive, reproductive and excretory tracts suggests their potential role in the disappearance of the cloaca in some vertebrate species, such as placental mammals and teleost fishes, and in the evolution of a more complex anatomical configuration, in which digestive, reproductive and excretory functions are more clearly separated.

Hoxa13 functions in the extra-embryonic compartment.

In contrast to all other *Hox* genes, only *Hoxa13* inactivation precludes the embryo from the completion of its *in utero* development (Fromental-Ramain et al., 1996b; Stadler et al., 2001). *Hoxa13* homozygous mutants display midgestation lethality and cannot be recovered after e15 (Fromental-Ramain et al., 1996b). However, mutant embryos present grossly normal morphology, and the embryonic lethality was initially ascribed to partial stenosis of the umbilical arteries, even if this phenotype is not fully penetrant (Warot et al., 1997). Subsequently, Shaut and collaborators uncovered a role for *Hoxa13* in the

development of the vasculature within the placental labyrinth, which is characterized by reduced branching and reduced size of the overall structure in mutant homozygous tissues. The defective vasculature within the placental labyrinth likely accounts for the mid-gestation lethality of *Hoxa13*-/- embryos. Lack of *Hoxa13* function in the mutant labyrinthine vasculature results in down-regulation of pro-vascular factors in endothelial cells, such as *Tie2*, *Foxf1* and *Enpp2*, suggesting that downregulation of these genes could partially account for the *Hoxa13*-/- placental phenotype (Shaut et al., 2008).

1.3 The murine chorioallantoic placenta

1.3.1 The placenta: overview.

In eutherian mammals, the embryo starts and completes its development in the mother's uterus, depending upon the mother for its survival during the entire pregnancy. During embryogenesis, the chorioallantoic placenta is the first organ to form and is essential to sustain embryonic survival and growth during gestation. The placenta forms the interface between the maternal and fetal environment, facilitating nutrient and gas exchanges, as well as removal of fetal waste products. The placenta is also an important source of pregnancy-associated hormones that alter maternal physiology during pregnancy

and acts as an immune barrier for the foetus, maintaining the separation of maternal and fetal circulation.

As in humans, the murine mature placenta is formed of two major components: the decidua and the labyrinth (Fig. 1.3). The outer maternal layer includes decidual cells from the uterus and the maternal vasculature. The placental labyrinth is formed by highly branched endothelium and by trophoblast cells, which play structural and functional roles in bringing the maternal and fetal vasculature into close association. The umbilical cord and its vasculature connect the placenta to the developing embryo.

All aspects of chorioallantoic development, including the formation of the allantois, i.e. the precursor of the umbilical cord, its growth, and the formation of the highly vascularized labyrinth layer are susceptible to genetic perturbations (Inman and Downs, 2007; Rossant and Cross, 2001; Watson and Cross, 2005). In the last decade, the study of different mouse mutants presenting aberrant development of the different chorioallantoic placenta components shed some light on the molecular basis of placental development. However, even if extra-embryonic tissues are clearly essential to sustain growth and development of the embryo, much work remains to be done in order to fully characterize the molecular mechanisms governing their development.

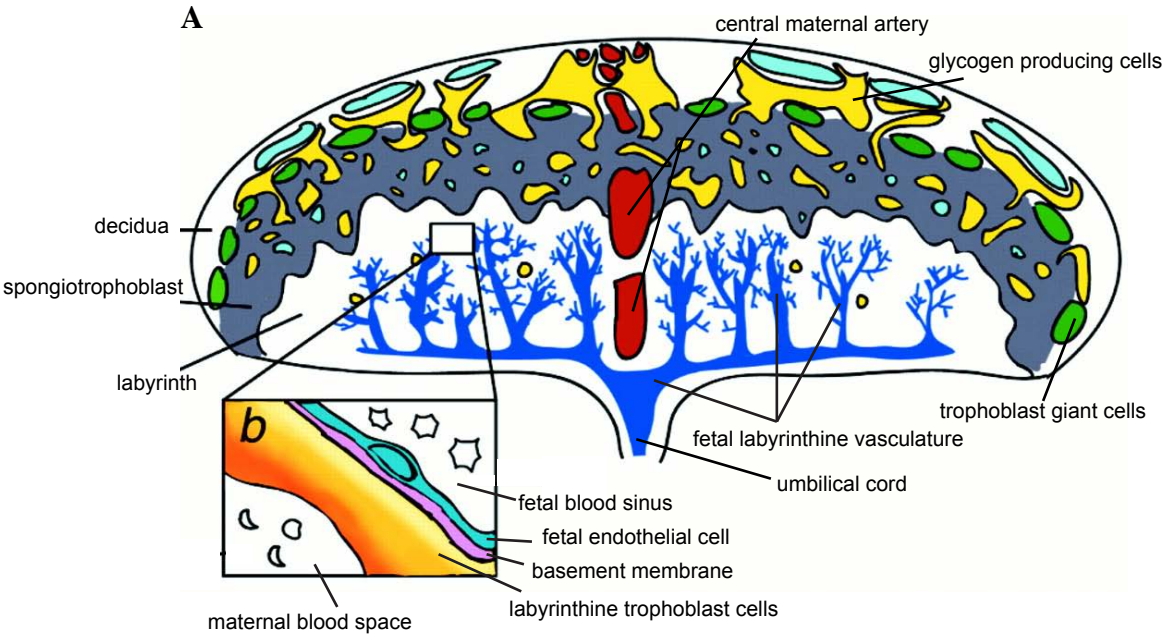

Figure 1.3 The murine placenta.
The major regions and cell types of the mouse placenta at e15.5. (A) Schematic representation of a sagittal section through the center of the placenta. On the top, the maternal part (decidua). Just below the spongiotrophoblast layer of the placenta (grey). Highly branched fetal vasculature within the labyrinth is represented in blue and is connected with the umbilical cord (bottom).
(b) Magnification of the boxed area in A, showing in more detail the labyrinthine feto-maternal interface (the zygote-derived tissue between fetal and maternal blood). In orange, the trilaminar layer of trophoblast cells which separates and mediates the exchanges between the maternal blood and the fetal vasculature.
(adapted from *Georgiades et al. 2001*).

1.3.2 Early development and the origin of embryonic and extra-embryonic lineages in the mouse.

Mouse gestation lasts around 20 days, and can be divided into three phases: pre-implantation, implantation and post-implantation. During this time, the fertilized egg develops and gives rise to both embryonic and extra-embryonic structures (Fig. 1.4). The development of embryonic and extra-embryonic components is tightly linked and synchronized during the entire pregnancy.

After fertilization, during the pre-implantation phase, the mouse zygote undergoes three rounds of cleavage, reaching 32-cell stage (e3.5). At this time, two cell populations are distinguishable and committed to different fates: the outer cell layer, or trophectoderm and a small cluster of inner cells, referred to as the inner cell mass. The spatial distribution of these two cell populations generates an inner fluid-filled cavity, the blastocoel. At this stage, the mouse embryo is called a blastocyst (Fig. 1.4). After an additional 24 hours of maturation, the blastocyst is ready to implant into the maternal uterine wall (e4.5). During the implantation process, the trophectoderm excavates a space in the uterine wall and becomes embedded into it, via a process that involves maternal participation through hormonal receptivity, and thus synchrony between the mother and the fetus. During the post-implantation phase, the trophectoderm begins to differentiate into extra-embryonic

ectoderm, and the inner cell mass gives rise to the epiblast and primitive endoderm lineages. The extra-embryonic ectoderm will subsequently originate the ectoplacental cone and the chorion. The ectoplacental cone will give rise to the outer population of trophoblast giant cells and the hormone secreting spongiotrophoblasts. The chorion will differentiate into the various labyrinth trophoblast cell subtypes. The primitive endoderm with its descendant, the extra-embryonic parietal and visceral endoderm, will form components of the parietal and visceral yolk sacs, structures that will function as temporary placenta, until the definitive chorioallantoic placenta is formed. The epiblast gives rise to the three primitive embryonic cell layers (embryonic ectoderm, endoderm and mesoderm), to the extra-embryonic mesoderm that forms the allantois that will subsequently give rise to the umbilical cord and to the amniotic ectoderm that forms to the amnion (reviewed e.g. in (Cockburn and Rossant, 2010; Simmons and Cross, 2005)). Recent data suggest that the three primitive embryonic cell layers do not entirely segregate at gastrulation and that common progenitors of both ectoderm and mesoderm can be identified at much later stages in the mouse (Tzouanacou et al, 2009).

The intimate association of labyrinth trophoblast cells and allantois/umbilical cord-derived vasculature eventually form the labyrinth layer of the placenta, which is the site of feto-maternal exchanges. The development of this essential structure is presented in the next section (see also Fig. 1.5).

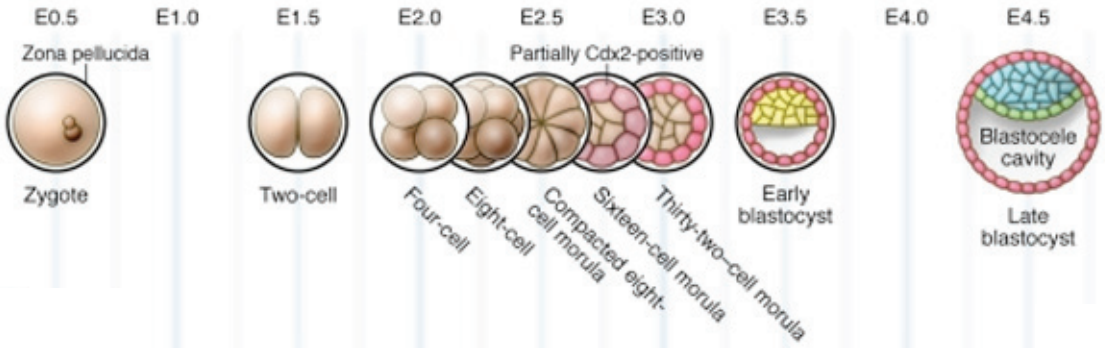

Figure 1.4 Stages of mouse preimplantation development.
In the mouse, the fertilized egg undergoes three rounds of cleavage, producing an eight-cell embryo that then undergoes compaction. From the eight-cell stage onward, cell divisions produce two populations of cells, those that occupy the inside of the embryo and those that are located on the outside. The blastocoel cavity begins to form inside the embryo beginning at the 32-cell stage and continues to expand as the embryo grows and matures into the late blastocyst stage.
(adapted from Cockburn and Rossant, 2010)

1.3.3 Labyrinth development.

Gastrulation and emergence of the allantois.

Between e4.5 and e6 the epiblast elongates and forms an internal cavity, assuming a U-shaped structure. Around e6.75 the process of gastrulation begins, with the formation of the primitive streak in the posterior region of the embryo. 24 hours after its formation, the primitive streak elongates towards its anterior limit, where a specialized structure referred to as the node will form. The node sends forward a population of cells in the anterior midline, called the notochord. These cells give rise to the definitive endoderm and to mesoderm of the axial midline. At the same time, cells emerge in lateral directions from the primitive streak, generating the nascent embryonic mesoderm. Cells emerging at specific times and AP locations along the primitive streak will give rise to different mesoderm derivatives ((Kinder et al., 1999; Lawson et al., 1991; Tam and Beddington, 1987)). Cells from the epiblast ingress into the posterior primitive streak and emerge as extra-embryonic mesoderm in the extra-embryonic space ((Beddington, 1981; Lawson et al., 1991; Tam and Beddington, 1987)). The cell population that first completes this process gives rise to the mesodermal lining of the exocoelomic cavity (e7.25). Subsequently, another cell population ingresses through the posterior primitive streak to emerge as the allantoic bud, which remains in close continuity with the posterior primitive streak (Lawson et al., 1991).

The development of the allantois proceeds in parallel with specific stages of embryonic development (Downs and Davies, 1993). At the neural plate stage (e7.25-e7.5), the allantois emerges from the primitive streak as a bud containing an outer and an inner layer. The outer layer of squamous epithelial cells, the mesothelium, is characterized by the presence of both adherens junctions and desmosomes. The inner cells are known as the allantoic core (Downs and Gardner, 1995; Downs et al., 2004). The vascularization of the allantois occurs *de novo*, like the vascularization of the yolk sac and embryo. At late allantoic bud stage, in the distal tip of the allantois, the first angioblast cells begin to differentiate from the allantoic mesenchyme. These cells are endothelial progenitors that will form the primary vascular plexus within the allantois (Downs et al., 1998; Drake and Fleming, 2000).

The molecular mechanisms leading to allantoic bud emergence are still poorly understood. However, loss-of-function inactivation for different genes leads to absence of allantoic bud emergence. Members of the Bmp family seem to have an essential role in this process. *Bmp-4* mutants gastrulate properly, but fail to develop the allantoic bud (Lawson et al., 1999; Winnier et al., 1995). Embryos carrying a mutation of another member of the Bmp family, *Bmp8b*, have delayed emergence of the allantoic bud and subsequent retardation of allantoic elongation (Ying et al., 2000). Furthermore, inactivation of the Bmp signaling intermediate *Smad1* results in the absence of allantoic bud in a subset of mutants (Lechleider et al., 2001). Mutants for a*fadin,* coding for a component of adherens and tight

junctions, also fail to develop the allantois, possibly due to defects in the establishment of the outer cell layer within the allantois (Zhadanov et al., 1999).

Elongation and vascularization of the allantois.

At headfold stage (e7.75-e8), the allantoic bud grows and elongates through three major mechanisms: addition of new cells from the primitive streak, allantoic cell proliferation and increase in the intercellular space, a process called cavitation (Brown and Papaioannou, 1993; Downs and Bertler, 2000; Tam and Beddington, 1987). At this time, mesenchymal cells within the allantois complete the process of de novo vascularisation, in which core cells of the allantois differentiate into Flk-1 expressing angioblasts, with a distal to proximal polarity. These cells will ultimately undergo endothelial differentiation and express the endothelial cell marker PECAM-1. The primary vascular plexus forms along the major axis of the allantois and, by 6-8 somite stage (e8.25-e8.5), it amalgamates with the developing vasculatures of the embryo and the yolk sac, just below the base of the allantois (Downs et al., 1998; Downs et al., 2004; Inman and Downs, 2006).

Different mouse mutants display defects in allantois enlargement and elongation, although the underlying mechanisms remain largely obscure (reviewed in (Inman and Downs, 2007)). Many of these mutants belong to the Bmp family, such as *Bmp2, Bmp4, SMAD1* and *SMAD4* mutants (Chang et al., 1999; Downs et al., 2004; Fujiwara et al., 2001; Lechleider et al., 2001; Ying and Zhao, 2001; Zhang and Bradley, 1996). Genetic

inactivation of the T box transcription factor *Tbx4* results in defects in allantoic growth associated with apoptosis in the distal allantois (Chapman et al., 1996; Naiche and Papaioannou, 2003). Mutants for the homeobox containing transcription factor *Cdx2* die between e3.5 and e5.5, as *Cdx2* function is essential for development of the trophoblast lineage. When chimeras were obtained by tetraploid complementation however, *Cdx2* mutants survived until e10, but displayed only a short rudimentary allantois (Beck et al., 1999; Chawengsaksophak et al., 2004). Another T box transcription factor, *brachyury* (*T*) is crucial for allantois growth and vascularisation. Different *brachyury* mutant alleles give rise to a short allantois, in which core cells undergo apoptosis and fail to form a functional vascular plexus (Gluecksohn-Schoenheimer, 1944; Inman and Downs, 2006). Key factors involved in regulating embryonic and yolk sac vascularisation are also expressed in the allantois (Downs, 1998; Downs et al., 2004; Dumont et al., 1995). Loss-of-function inactivation of *Vegf, Flk-1, Flt-1, Tie1* and *Tie2* are embryonic lethal due to defective vasculogenesis. Surprisingly, no specific defects in allantoic vascularisation were detected in these mutants, although this may be because extra-embryonic structures were examined only grossly. (Carmeliet et al., 1996; Ferrara et al., 1996; Fong et al., 1995; Hiratsuka et al., 1998; Hiratsuka et al., 2005; Sato et al., 1995; Shalaby et al., 1995).

Chorio-allantoic union.

Once the allantois has enlarged and elongated, at 6-8s embryonic stage (e8.5), it reaches the chorionic surface and unites with it. This process requires specific factors

produced by both the chorion and the allantois. Grafting experiments have demonstrated that chorio-allantoic union is dependent upon the developmental maturity of the allantois, while the chorion is always receptive to the allantois (Downs, 1998). The process of chorio-allantoic union relies in part upon the expression of vascular adhesion molecule 1 (VCAM-1) and α4-integrin, a binding partner of VCAM-1, expressed in the distal allantois and in the chorion, respectively. In mutants for these factors, the allantois forms and elongates, but fails to contact the chorion (Gurtner et al., 1995; Kwee et al., 1995; Yang et al., 1995). However, in a small proportion of VCAM-1 and α4-integrin mutants, the allantois does unite with the chorion, suggesting that other molecular mechanisms are involved in this process. Accordingly, a large number of mice mutants show defects in chorio-allantoic union, in almost half of the cases, presenting an incompletely penetrant phenotype (reviewed in (Inman and Downs, 2007)). For example, in a portion of *Cdx2*/*Cdx4* compound mutants the allantois fails to attach to the chorion, even if VCAM-1 and α4-integrin are normally expressed (van Nes et al., 2006).

Chorion vascularization.

Once the allantois has contacted the chorion, its distal tip spreads over the chorionic surface, probably accompanied by the formation of hydrophobic space in the distal part of the allantois. Around e9, the allantoic vasculature starts to invade the chorion and simultaneously, the trophoblast surface starts to fold, generating villous structures. This process is named chorioallantoic branching morphogenesis (reviewed in (Cross et al.,

2006)). The sites where the chorionic plate folding occurs and where evagination of the allantoic vasculature takes place are marked by the expression of the transcription factor Glial cell missing 1 (Gcm1). *Gcm1* begins to be expressed in the chorionic plate at e8, and during branching of the allantoic vasculature, remains expressed at the distal tip of elongating branches. *Gcm1* mutants fail to initiate chorioallantoic branching and are arrested at a flat chorion stage (Anson-Cartwright et al., 2000).

Several observations suggest that the process of chorioallantoic branching requires close interaction and molecular crosstalk between the trophoblast cell population and the allantoic mesoderm and that the fusion of the allantois with the chorion is required to trigger important modifications and differentiation in trophoblast stem cells (Cross et al., 2006). Thus, in various mutants demonstrating impaired chorioallantoic fusion, the chorionic plate does not develop villous invaginations and the trophoblast lineage fails to properly differentiate.

Several genes are essential for proper chorioallantoic branching morphogenesis (reviewed in (Inman and Downs, 2007; Rossant and Cross, 2001)). Different loss-of-function mutations affect allantoic vasculature branching. For example, those *Cdx2*/*Cdx4* compound mutants that successfully undergo chorioallantoic union show decreased vascular branching within the labyrinth (van Nes et al., 2006). Various mutants for components of the Notch signalling pathway, such as *Notch1*/*Notch4, Hey1*/*Hey2* and *Dll4,* present a similar phenotype (Duarte et al., 2004; Fischer et al., 2004; Krebs et al., 2000).

Many other mutants show impaired vasculogenesis in the labyrinth due to defective trophoblast lineage or have defects of unknown origin. However, it is clear that defective allantoic or chorionic differentiation can alter the development of surrounding tissue complicating the understanding of the defect origin (Rossant and Cross, 2001).

Prior to e10.5, embryonic development is mainly sustained by diffusion of gases, nutrients and waste products through the yolk sac (also referred to as choriovitelline placenta). However, after this stage, failure to establish a functional chorioallantoic placenta, in which the labyrinthine vasculature is properly branched, is detrimental for embryonic survival, leading to mid-gestation lethality due to reduced or impaired exchange between the mother and foetus (Rossant and Cross, 2001).

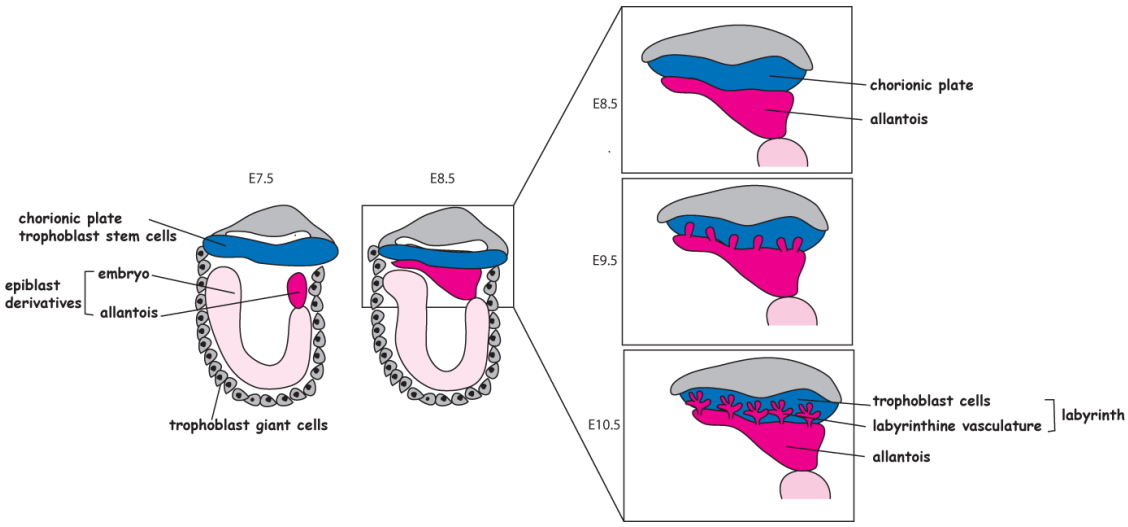

Figure 1.5 Labyrinth development in the mouse.
The allantois, the precursor of the umbilical cord, is an epiblast derivative from which the labyrinthine vasculature originates. At late neural plate stage, *de novo* vasculogenesis initiates at the distal tip of the allantois. Then the allantois fuses with the chorion around e8.5. After chorio-allantoic attachment the vasculature of the allantois spreads and branches into the chorion giving origin to the vasculature of the labyrinth. Proper branching of the initial chorio-allantoic interface ensures the enlargement of the surface for feto-maternal exchanges, which is essential to support the increasing metabolism of the growing embryo.

1.4 *Hox* gene regulation.

1.4.1 *Hox* gene regulation in the primary body axis.

In the mouse, *Hox* gene expression in the primary body axis can be subdivided into three distinct phases: the initiation of gene expression, the establishment of the definitive expression pattern and its subsequent maintenance during later stages of embryonic development (Deschamps et al., 1999).

Initiation of *Hox* gene expression.

Hox genes begin to be expressed during gastrulation, at the late streak stage, in cells of the posterior primitive streak fated to become extra-embryonic mesoderm. Once activated, *Hox* gene expression domains expand to more anterior levels, up to the node region, from where the embryonic primary axis elongates (Deschamps and Wijgerde, 1993). The timing of its initial activation determines the time at which each *Hox* gene expression domain will reach the node region. However, lineage-tracing experiments demonstrated that the definitive *Hox* expression patterns are not fixed at the node, but will be defined later and in more anterior regions (Forlani et al., 2003). The initial activation of *Hox* gene transcription is regulated by events related to the formation and extension of the primitive streak, such as Wnt, Fgf and possibly retinoic acid (RA) signalling (Ciruna and Rossant, 2001; Forlani et al., 2003; Hogan et al., 1992).

Establishment of expression domains.

Cells leaving the primitive streak early on contribute to future anterior somites, and only express *3'Hox* genes, while cells leaving the streak later express both 3' and more 5' *Hox* genes. However, this early expression program does not correspond to the definitive "Hox code" of the descendants of these cells, which will be only fixed later on by additional regulatory signals. Initiation, anterior extension and establishment of *Hox* gene expression domains are tightly linked to the emergence, extension and segmentation of the body axis (Deschamps and van Nes, 2005). Different factors have been identified as possible direct or indirect upstream regulators of *Hox* genes in both mesoderm and neurectoderm derivatives. During axial elongation, cells leaving the node are exposed to gradients of Wnt and Fgf signals, both stronger in the posterior embryonic domains (Aulehla et al., 2003; Dubrulle et al., 2001), as well as to retinoic acid (RA) gradient, stronger in anterior domains (Dubrulle and Pourquie, 2004). In addition, *Hox* genes may be also related to the segmentation of the mesoderm during somitogenesis. Several 3' *Hox* genes display cyclic transcription in the pre-somitic mesoderm (PSM), correlated to the cyclic production of new somites (Zakany et al., 2001). Perturbation of Notch signalling, an essential player in the segmentation clock, affects *Hox* gene expression in the PSM (Zakany et al., 2001), or results in a shift in *Hox* expression domains that produces axial skeletal defects (Cordes et al., 2004). RA signalling is also critical in the establishment of *Hox* expression boundaries in the hindbrain (Gavalas and Krumlauf, 2000). RA binds to the

intracellular retinoid acid receptor (RAR), which, through heterodimerization with the retinoid X receptor (RXR), binds to retinoid acid response elements (RAREs). Such elements were identified in the vicinity of group 1 to 4 *Hox* genes, and are required for appropriate *Hox* expression in rhombomeres, indicating that RA directly regulates *Hox* gene expression (e.g. (Dupe et al., 1997; Marshall et al., 1994; Studer et al., 1994). In the hindbrain, cross-interaction between *Hox* genes and the transcription factors *Krox20* and *Kreisler* have been shown to establish the definitive expression patterns for 3' *Hox* genes (Manzanares et al., 1999; Manzanares et al., 1997; Manzanares et al., 2002; Nonchev et al., 1996; Sham et al., 1993). The 3' *Hox* expression in the hindbrain also involves auto- and cross-regulatory loops that are presumably involved in the maintenance and reinforcement of *Hox* gene expression (Gould et al., 1997; Maconochie et al., 1997; Manzanares et al., 2001; Packer et al., 1998; Popperl et al., 1995; Studer et al., 1994).

Other key regulators of *Hox* genes in the establishment of the AP patterning are genes of the *Cdx* family of transcription factors. *Cdx* genes are homologous to the *Drosophila caudal* gene and are closely related to *Hox* genes, as they are believed to derive from the same common ancestral *ProtoHox* cluster (Pollard and Holland, 2000). The *Cdx* family is composed of three members: *Cdx1, Cdx2* and *Cdx4*. During early embryonic development, these genes are expressed similarly to *Hox* genes, with nested expression domains along the AP axis (reviewed in (Young and Deschamps, 2009)). *Cdx* mutants display vertebral patterning defects, correlating with perturbation of the "Hox code" from

cervical to caudal levels (Houle et al., 2003; van den Akker et al., 2002). Moreover, Cdx proteins can directly regulate *Hox* gene expression, via *Cdx* binding sites that are found clustered in the *Hox* clusters (Charite et al., 1998; Subramanian et al., 1995). *Cdx* genes are regulated by Wnt, Fgf and RA signalling, and it was proposed that they convey these signals to *Hox* genes (Lohnes, 2003).

Along with these molecular interactions of transcription factors and signalling pathways, the sequential transcriptional activation of *Hox* genes during early embryonic development, as well as in the differentiation of ES cells *in vitro*, is accompanied by higher order chromatin dynamics (reviewed in (Soshnikova and Duboule, 2009a; Sproul et al., 2005)). Activating and repressive histone marks, such as trimethylation at lysine 4 or trimethylation at lysine 27 as well as acetylation at lysine 9 of histone H3, follow inverse temporal collinear changes in their distribution from 3' to 5' of the cluster (Chambeyron and Bickmore, 2004; Soshnikova and Duboule, 2009b). These chromatin modifications precede the actual *Hox* gene activation. However, the histone mark distribution is largely preserved even in presence of a split *Hox* cluster, ruling out the existence of a spreading mechanism of these chromatin modifications (Soshnikova and Duboule, 2009b). Mutations in *Polycomb* group genes, that code for the enzymatic complexes that deposit these marks, result in heterochronies in *Hox* gene activation, confirming a functional role of these chromatin modifications (Bel-Vialar et al., 2000). Furthermore, experiments performed both in differentiating ES cells as well as in embryonic tissues demonstrate that the overall

DNA organization changes during gene collinear transcriptional activation, and inactive and active genes are localized in distinct three-dimensional domains of the nucleus (Chambeyron et al., 2005; Morey et al., 2007; Noordermeer et al., 2011).

Once *Hox* genes are activated, the correct anterior limit of expression for each of them has to be established. As the vertebrate body extends by posterior growth, it was proposed that the temporal progression of *Hox* gene activation, along with axis elongation, could directly determine the establishment of the anterior limit of expression at later stages (Duboule, 1994). In chicken embryos, over-expression of 5' *Hox* genes in epiblast cells delay their ingression through the primitive streak, modifying the final axial position they contribute to (Iimura and Pourquie, 2006). However, mice with engineered heterochronies in gene activation do not systematically show altered anterior limit of gene expression, suggesting the existence of multiple superimposed regulatory mechanisms underlying temporal *Hox* gene activation in the trunk (Kondo and Duboule, 1999; Tschopp et al., 2009; van der Hoeven et al., 1996). In the recent model for *HoxD* regulation in the trunk, the initiation of the temporal collinear gene activation is under the control of a centromeric-located repressive influence and a telomeric- based activation mechanism, thus the time of activation of each gene is dependent on its location within the cluster. The final spatial localization of *Hox* transcripts, in contrast, seems to rely largely on local regulatory elements acting at short distance and located inside the cluster (Tschopp et al., 2009).

Maintenance of gene expression.

Polycomb group (*PcG*) and *Trithorax* group (*TrxG*) genes were first identified in *Drosophila* where, when mutated, give rise to homeotic transformations. They play a key role in preserving *Hox* gene expression once the expression domains are established (reviewed in (Maeda and Karch, 2006; Ringrose and Paro, 2007)). *PcG* and *TrxG* gene function is largely conserved between *Drosophila* and vertebrates (Gould, 1997). Both gene groups code for proteins involved in epigenetic modification of the chromatin at specific sites, *via* histone modifications that are inherited after cell division. These enzymes, in addition to their function on *Hox* clusters, also regulate the chromatin state at many other genomic loci. *PcG* genes are required to maintain *Hox* genes in a silent state outside their normal expression domains, while *TrxG genes* are essential for maintenance of *Hox* gene expression. Both groups bind as multiprotein complexes to *cis* regulatory elements located in the proximity of target gene promoters. Some *PcG* complexes were shown to promote trimethylation of lysine 27 of histone H3, while *TrxG* complexes promote trimethylation of lysine of the same histone (Byrd and Shearn, 2003; Cao and Zhang, 2004). These histone modifications usually correlate with silent or active transcriptional states genome-wide, however how exactly they affect transcription remains to be determined.

In the mouse, *PcG* mutations lead to anteriorization of *Hox* gene expression causing posterior homeotic transformations, as for instance in the case of *Bmi1*, *mel18, M33* or *Eed* mutants (Akasaka et al., 1996; Core et al., 1997; van der Lugt et al., 1996; van der Lugt et

al., 1994; Wang et al., 2002). Conversely, inactivation of the *TrxG* gene *Mll* does not interfere with gene activation, but leads to subsequent loss of *Hox* expression (Yu et al., 1998; Yu et al., 1995).

1.4.2 Local *cis*-regulatory elements and regulatory landscapes.

Hox gene transcriptional regulation, in both time and space, apparently relies on the complex interaction of many different regulatory mechanisms at work in *cis*. Different mechanisms of regulation are likely to be at work both at the gene and cluster level. Spatiotemporal collinearity is the result of a balanced interaction between intrinsic regulatory elements and mechanisms of global regulation ((Spitz and Duboule, 2008)).

Cis- regulatory elements are non coding DNA sequences that modulate gene activity, through both activation and repression of transcription, and can be located in the immediate vicinity of target gene promoters or in remote locations, up to 1 Mb distance from their targets (reviewed e.g. (Ong and Corces, 2011) (Kleinjan et al., 2001; Lettice et al., 2003)). Recently developed techniques, such as chromosome conformation capture (3C) and its variants, have allowed the spatial organization of DNA loci *in vivo* to be directly addressed (Gavrilov et al., 2009). The results obtained strongly suggest that gene regulation at such genomic distance is achieved by the formation of chromatin loops that bring distant regulatory elements into close proximity with target promoters (reviewed e.g. (Ong and Corces, 2011)).

In the main body axis, important aspects of the spatial *Hox* transcript distribution can be explained by the action of local and short-range regulatory elements. In fact, when randomly integrated into the genome, most of the larger transgenes were able to recapitulate *Hox*-like expression patterns in the trunk (Charite et al., 1995; Whiting et al., 1991; Zakany et al., 1988), but not in more recently evolved structures, like the limbs and genitals (Gerard et al., 1993; Renucci et al., 1992). These expression patterns were only recovered when the same transgenes were targeted in the context of their endogenous cluster environment (Spitz et al., 2001; van der Hoeven et al., 1996). Subsequent experiments demonstrated that the expression of *Hox* genes in evolutionarily more recent structures, like the digits and genitals, depends on global enhancer elements located in regions considerably distant from the cluster (reviewed in (Spitz and Duboule, 2008)).

Substantial efforts have been used to shed light on the regulatory mechanisms associated with *Hox* gene expression during limbs development, as a paradigm for the emergence of evolutionary innovations. A transgenic approach involving large, randomly tagged BACs covering the region 5' to the *HoxD* cluster, identified a segment of about 40 kb, referred to as global control region (GCR). The GCR lies around 200 kb from *Hoxd13* and is able to drive reporter expression in the limbs and genitals (Spitz et al., 2003). The limb enhancer activity was subsequently assigned to a 5 kb highly conserved fragment (region B (Gonzalez et al., 2007)). However, the GCR alone is not able to fully recapitulate the endogenous *Hoxd* gene expression in limbs. Another region, Prox, which was subsequently

identified approximately 50 kb upstream to *Hoxd13*, also drives reporter expression in limbs when directly linked to the reporter, but is not able to activate *Hoxd* genes at a distance in transgenic assays (Gonzalez et al., 2007). Interestingly, even if they display different patterns, when linked together in a reporter transgene, GCR and Prox show synergistic activity, resulting in a more *bona fide* recapitulation of endogenous 5'*Hoxd* gene expression (Gonzalez et al., 2007). Moreover, a transgene including GCR linked to a human BAC including Prox and posterior *HoxD* cluster is able to partially rescue the limb phenotype associated with a lack of 5' *Hoxd* genes (Gonzalez et al., 2007). Thus, global regulatory mechanisms mediate the expression of 5'*Hoxd* and neighboring genes such as *Evx2* and *Lnp* in the developing limbs and genitalia and rely on at least two distinct enhancers located upstream of the *HoxD* cluster. A similar situation was also described at the *HoxA* locus, as *Hoxa13* also seems to be part of a regulatory landscape with *Evx1* and other genes located further away in the chromosome showing expression in limb and genitalia (Lehoczky et al., 2004). Moreover, a sequence showing high conservation with region B was identified in the vicinity of *Evx1*, but failed to drive clear reporter expression in limbs in transgenic assays (Lehoczky et al., 2004). Experiments based on tagged BAC transgenes suggest that at least two elements centromeric to *Evx1* are able to partially recapitulate endogenous *Hoxa* expression in limbs and genitals (Lehoczky and Innis, 2008), however proof that these sequences are *bona fide* regulatory elements for *Hoxa* genes has not been provided.

Similarly, evidence suggests that an element responsible for *Hoxd* gene expression in the early limb bud and the intestinal hernia (ELCR) is located on the opposite side of the *HoxD* cluster (Zakany et al., 2004). The trans-allelic targeted meiotic recombination technique (TAMERE) (Herault et al., 1998) enabled experiments determining that in the early limb buds, the temporal sequence of *Hoxd* gene expression is controlled by their position relative to the 3' extremity of the cluster. The restriction of posterior gene expression to the posterior part of the limb bud, in contrast, is dependent on the gene position relative to the 5' extremity, which exerts a repressive effect (Tarchini and Duboule, 2006). Interestingly, a similar mechanism underlies *Hoxd* gene expression in the trunk at early stages of embryonic development (Tschopp et al., 2009). Such a dependence of expression territory on the genomic configuration of the complex was illustrated by the changes in *Hoxd* gene expression caused by Sequential Targeted Recombination INduced Genomic rearrangement (STRING)-generated inversions of large DNA regions flanking the *HoxD* cluster and by a 3 Mb inversion resulting in the split of the *HoxD* cluster in two sub-clusters (Spitz et al., 2005).

A wealth of data obtained in the last 15 years therefore describe a picture in which important parts of the ancient *Hox* regulatory system are located within the cluster, while novel regulatory elements lie outside it, in large regulatory landscapes. This arrangement likely came about to avoid interference with control elements related to ancestral *Hox* functions (Fig. 1.6).

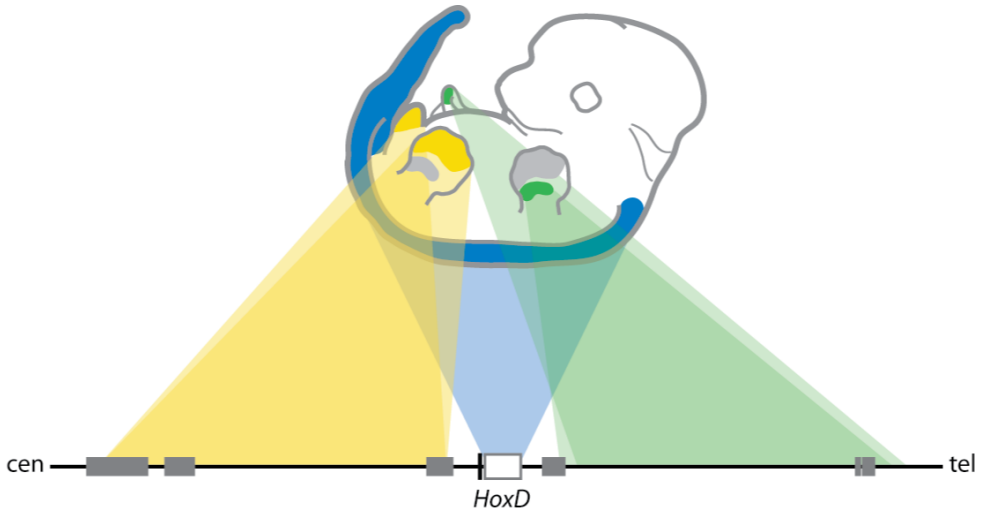

Figure 1.6 The global regulatory organization of the murine *HoxD* locus. Regulatory elements responsible for setting up spatial collinearity in the primary body axis are mostly located within the gene cluster itself (blue). Expression specificities in more recently evolved embryonic structures are driven by enhancer elements residing in the flanking gene deserts. This is the case, for example, for the distal limb bud and the genitalia, with the responsible regulatory elements located on the centromeric side (yellow), whereas enhancers driving *Hoxd* gene expression in the proximal limb and the intestinal hernia are found on the telomeric side (green). (*Tschopp and Duboule, 2011*)

Aim of the thesis.

In the last two decades evidence was obtained suggesting that *Hox* genes have been co-opted for the patterning of evolutionary novel embryonic structures such as limbs and external genitalia. Growing evidence suggest that the recruitment of *Hox* genes to achieve additional functions relies largely upon the acquisition of novel regulatory mechanisms, distinct from the ones already at work in the trunk.

Recent studies have shown that the most 5' genes of the *HoxA* cluster, namely *Hoxa13*, is functional not only in the embryo proper, where it is required for proper limb and urogenital development, but is also essential in the extra-embryonic compartment, for the proper expansion of the vasculature within the placental labyrinth. Inactivation of *Hoxa13* leads, in fact, to embryonic lethality due to impaired feto-maternal exchanges. This suggests that the recruitment of *Hoxa13* in the extra-embryonic tissues might have been pivotal for the evolution of developmental strategies associated with the emergence of placental species.

The goal of my doctoral studies was to better understand the regulatory mechanisms underlying *Hoxa13* recruitment in the extra-embryonic compartment. Using expression analysis, genetic rearrangements and transgenic analysis I investigated whether *Hoxa* function in the extra-embryonic compartment is restricted to *Hoxa13* and I explored the regulatory mechanisms underlying *Hoxa13* expression in the extra-embryonic tissues.

Moreover, through the analysis of *Hoxa* gene expression in a non-placental species, I tried to ascertain the point of vertebrate evolution at which *Hox* genes were recruited to the extra-embryonic compartment. Finally, the generation of a new genetic tool allowed me to perform genetic lineage-tracing analyses to help understanding the overall *Hoxa13* contribution to embryonic and extra-embryonic structures.

Chapter 2

Recruitment of 5'*Hoxa* genes in the allantois is essential for proper extra-embryonic function in placental mammals.

Martina Scotti and Marie Kmita *

Laboratory of Genetics and Development, Institut de Recherches Cliniques de Montréal (IRCM), 110 avenue des Pins Ouest, H2W1R7, Université de Montréal, Montréal Québec, Canada.

At the time of the submission of this thesis this manuscript has been accepted for publication in Development (DEVELOP/2011/075408 Vol: 139 Issue: 04).

* Corresponding author: Marie Kmita

2.1 Author contribution:

I personnaly performed all the experiments described in this study and realized all figures. The manuscript was written by Dr. Marie Kmita.

2.2 Abstract:

The *Hox* gene family is well known for its functions in establishing morphological diversity along the anterior-posterior axis of developing embryos. In mammals, one of these genes, namely *Hoxa13*, is critical for embryonic survival as its function is required for the proper expansion of the fetal vasculature in the placenta. Thus it appears that the developmental strategy specific to placental mammals is linked, at least in part, to the recruitment of *Hoxa13* function in developing extra-embryonic tissues. Yet, the mechanism underlying this extra-embryonic recruitment is unknown. Here we provide evidence that this functional novelty is not exclusive to *Hoxa13* but shared with its neighboring *Hoxa11* and *Hoxa10* genes. We show that the extra-embryonic function of these three *Hoxa* genes stems from their specific expression in the allantois, an extra-embryonic hallmark of amniote vertebrates. Interestingly, *Hoxa10-13* expression in the allantois is conserved in chick embryos, which are non-placental amniotes, suggesting that the extra-embryonic recruitment of *Hoxa10, Hoxa11* and *Hoxa13* most likely arose in amniotes, i.e. prior to the emergence of placental mammals. Finally, using a series of targeted recombination and transgenic assays, we provide evidence that the regulatory mechanism underlying *Hoxa* expression in the allantois is extremely complex and relies on several *cis*-regulatory sequences.

2.3 Introduction :

The *Hox* gene family is well known for its major role, conserved throughout the animal kingdom, in the establishment of the body architecture during embryogenesis (Kmita and Duboule, 2003; Krumlauf, 1994; Young and Deschamps, 2009). In addition to this ancestral function, *Hox* genes have been recruited in the course of evolution to achieve a variety of different functions, including the morphogenesis of evolutionarily novel structures (Pearson et al., 2005). The genome of most vertebrates contains 39 *Hox* genes physically grouped into four clusters, referred to as *HoxA, HoxB*, *HoxC* and *HoxD* clusters. Individual inactivation of the various *Hox* genes revealed that *Hoxa13* is the only member of this gene family required for embryonic survival (Fromental-Ramain et al., 1996b; Shaut et al., 2008; Stadler et al., 2001). Accordingly, mutants carrying deletion of the *HoxB, HoxC* or *HoxD* cluster are viable, at least until birth (Medina-Martinez et al., 2000; Spitz et al., 2001; Suemori and Noguchi, 2000). The lethality of *Hoxa13*-/- embryos is due to impaired expansion of the fetal vasculature in the placental labyrinth, which precludes adequate exchanges between maternal and fetal blood to ensure embryonic survival (Shaut et al., 2008). Thus, at least in mice, the function of *Hoxa13* is not restricted to the embryo proper. Importantly, it also suggests that the function of *Hoxa13* may have played a critical role in the emergence of the developmental strategy characterizing placental mammals. In this study we have addressed two key questions relevant to this role: how *Hoxa13* has been

recruited in the extra-embryonic compartment and is this recruitment restricted to placental vertebrates?

We present evidence that *Hoxa10* and *Hoxa11*, the closest neighboring genes to *Hoxa13*, also contributes to the proper formation of the labyrinthine vasculature indicating that extra-embryonic recruitment is not restricted to *Hoxa13*. We show that the extra-embryonic function of these *5'Hoxa* genes is linked to their expression in the allantois, a mesoderm derivative of the posterior primitive streak and hallmark of amniote embryos (Downs, 2009). Interestingly, we found that *5'Hoxa* genes are also expressed in the allantois of a non-placental amniote suggesting that the extra-embryonic recruitment of 5'*Hoxa* genes predates the emergence of placental vertebrates. Finally, our work reveals a specific transcriptional control underlying 5'*Hoxa* extra-embryonic expression and we propose that the emergence of the reproductive strategy of placental species was tightly linked to the evolution of *Hoxa* gene regulation.

2.4 Results:

2.4.1 *Hoxa10* and *Hoxa11* together with *Hoxa13* contribute to the development of the labyrinthine vasculature.

Inactivation of individual *Hox* genes in mice has revealed that *Hoxa13* is the only member whose function is required for embryonic survival (Fromental-Ramain et al., 1996b; Shaut et al., 2008). Unexpectedly, while live *Hoxa13*-/- embryos can be recovered

at embryonic day (e) 14.5 (Fromental-Ramain et al., 1996b; Shaut et al., 2008), we found that embryos homozygous for the deletion of the entire *HoxA* cluster (referred to as *HoxAdel/del* hereafter) do not survive later than e12. As mid-gestation lethality is typically related to cardio-vascular and/or placental defects (Copp, 1995) and mortality of *Hoxa13*-/- embryos is associated with placental dysfunction (Shaut et al., 2008), we hypothesized that the early lethality of *HoxAdel/del* mutants is the consequence of an exacerbated placental defect as compared to the single *Hoxa13* inactivation. Consistent with this assumption, abnormal placental morphology and marked reduction of the endothelium within the labyrinth is observed in all e10.5 *HoxAdel/del* placentas analyzed (Fig. 2.1), while *Hoxa13*-/- placenta remains undistinguishable from wild type specimens until e11.5 (Shaut et al., 2008). Previous studies identified the requirement of *Hoxa10* and *Hoxa11* for the proper function of the uterus (Benson et al., 1996; Gendron et al., 1997; Satokata et al., 1995) raising the possibility that the more severe phenotype of *HoxAdel/del* placenta could be due to a combination of loss of *Hoxa13* function in the labyrinth and reduced *HoxA* dosage in the mother's uterus. However, epiblast-specific conditional inactivation of the *HoxA* cluster, using the *HoxAflox* mice (Kmita et al., 2005) and the *mox2Cre* deleter strain (Tallquist and Soriano, 2000), resulted in the same placental phenotype as *HoxAdel/del* mutants (not shown) indicating that this phenotype is due to the loss of *Hoxa* genes in epiblast derivatives.

The vasculature of the labyrinth originates from the allantois (Inman and Downs, 2007; Rossant and Cross, 2001), a mesoderm derivative of the posterior primitive streak (Downs et al., 2004; Kinder et al., 1999; Lawson, 1999). Allantoic vascularization occurs *de novo* similarly to the embryo and yolk sac vascularization (Downs et al., 1998; Drake and Fleming, 2000). Following the beginning of vasculogenesis, the distal tip of the allantois fuses to the chorion and subsequent expansion of the distal allantoic vascular plexus within the chorionic plate gives rise to the fetal vasculature of the labyrinth (Inman and Downs, 2007; Rossant and Cross, 2001). To establish which *Hoxa* genes are involved in the development of the labyrinthine vasculature, we analyzed the expression of all *Hoxa* genes starting at allantoic bud-stage (e.7.5). As shown in figure 2.2, *Hoxa13* is expressed in the allantois together with its closest neighbors, *Hoxa10* and *Hoxa11,* both prior to and after chorio-allantoic fusion. Unexpectedly, this co-expression is transient and by e9.5 the extra-embryonic expression of *Hoxa10* and *Hoxa11* is only detected in the maternal part (decidua) and not in the labyrinth (Fig.2.2 and Fig. S2.1).

2.4.2 5'*Hoxa* genes are expressed in progenitors of the labyrinthine vasculature.

The early and transient co-expression of *5'Hoxa* genes suggests that the precocious vascular defect in *HoxAdel/del* placenta, when compared to the single *Hoxa13* loss of function, is due to the combined 5'*Hoxa* inactivation in the allantois and/or nascent chorio-allantoic interface. However, at the stage of chorio-allantois fusion, there is no apparent

reduction of the endothelial cell population in *HoxAdel/del* allantois (Fig. S2.2), thereby excluding impaired endothelial differentiation and/or expansion in the allantois as a cause for the labyrinthine phenotype. In turn, this result raises the possibility that 5'*Hoxa* expression actually occurs in progenitor cells of the labyrinthine vasculature but its functional outcome is only detectable at later stages of labyrinth development. In an attempt to clarify this issue, we investigated the fate of the allantoic cells expressing these genes. For this purpose, we used a mouse line driving expression of the Cre recombinase in all cells in which *Hoxa13* is normally expressed such that, in presence of a Cre reporter transgene, *Hoxa13*-expressing cells and their descendants permanently express the reporter transgene. As genetic fate mapping is a three step-process (activation of *Cre* transcription, recombination of the reporter transgene and synthesis of the reporter protein), we first established the delay existing between *Cre* transcriptional activation (i.e. *Hoxa13* activation) and the actual expression of the reporter protein. We found that the reporter protein is detectable 20-24h after the initial *Cre* transcription (not shown). To verify that the *Hoxa13Cre* allele is functional in all cells normally expressing *Hoxa13*, we first looked at *Cre*-reporter expression in developing limbs, where *Hoxa13* has been extensively studied and where, as in the allantois, its transcriptional activation occurs in mesenchymal cells. One day after *Hoxa13* transcriptional activation, Cre reporter expression is found in all mesenchymal cells of distal limb buds (Fig. S2.3A-B), providing evidence that our *Hoxa13Cre* allele is an efficient tool for tracing the fate of *Hoxa13*-expressing cells.

In the allantois, reporter expression is first detected at e8.25 (Fig. 2.3B), consistent with the delay existing between *Cre* transcriptional activation and Cre-mediated recombination, such that reporter expression at e8.25-8.5 highlights the fate of the first *Hoxa13* expressing cells and their progeny (referred to as Hoxa13lin+ cells hereafter). Interestingly, while *Hoxa13* is predominantly expressed in the proximal domain of the allantois at e7.5 (Fig. 2.3A), at e8.25-8.5 a large proportion of Hoxa13lin+ cells are located at the chorio-allantoic interface/nascent labyrinth and only few Hoxa13lin+ cells are found in the proximal allantois (Fig. 2.3B). This early fate-map indicates that a significant subset of cells in which *Hoxa13* is initially activated contributes to the formation of the labyrinth. Surprisingly, at e8.5, virtually none of theses cells are of endothelial identity as revealed by co-immunostaining for the platelet endothelial cell adhesion molecule 1 (PECAM-1 also known as CD31, Fig. 2.3C-E). However, the proportion of Hoxa13lin+ cells expressing the endothelial marker CD31 (Hoxa13lin+/CD31+) increases progressively during embryogenesis (Fig. 2.4) and at late gestation, all Hoxa13lin+ cells are part of the fetal vasculature in the labyrinth, forming the labyrinthine endothelium as well as vascular smooth muscles that surround larger blood vessels at the base of the labyrinth (Fig. 2.4 and not shown). Consistent with the pool of Hoxa13lin-/CD31+ cells in the nascent labyrinth and undetectable *Hoxa13* expression beyond e9, the endothelium in the mature labyrinth is formed of both Hoxa13lin positive and negative cells (Fig. S 2.3C-E). In marked contrast, the endothelium of the mature umbilical cord is completely deprived of Hoxa13lin+ cells, which are found exclusively adjacent to the endothelium and forming vascular smooth

muscles (Fig. 2.4J-L). Together these results show that endothelial differentiation of Hoxa13lin+ cells takes place exclusively in the labyrinth and suggest that the ultimate fate of this cell population is influenced by extrinsic factors. However, *Hoxa13* appears dispensable for endothelial differentiation as the fate map of *Hoxa13*-expressing cells in absence of Hoxa13 protein shows that Hoxa13lin+ cell population is reduced but remains capable of differentiating into endothelial cells (Fig. S2.4)

2.4.3 Expression of 5'*Hoxa* genes in the allantois is required for embryonic survival.

Our fate map and in situ data suggest that 5'*Hoxa* function in proper expansion of the labyrinthine endothelium is associated with their expression in endothelial cell progenitors initially located in the allantois. As a consequence, gene inactivation after e8.5 should have little or no effect on the development of the labyrinthine vasculature. To identify the temporal requirement of 5'*Hoxa* function, we took advantage of the spatial and temporal specificity of the *Hoxa13Cre* allele. Since *Hoxa13* coding sequence is disrupted in the *Hoxa13Cre* allele, we generated *Hoxa13Cre/HoxAflox* mutants in which *Hoxa13* inactivation occurs in all cells normally expressing *Hoxa13* but with the 20 to 24h delay inherent to the Cre-mediated recombination. We found that *Hoxa13Cre/HoxAflox* mutants are fully viable and accordingly the vasculature of *Hoxa13Cre/HoxAflox* labyrinth is undistinguishable from that of wild type specimens (Fig. 2.5A-C). This conditional inactivation has a drastically distinct effect on limb development, during which *Hoxa13*

expression is detectable over several days. Indeed, *Hoxa13Cre/HoxAflox* mice exhibit limb defects (Fig. 2.5D-E) reminiscent of the phenotype associated with complete *Hoxa13* inactivation (Perez et al., 2010), thereby demonstrating the efficiency of *Hoxa13Cre*-mediated inactivation of the *HoxAflox* allele. Together, these results provide evidence that transient *Hoxa13* expression in the allantois is sufficient to ensure proper vasculature development in *Hoxa13Cre/HoxAflox* labyrinth and survival of the embryo. Thus, expression of *Hoxa13* in the allantois up to chorio-allantoic fusion stage is key for proper function of the placental labyrinth.

2.4.4 Extra-embryonic recruitment of 5'*Hoxa* genes is specific to the allantois and is not restricted to placental mammals.

The placental phenotype of both *Hoxa13-/-* and *HoxAdel/del* mutants (Shaut et al., 2008; this study) provides evidence that 5'*Hoxa* genes play a key role in the proper formation of the labyrinthine vasculature. In contrast, the vasculature in mutant and wild type yolk sacs is indistinguishable (Fig. S 2.5A-D). Accordingly, analysis of *Hoxa13Cre/+; Rosa26R* conceptus shows that Hoxa13lin+ cells do not contribute to the formation of the yolk sac (Fig. S 2.5E), thus indicating that the extra-embryonic recruitment of *Hoxa* genes is specific to the allantois and its derivatives. Since the allantois is an extra-embryonic hallmark of amniote vertebrates, the recruitment of 5'*Hoxa* genes in this tissue could have arisen prior to the emergence of placental species. To test this possibility, we investigated *Hoxa* expression in chick embryos. In this non-placental amniote, 5'*Hoxa* genes are also

specifically expressed in the allantois (Fig. 2.6A) indicating that extra-embryonic recruitment of 5'*Hoxa* genes is not restricted to placental species. Previous studies revealed that the allantois is a mesoderm derivative of the posterior primitive streak that buds and extends into the exocoelom (Downs et al., 2004; Kinder et al., 1999; Lawson, 1999). Knowing that vertebrate *Hox* genes are activated in epiblast cells prior to ingression through the primitive streak (Iimura and Pourquie, 2006), the possibility exists that the extra-embryonic expression of 5'*Hoxa* genes is a mere collateral effect of the emergence of the allantois, i.e activation of *5'Hoxa* genes in the epiblast prior to formation of the epiblast-derived "appendage" into the exocoelom. However, at early stages, Hoxa13lin+cells are located exclusively in the extra-embryonic compartment (Fig. 2.4A) indicating that the initial activation of 5'*Hoxa* genes occurs in epiblast-derived cells only once these cells are already engaged in the extra-embryonic fate. This specificity suggests that the activation of 5'*Hoxa* genes in the allantois is most likely independent of the mechanism underlying initial *Hox* activation in the embryo proper.

2.4.5 The transcriptional control of 5'*Hoxa* genes in the allantois involves an enhancer-sharing mechanism.

To gain insights into the mechanism underlying the recruitment of 5'*Hoxa* genes in the allantois, we next investigated whether it is linked to particular features of 5'*Hoxa* promoters or associated with an enhancer-sharing mechanism. To address this issue, we first investigated the expression of the transgene located at the 5'end of the *HoxA* cluster in

HoxAflox embryos. This transgene, located 3.5kb away from *Hoxa13*, contains the housekeeping phosphoglycerate kinase-1 (PGK) promoter, previously shown to respond to enhancer activity spanning the transgene insertion site (Herault et al., 1999). When randomly inserted or targeted at the 5' end of the *HoxD* cluster, this promoter has no detectable activity in the allantois (Kmita et al., 2000b). In contrast, when targeted to the 5' end of the *HoxA* cluster, it becomes robustly expressed in the allantois (Fig. 2.6C) revealing the existence of an "allantois" enhancer whose activity is shared between neighboring genes. Interestingly, this locus-specific expression persists in absence of the *HoxA* cluster (Fig. 2.6D) suggesting that the enhancer is located outside the *HoxA* cluster. Yet, *Evx1*, the closest 5'*Hoxa* neighboring gene outside the *HoxA* cluster, is not expressed in the allantois (Fig. 2.6E), raising the possibility that the "allantois" enhancer is located within the *Hoxa13-Evx1* intergenic region but in the vicinity of *Hoxa13*. To test this hypothesis, we first generated transgenic mice carrying this 50kb region linked to the *lacZ* reporter gene (*IR50* in Fig. 2.6F). Out of five independent lines, one fails to express the reporter but the four other lines show *lacZ* expression in the allantois as well as chorio-allantoic interface at e8.5 (Fig. 2.6F). Interestingly, at e9, the transgene is not expressed in the labyrinth and becomes downregulated in the allantois (Fig. 2.6F and not shown), reminiscent of the 5'*Hoxa* expression pattern. Together these results show that the *Hoxa13-Evx1* intergenic region contains a regulatory element capable of activating gene expression in the allantois. To test whether this element is necessary and sufficient to drive the expression of 5'*Hoxa* genes in the allantois, we next analyzed the impact of deleting the endogenous *Hoxa13-*

Evx1 intergenic region. Unexpectedly, expression of 5'*Hoxa* genes and the PGK-transgene remain detectable in the allantois of homozygous embryos carrying this deletion (Del5, Fig. 2.7) indicating the existence of additional regulatory element(s) underlying 5'*Hoxa* expression in the allantois. Accordingly, Del5 homozygous embryos survive until birth.

The presence of a transcriptional enhancer in the *Hoxa13-Evx1* intergenic region raises the possibility that the recruitment of 5'*Hoxa* genes in the allantois originates from the appearance of an evolutionary novel transcriptional regulatory element. Alternatively, this element could have been already functional in another tissue prior the emergence of amniotes and the presence of appropriate transcription factors in the allantois resulted in its functional co-option therein. Analysis of our IR50 transgenic lines shows that the *Hoxa13-Evx1* intergenic region triggers also reporter gene expression in the tail bud and developing limbs (Fig. S 2.6, top), two domains where 5'*Hoxa* genes are expressed. In an attempt to assess whether these expression domains rely on distinct or shared regulatory elements, we subdivided the 50kb intergenic region into smaller DNA fragments, each one linked to the *lacZ* reporter gene driven by the *b-globin* minimal promoter (referred to as *b-lacZ*). To avoid variations in transgene expression due to position effects, each transgene was flanked with the H19 insulator sequence. We generated 12 distinct transgenes (named "a" to "l" in Fig. S 2.6) and for each of them, we analyzed at least five transgenic embryos at e8.5 and at least three at e12.5 (see supplementary table 1). At e12.5, four of these transgenes trigger *lacZ* expression (Fig. S 2.6, transgenes # c, f, g and l). Three of them show staining in limbs (Fig. S 2.6, #c, f, g) that recapitulates partially the IR50 expression pattern. We next

analyzed these transgenes at e8.5 and did not detect any b-Gal staining, except for embryos carrying the transgene "l", in which staining is observed in the midbrain (not shown). These results suggest that regulatory elements capable of triggering gene expression in limbs are not functional in the allantois. We then tested expression of the eight other transgenes at e8.5 but strikingly none of them shows expression in the allantois or tail bud. Consistent with the lack of tail bud expression at e8.5, none of the e12.5 transgenic embryos express the *lacZ* reporter in the developing tail (Fig. S 2.6). Together these results show that, while the entire *Hoxa13-Evx1* intergenic region results in reporter expression in the allantois, tail bud and developing limbs, sub-domains of this DNA fragment are only able to trigger reporter expression in limb buds when assayed individually.

2.5 Discussion.

The embryonic lethality resulting from impaired vascular development in the labyrinth of *Hoxa13* mutant revealed that in mice, and possibly other vertebrate species, the function of *Hox* genes is not restricted to the embryo proper. This discovery raises the question of the evolutionary history underlying the extra-embryonic recruitment of *Hoxa13*. In this study, we used a combination of targeted genomic rearrangements, transgenesis and genetic fate mapping to gain insights into the transcriptional regulation underlying *Hoxa13* function in the placental labyrinth. The expression data, genetic fate mapping and conditional gene inactivation presented here further reveal that the primary extra-embryonic function of *Hoxa13* relies on its expression in a subset of cells forming the allantois, well

before defects in the labyrinthine vasculature are detectable in *Hoxa13*-/- mutant. Interestingly, *Cdx* function in labyrinth development also relies on their expression in endothelial progenitors in the allantois (van Nes et al., 2006; Young et al., 2009) and reduced *Cdx* dosage results in a phenotype similar to that of *HoxAdel/del* labyrinth. Such similarity between *Cdx* and *Hox* mutants is consistent with the role of Cdx proteins as regulators of *Hox* genes, as illustrated for some *Hox* genes during anterior-posterior patterning of the axial skeleton (reviewed in e.g (Young and Deschamps, 2009) and suggests that the role of *Cdx* genes in proper labyrinth formation is mediated, at least in part, by *Hox* genes. While the allantois contains progenitor cells of both labyrinthine and umbilical cord endothelium, those expressing *Hoxa13* do not contribute to the umbilical cord endothelium. This specificity could be explained by a cell non-autonomous effect, whereby signaling from trophoblast cells would be required for endothelial differentiation of *Hoxa13*-expressing cells and their descendants. Consistent with this hypothesis, evidence has been obtained that cross-talks between trophoblast and allantois cells play a key role in the development of the fetal vasculature in the labyrinth (Rossant and Cross, 2001). Noteworthy, recent analysis of the fate map of *Tbx4*-expressing cells provided evidence for a key role of peri-vascular cells during vasculogenesis in the allantois (Naiche et al., 2011). However, in contrast to *Tbx4* (Naiche and Papaioannou, 2003), *Hoxa13* is dispensable for endothelial differentiation. Instead our fate map shows reduced Hoxa13lin+ cell population in *Hoxa13*-/- labyrinth, consistent with decreased expansion of the endothelial network.

The downregulation of *Tie2, Foxf1* and *autotaxin (Enpp2),* which are *Hoxa13* target genes (McCabe and Innis, 2005; Shaut et al., 2008), was proposed to account for the reduced fetal vasculature in *Hoxa13*-/- labyrinth (Shaut et al., 2008). The function *autotaxin* and *Foxf1* is actually required in the allantois where their inactivation prevents chorio-allantoic fusion and *de novo* vasculogenesis (Mahlapuu et al., 2001; van Meeteren et al., 2006). Our finding that cells forming the endothelium of the allantois/umbilical cord originate from cells in which *Hoxa13* is never expressed thus provides an explanation for proper formation of the endothelium in *Hoxa13*-/- allantois/umbilical cord. Nonetheless, this does not exclude that down-regulation of *autotaxin* and/or *Foxf1* in *Hoxa13*-expressing cells affects the development of the labyrinthine vasculature. Understanding the respective role of *autotaxin*, *Foxf1* and *Tie2* in *Hoxa13*-/- labyrinth phenotype will require their conditional inactivation in *Hoxa13*-expressing cells.

Although endothelial cells in the allantois do not express *Hoxa13*, analysis of the *Hoxa13Cre/HoxAflox* mutant shows that the slight delay inherent to the Cre-mediated gene deletion is sufficient to ensure proper expansion of the fetal vasculature in the labyrinth and thus, embryonic survival. This result suggests that *Hoxa13* expression in the allantois is critical for subsequent development of the labyrinthine vasculature and is consistent with our *in situ* hybridization analysis showing that *Hoxa13* as well as *Hoxa10* and *Hoxa11*

expression is only detectable until e9. The discrepancy between our expression data and that reported previously by Shaut et al. (2008) likely results from the difference in the experimental approach chosen. Indeed, while we used whole-mount *in situ* to visualize *Hoxa13* transcripts, Shaut et al. analyzed the fluorescence of the *Hoxa13-GFP* allele, i.e. the protein produced by this targeted allele. Nevertheless, proper labyrinth development in our conditional mutant, together with the genetic fate map of *Hoxa13*-expressing cells and *in situ* data, indicates that the primary function of *Hoxa13* in the extra-embryonic compartment relies on its early expression in the allantois. As a consequence, implementation of the mechanism underlying *Hoxa13* transcriptional activation in the allantois was likely critical for species requiring the function of a chorio-allantoic placenta to ensure embryonic survival. Our analysis also shows that *Hoxa10* and *Hoxa11* are co-expressed with *Hoxa13* in the allantois indicating that extra-embryonic recruitment was not restricted to *Hoxa13*. Analysis of several targeted rearrangements within and outside the *HoxA* cluster reveals that the mechanism underlying expression of these 5'*Hoxa* genes in the allantois involves at least two transcriptional enhancers, one of which is located within the 50 kb *Hoxa13-Evx1* intergenic region. Surprisingly, subdivision of this intergenic region into smaller DNA fragments failed to recapitulate reporter gene expression in the allantois. Similar result was obtained for the tail bud/trunk expression. In contrast, three of these overlapping transgenes were able to drive reporter expression in developing limbs, which recapitulates the limb enhancer activity of the entire 50 kb region (IR50 transgene), thereby establishing that allantois and tail bud expression rely on *cis*-regulatory sequences

distinct from those driving expression in limbs. Loss of reporter expression in the allantois and tail bud upon fractioning of the *Hoxa13-Evx1* intergenic region raises the possibility that both expression patterns could rely on the same regulatory sequences. In this view, the extra-embryonic recruitment of 5'*Hoxa* genes could be the consequence of the functional co-option of the tail bud enhancer in the allantois, both tissues being epiblast derivatives. However, in contrast to the IR50 transgene, 5'*Hoxa* genes are expressed in the allantois but not in the tail bud, at least up to e8.5. Thus, if expression of the IR50 transgene is driven by the same regulatory sequences in allantois and tail bud, absence of 5'*Hoxa* expression in the tail bud implies the existence of a repression mechanism preventing activation of the 5'*Hoxa* genes in this tissue, consistent with the recent finding that precocious expression of 5'*Hox* genes in the tail bud is detrimental for the posterior elongation of mice embryos (Young et al., 2009). Nonetheless, the fact that allantois expression could not be triggered using fragments of the *Hoxa13-Evx1* intergenic region suggests that integrity of the latter 50kb region is required to drive reporter expression in the allantois. It is widely accepted that long distance enhancer-promoter interaction involves chromatin looping. In this view, it is possible that both allantois and tail bud enhancers located in the *Hoxa13-Evx1* intergenic region require a defined three-dimensional chromatin organization to establish proper contacts with their target promoters. As a consequence, fractioning of the intergenic region would result in loss of proper chromatin organization while the distance between the enhancer and the minimal promoter of the reporter might be too large to ensure efficient transcriptional activation without chromatin looping. Consistent with this hypothesis,

analysis of *Hoxd* genes' regulation in developing limbs revealed that the underlying control is extremely complex and cannot be easily assessed through the analysis of simple reporter transgenes (Tschopp and Duboule, 2011).

Although, it remains to be established whether the recruitment of 5'*Hoxa* function in the allantois was elicited by the co-option of tail bud enhancer(s) or the implementation of evolutionary novel cis-regulatory sequences, *Hoxa13*-/- and *HoxAdel/del* placental phenotypes suggest that 5'*Hoxa* expression in the allantois is vital for the survival of mouse embryos and most probably for other placental species. Expression analysis in the allantois of chick embryos, which are non-placental amniotes, suggests that 5'*Hoxa* extra-embryonic recruitment likely occurred in amniotes, prior to the emergence of placental animals. It is thus likely that recruitment of *5'Hoxa* genes in the allantois has subsequently played a key role in the implementation of the developmental strategy that characterizes placental species. It will be of particular interest to investigate whether the regulatory mechanism controlling 5'*Hoxa* expression in the allantois is conserved between placental and non-placental amniotes or whether it has evolved concomitantly with the emergence of placental species.

2.6 Materials and Methods.

2.6.1 Mouse strains.

HoxAflox, Hoxa13null, *Rosa26*R, *mT/mG, mox2Cre* and *CMV:Cre* lines were previously described (Dupe et al., 1997; Fromental-Ramain et al., 1996b; Kmita et al., 2005; Muzumdar et al., 2007; Soriano, 1999; Tallquist and Soriano, 2000). The *HoxAdel* line was generated by crossing *HoxAflox* mice with *CMV:Cre* partners. The TAMERE approach (Herault et al., 1998) was used to generate *HoxAdelneo* and *del(5')* mutants (Kmita and Duboule, unpublished). *HoxAdelneo* was obtained from meiotic recombination of the *HoxAflox* allele and *del(5')* from meiotic recombination between the *Evx1flox* (Goldman and Martin, unpublished) and *HoxAflox* alleles. In the *Hoxa13Cre* allele, *Hoxa13* first exon is replaced with the *Cre:IRES:Venus* cassette (Scotti and Kmita, in preparation). The *IR50* transgene was generated using the recombineering technique (Copeland et al., 2001). a-l transgenes carry the chicken βglobin minimal promoter and a LacZΔCpG NLS reporter. H19 insulators are located at both extremities of the transgenes. All transgenic embryos were generated by pronuclear injection.

2.6.2 In Situ Hybridization, Immunohystochemistry and X-gal staining.

Whole mount in situ hybridizations were carried out using standard procedures (Kondo et al., 1998b; Nieto et al., 1996). Chicken probes are as previously described (Burke et al., 1995). Mouse *Hoxa1* and *Hoxa13* probes are described in (Dupe et al., 1997) and (Warot et al., 1997). Probe templates for *Hoxa2, Hoxa3, Hoxa4, Hoxa5*, *Hoxa7*, *Hoxa9, Hoxa10* and *Hoxa11* were provided by, respectively, J. Deschamps, C. Fromental-Ramain et B. Tarchini. The *hygromycine* probe was generated using the 600bp EcoRI-HincII coding sequence.

Immunohistochemistry was carried out on 10-12 mm cryosections according to standard procedures or on whole-mount specimens as previously described (Gregoire and Kmita, 2008). Antibodies against CD31 (BD Bioscences 1: 100) and beta-galactosidase (Cappel 1:1000) were used. The *mT/mG* Cre reporter allele expresses GFP at the cell membrane and thus direct GFP fluorescence was used for co-localization with CD31, which is also expressed at the cell membrane. X-gal staining on embryos and placentas was carried out as described in (Downs and Harmann, 1997) and according to (Zakany et al., 1988) for older specimens. Immunostaining on sections were imaged using ZEISS LSM710 confocal microscope. For all analyses of placenta sections, we used only sections that encompassed the junction with the allantois/umbilical cord to ensure accurate comparison

of the various placenta specimens. For each genotype and stage, analyses were performed on a minimum of three placentas.

2.7 Acknowledgments.

We are grateful to Annie Dumouchel, Mark Cwajna and TongYu Wang for technical help, Basile Tarchini for assistance in cloning procedures and sharing reagents and members of the lab for insightful discussion. We thank Qinzhang Zhu and Li Lian for ES cell and transgene injections. We are particularly grateful to Denis Duboule for sharing mice and Gail Martin and Devorah Goldman for providing the *Evx1flox* mouse. Recombineering material was kindly provided by Neal Copeland and Nancy Jenkins and the Venus/PCS2 vector was obtained from Atsushi Miyawaki. We thank Karen Downs for precious comments on our results and Jacqueline Deschamps, Artur Kania, Rolf Zeller and Aimée Zuniga for critical reading of the manuscript. This work was supported by the Canadian Institute of Health Research (CIHR-82880) and the Canada Research Chair program (to MK). MS was supported by a PhD fellowship from the Molecular Biology program of the University of Montreal.

2.8 Legends to figures.

Figure 2.1 Deletion of the *HoxA* cluster leads to impaired vasculature in the placental labyrinth.

Histology of wild type (**A**) and mutant (**B**) placentas at e10.5 as revealed by hematoxylin and eosin staining on paraffin sections. At high magnification (**C-D**), the mutant labyrinth appears more compact, likely as a consequence of reduced fetal vasculature (**D**). (**E-F**) Whole mount CD31 immunostaining labelling the vascular endothelium of wild type (**E**) and *HoxAdel/del* (**F**) hemi-placentas at e10.5. (**G, H**) Magnifications of boxed areas in (**E, F**). In the wild type placenta, the vasculature expands into the entire labyrinth (**E**, **G**). In the mutant (**F**, **H**) large labyrinth regions are deprived of vasculature and characterized by absence of brown staining (**H**, black dotted lines delimit vasculature-deprived regions within the labyrinth). Immunohistochemical analysis of CD31 expression on cryosections of wild type (**I**) and mutant (**J**) placentas at e10.5 (n=11). Yellow arrows point to the large regions deprived of endothelial cells in the mutant labyrinth (**J**). In all panels white dotted lines mark the boundary between the labyrinthine region and the decidua. dec, decidua; lab, labyrinth. Scale bars 200 μm.

Figure 2.2 *Hoxa10*, *Hoxa11* and *Hoxa13* are the only members of the *HoxA* cluster expressed in the allantois.

Wild type expression patterns of *Hoxa* genes as revealed by whole mount *in situ* hybridization on e7.5 (top), e8.5 (middle) and e9.5 (bottom) conceptuses. At e7.5 and e8.5, only the most 5' located genes (*Hoxa10*, *Hoxa11* and *Hoxa13*) are expressed in the allantois (black arrows). Note that these genes are expressed prior genes located at more 3' positions. At e8.5, all *Hoxa* genes are transcriptionally activated, but none of the group 1 to 9 *Hoxa* genes are expressed in the allantois (white arrows). In contrast, 5'*Hoxa* expression in the allantois is barely, if at all, detectable in e9.5 allantois and there is no evidence for *Hoxa* expression in the labyrinth (bottom panel, dotted circles).

Figure 2.3: Initial expression of *Hoxa13* does not occur in endothelial cells of the allantoic vasculature.

(**B**) Whole mount X-gal staining *Hoxa13Cre/+;Rosa26R/+* conceptus at e8.5 reveals the fate of cells that have expressed *Hoxa13* at e7.5 (**A**). Note the significant proportion of *Hoxa13*lin+ cells at the chorio-allantoic interface. (**C-E**) Immunostaining on allantois cryosections showing that most of *Hoxa13*lin+ cells (green) do not express the endothelial cell marker CD31 (red) at e8.5. The *mT/mG* Cre reporter allele expresses GFP at the cell membrane and thus was used for co-localization with CD31, which is also

expressed at the cell membrane. Nuclei are labeled with DAPI (gray staining). Dotted lines in panel **B-E** highlight the limit between the allantois and chorionic plate. all, allantois. cho, chorionic plate. E, embryo. Scale bars 100 μm.

Figure 2.4: Hoxa13lin+ cells become progressively endothelial only in the labyrinth.

(**A**) beta-galactosidase activity reveals that Hoxa13lin+ cells is restricted to the allantois and placental labyrinth. (**B-D**) Co-immunostaining for Hoxa13lin+ cells and endothelial cells at e9.5. (**E**) Whole mount X-gal staining on e16.5 placenta. Immunostaining showing both *Hoxa13lin+* and endothelial cells in mature placental labyrinth (**F-H**) and umbilical cord (**J-L**) at e16.5. *mT/mG* Cre-reporter was used to mark Hoxa13lin+ cells such that both the reporter protein and CD31 signals are targeted to the cell membrane and allows unambiguous detection of protein co-localization (**D,** white arrows). Nuclei are labeled with DAPI (gray staining). (**I**) Percentage of Hoxa13lin+ signal co-localized with CD31+ signal at distinct stages of labyrinthine development. Scale bars 30 μm.

Figure 2.5: Delay in the induction of *Hoxa13* inactivation is sufficient to ensure proper development of the labyrinth and survival of the embryo.

(**A-C**) CD31 immunostaining on placenta cryosections at e14.5. *Hoxa13Cre/HoxAflox* labyrinthine vasculature (**B**) is comparable to wild type (**A**). (**D-E**) Forelimbs and hindlimbs of control (left, *HoxAflox/+*) and mutant (right, *Hoxa13Cre/HoxAflox*) mice at 6 months of age. Mutant limbs show a fully penetrant phenotype associated with the loss of *Hoxa13*, such as lack of digit 1 (white asterisk), shortening and malformation of the other digits in the forelimb and fusion of digit 2, 3 and 4 in the hindlimb (black arrows). Scale bars 200 μm.

Figure 2.6: Expression of *5'Hoxa* genes in chick allantois, and evidence for a shared allantois enhancer in mice.

(**A**) Whole mount *in situ* hybridization on chick embryos at stage HH18. *Hoxa13* and *Hoxa11* are expressed in the allantois (middle and right panels) but not *Hoxa9* (left panel), illustrating that 5'*Hoxa* expression in the allantois is not restricted to placental species. Schematic representation of the wild-type *HoxA* cluster (**B**) and alleles carrying rearrangements or deletions within the *HoxA* cluster (**C, D** and **E**). For each allele,

expression pattern for 5' *Hoxa* genes, *Evx1* or *PGK* transgenes is shown. (**B)**, Wild type expression of *Hoxa13*. (**C)**, The *PGK* promoter is activated in the allantois when inserted at the 5' end of the *HoxA* cluster (*HoxAflox* allele). (**D)**, The *PGK* transgene remains expressed in the allantois even in absence of the entire *HoxA* cluster (*HoxAdel*$^{neo+}$). (**E)**, *Evx1* expression remains excluded from the allantois even when the HoxA cluster is deleted (*HoxADel* allele). Wild-type expression of *Evx1* (black box). (**F)**, The IR50 transgene, containing the 50kb *Hoxa13-Evx1* intergenic region linked to the minimal promoter and lacZ reporter, is expressed in the allantois.

Figure 2.7: Deletion of the *Hoxa13-Evx1* intergenic region does not prevent *Hoxa10*, *Hoxa11* and *Hoxa13* expression in the allantois.

Whole mount *in situ* hybridization for *5'Hoxa* genes or PGK transgenes in *HoxAflox/flox* (top) and *Del(5')/Del(5')* embryos (bottom) at e8.5. These rearrangements in the vicinity of the *HoxA* cluster do not prevent 5' *Hoxa* expression in the allantois nor that of the PGK-transgene. Note that deletion of the 50kb *Hoxa13-Evx1* intergenic region (*Del5'*) does not interfere with 5'*Hoxa* expression in the tail bud. Arrows point to the allantois.

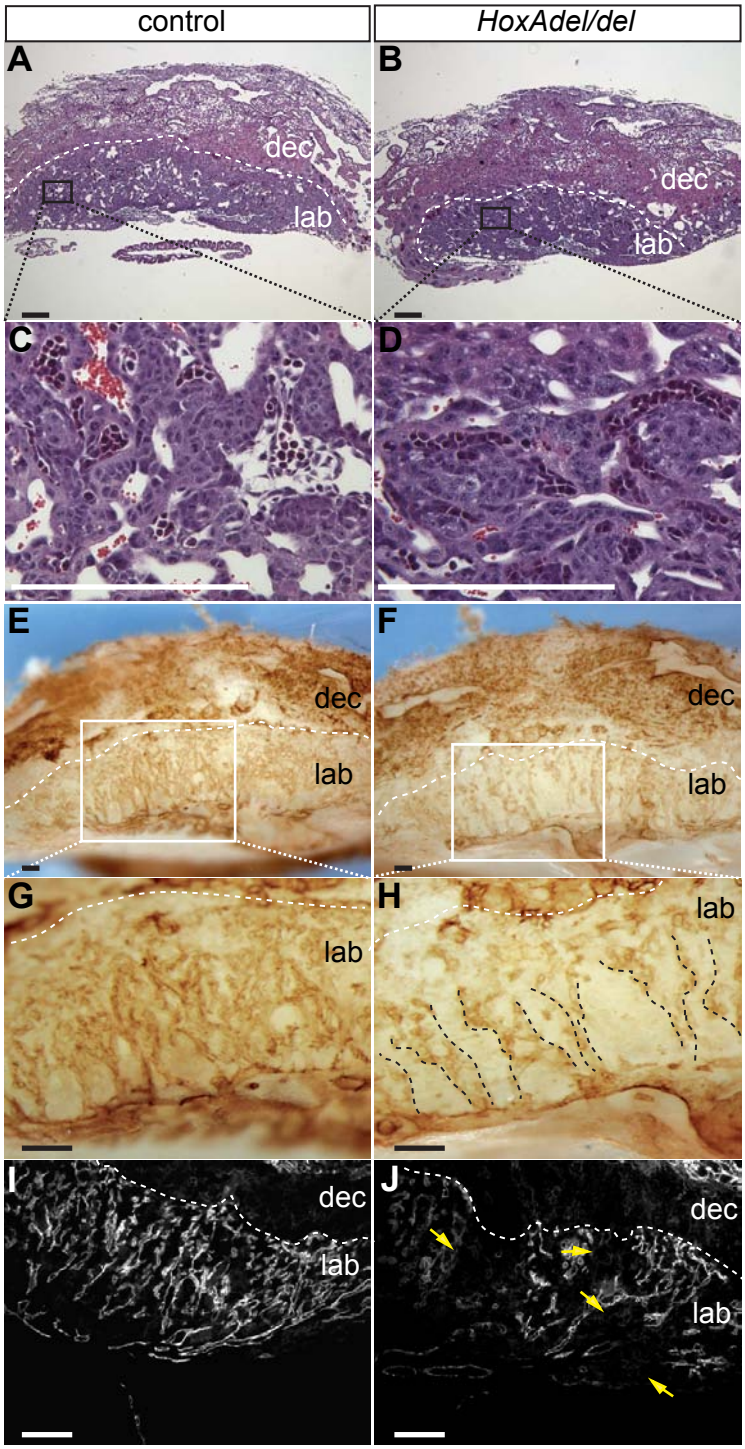

Figure 2.1 Deletion of the *HoxA* cluster leads to impaired vasculature in the placental labyrinth.

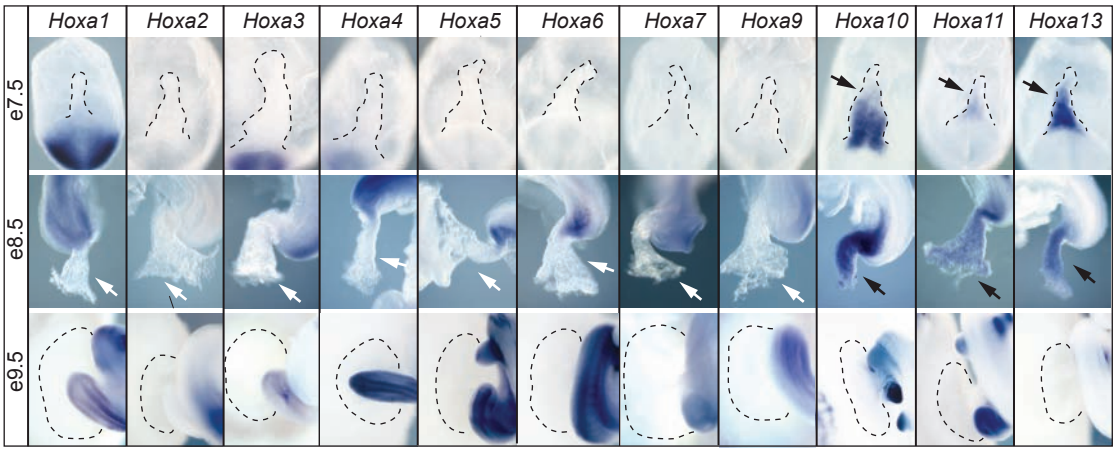

Figure 2.2 *Hoxa10, Hoxa11* and *Hoxa13* are the only members of the *HoxA* cluster expressed in the allantois.

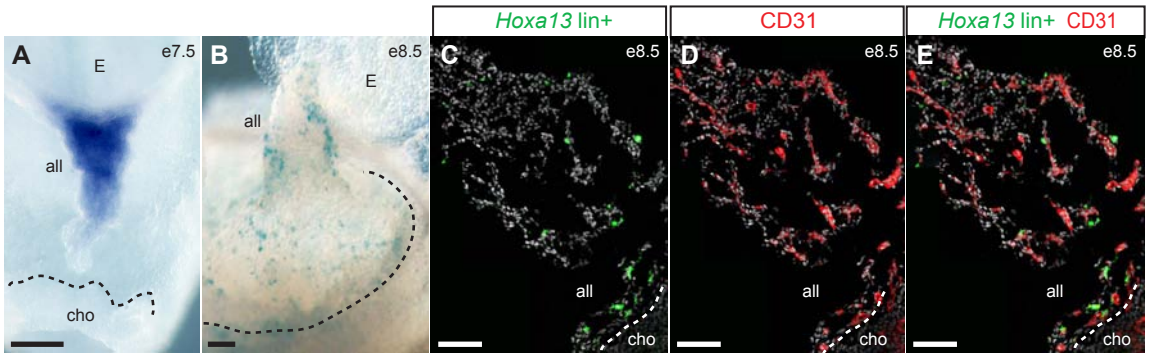

Figure 2.3 Initial expression of *Hoxa13* does not occur in endothelial cells of the allantoic vasculature.

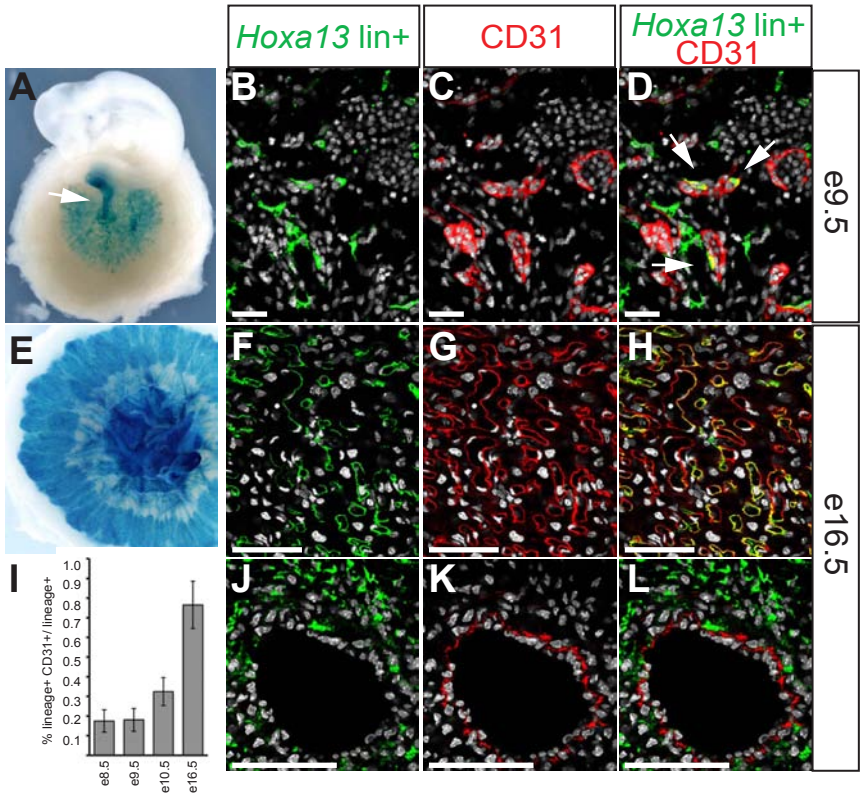

Figure 2.4 Hoxa13lin+ cells become progressively endothelial only in the labyrinth.

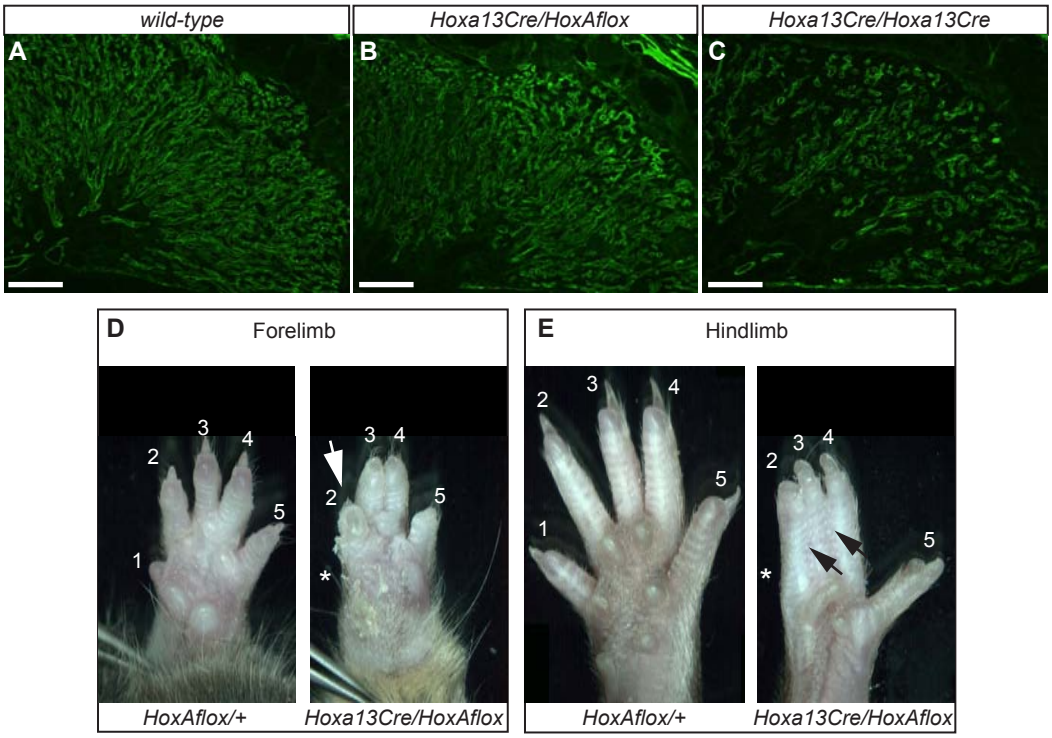

Figure 2.5 Delay in the induction of *Hoxa13* inactivation is sufficient to ensure proper development of the labyrinth and survival of the embryo.

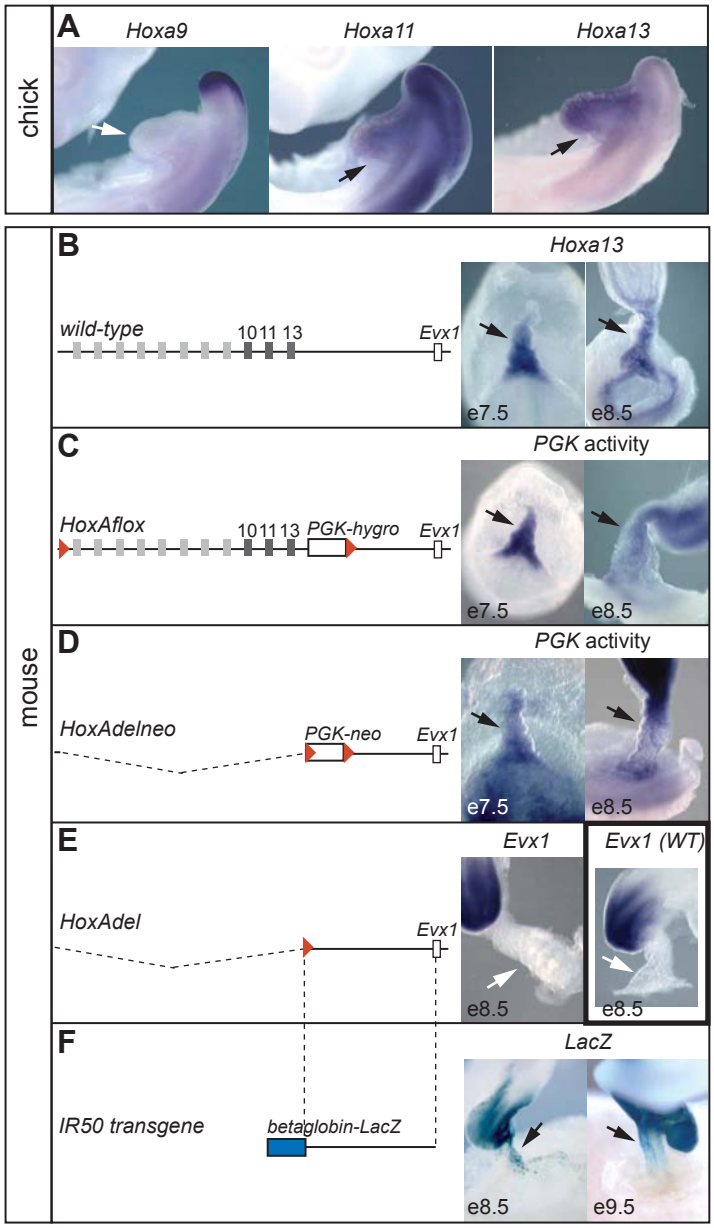

Figure 2.6 Expression of 5'*Hoxa* genes in chick allantois, and evidence for a shared allantois enhancer in mice.

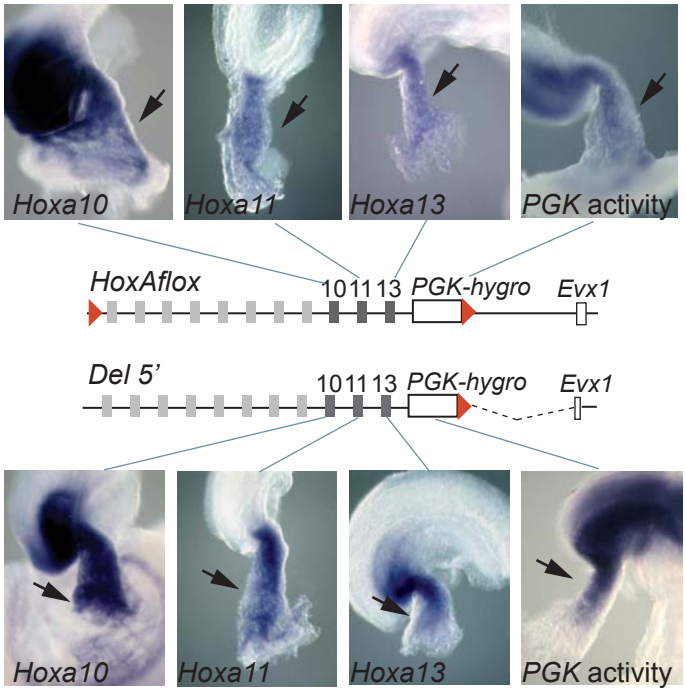

Figure 2.7 Deletion of the *Hoxa13-evx1* intergenic region does not prevent *Hoxa10*, *Hoxa11* and *Hoxa13* expression in the allantois.

2.9 Legends to supplementary figures.

Figure S 2.1 Expression of *Hoxa10* and *Hoxa11* is detected at early stages in the allantois, but is not maintained in the allantois-derived labyrinthine vasculature.

Wild type expression patterns of *Hoxa10* and *Hoxa11* at different stages of development as revealed by whole mount *in situ* hybridization. At e8.5 (**A,B**), 5'*Hoxa* genes expression is only detected in the allantois and is excluded from the chorionic plate (arrows). At e9.5 (**C,D**) , e10.5 (**E,F**) and e12.5 (**G,H)** 5'*Hoxa* genes are detected in the embryo proper and in the decidua, but not in the labyrinth. **F**, insert, whole mount *in situ* hybridization for *Hand1* showing expression in the labyrinth. The *Hand1* RNA probe was provided by A.Galli. E, embryo; lab, labyrinth; dec, decidua.

Figure S 2.2 Inactivation of *Hoxa* genes does not interfere with the formation of the primary vascular plexus within the allantois.

Whole mount CD31 immunostaining on control (**A,B**) and *HoxAdel/del* (**C,D**) allantois at 2 somite- (**A,C**) and 14 somite- (**B,D**) stage reveals the spatial distribution of endothelial cells. All allantois were imaged and photographed using a ZEISS LSM710 confocal microscope. prox, proximal; dist, distal; E, embryo. Scale bar 100 μm.

Figure S 2.3 The fetal vasculature of the mature labyrinth is formed of Hoxa13lin+ and Hoxa13lin- endothelial cells.

(**A,B**) *Hoxa13* lineage in distal forelimb buds of e11.5 *Hoxa13Cre/+; mT/mG* embryos illustrates that the *Hoxa13Cre* is an efficient tool to trace the fate of *Hoxa13* expressing cells. Hoxa13lin+ cells express the green fluorescent protein (mG) while cells in which there is no Cre-mediated recombination express Tomato (mT-red staining). The only cells expressing mT are ectodermal cells and blood cells, which do not express *Hoxa13*. (**C-E**) CD31 immunostaining on cryosections of e16.5 *Hoxa13Cre/+; mT/mG* labyrinth. Arrows point to capillaries formed of both Hoxa13lin+ and Hoxa13lin- cells. Few capillaries are only formed of Hoxa13lin- cells (compare **C** and **D**). Scale bar 35 μm.

Figure S 2.4: *Hoxa13* function is dispensable for endothelial cell differentiation.

Fate mapping of *Hoxa13*-expressing cells in e14.5 control (**A-C**) and *Hoxa13* null (**D-F**) placental labyrinths. In absence of *Hoxa13* function, there is a significant reduction of the Hoxa13lin+ cell population (compare **A** and **D**) that coincides with the reduced endothelial cell population (**B,E**). Even in absence of *Hoxa13* function, most of Hoxa13lin+ cells are endothelial (CD31+) cells (**C,F**). Scale bars 200 μm.

Figure S 2.5: The yolk sac from *HoxAdel/del* mutant is indistinguishable from wild-type yolk sac.

Wild type (**A,B**) and *HoxAdel/del* (**C,D**) samples at e11 photographed immediately after dissection. *HoxAdel/del* embryos have properly vascularized yolk sacs and are indistinguishable from yolk sacs of wild type littermates. Accordingly, X-gal staining on *Hoxa13Cre/+; Rosa26R* specimens shows no Hoxa13lin+ cells in the yolk sac (**E**).

Figure S 2.6: Loss of allantois expression upon subdivision of the *Hoxa13-Evx1* intergenic region.

Schematic representation of sequence conservation of the *Hoxa13-Evx1* intergenic region between mouse, human and chick (VISTA browser alignment). Top panel: *IR50* transgenic embryo at e12.5 and magnification of the forelimb. Bottom panel: representation of the IR subclones (*a-l*). Subdivision of the *Hoxa13-Evx1* intergenic region has been designed to maintain the integrity of conserved DNA sequences and each two neighboring DNA fragments are overlapping at their common extremity. *c, g* and *f* transgenes express the reporter gene in the forelimb at e12.5 (see arrows and magnification of the forelimbs). Transgene "*l*" is not expressed in the forelimb, but in the central nervous system at e12.5 (arrowheads). Right panel, magnification of the staining in the neural tube (dorsal view). The latter pattern, absent in IR50 transgenic embryos, is reminiscent of *Evx1* expression in the neural tube. Since, the reporter in the IR50 transgene is located at the opposite end compared to region "l", absence of neural tube expression in IR50 transgenic embryos suggests that this expression pattern is under the control of a short-range cis-regulatory element or restricted to *Evx1* as a consequence of an insulator element.

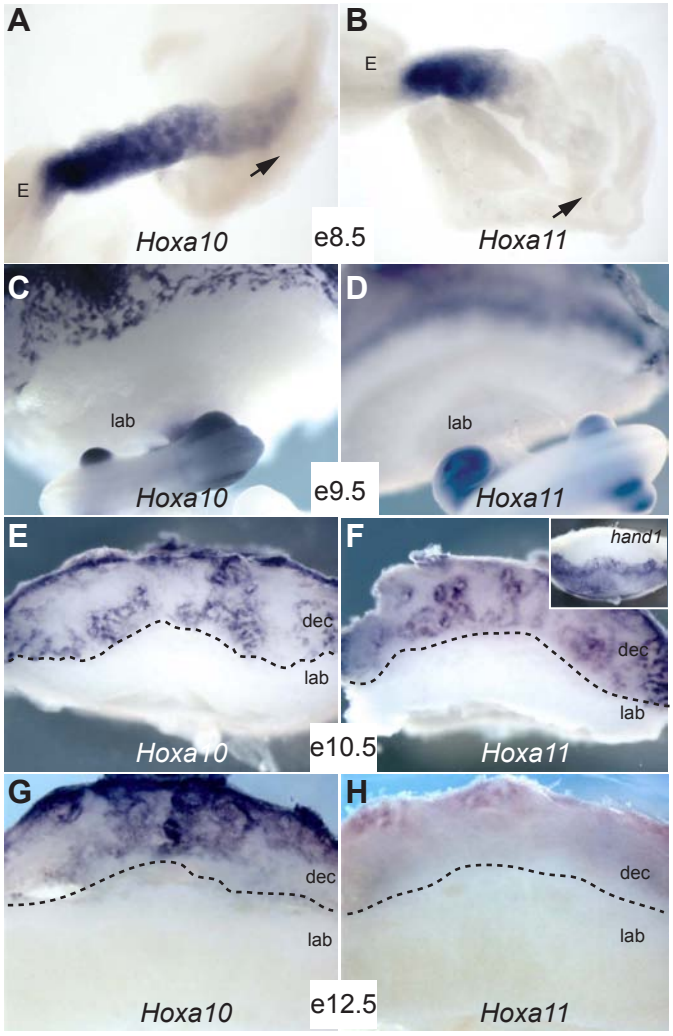

Figure S 2.1 Expression of *Hoxa10* and *Hoxa11* is detected at early stages in the allantois, but is not maintained in the allantois-derived labyrinthine vasculature.

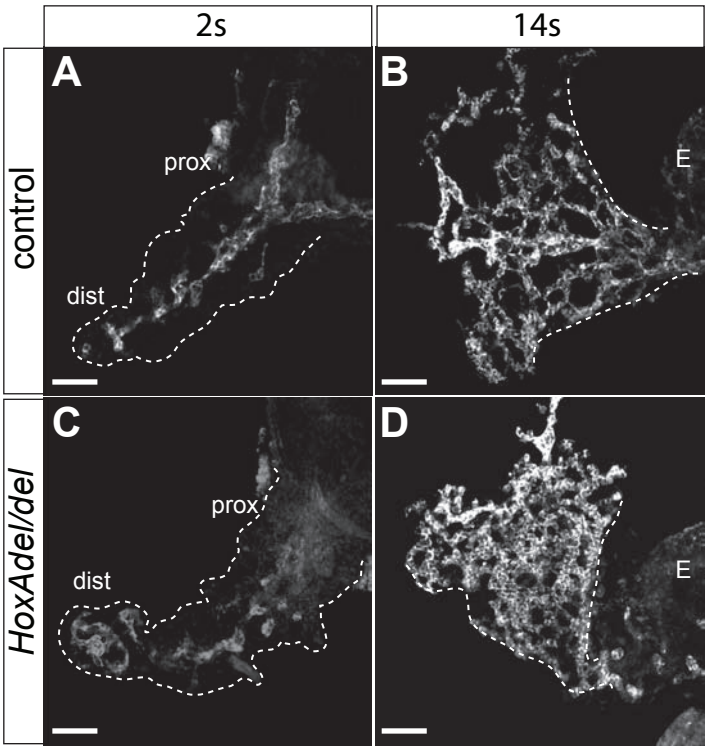

Figure S 2.2 Inactivation of *Hoxa* genes does not interfere with the formation of the primary vascular plexus within the allantois.

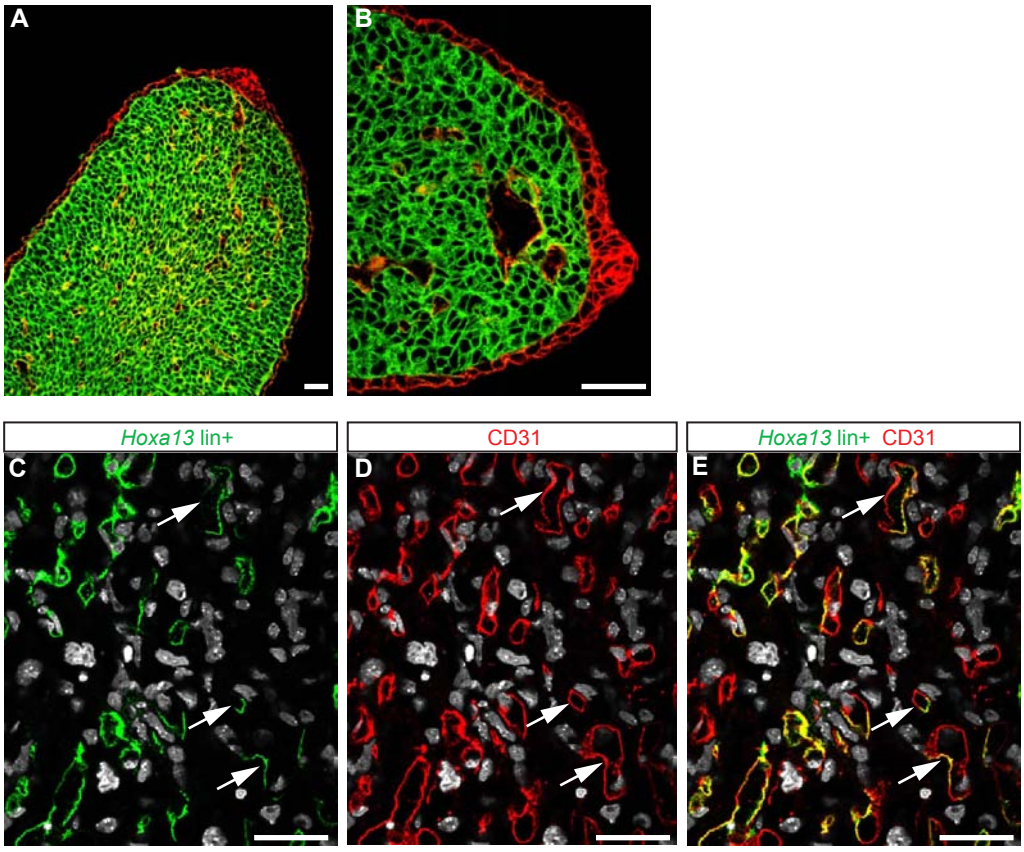

Figure S 2.3 The fetal vasculature of the mature labyrinth is formed of Hoxa13lin+ and Hoxa13lin- endothelial cells.

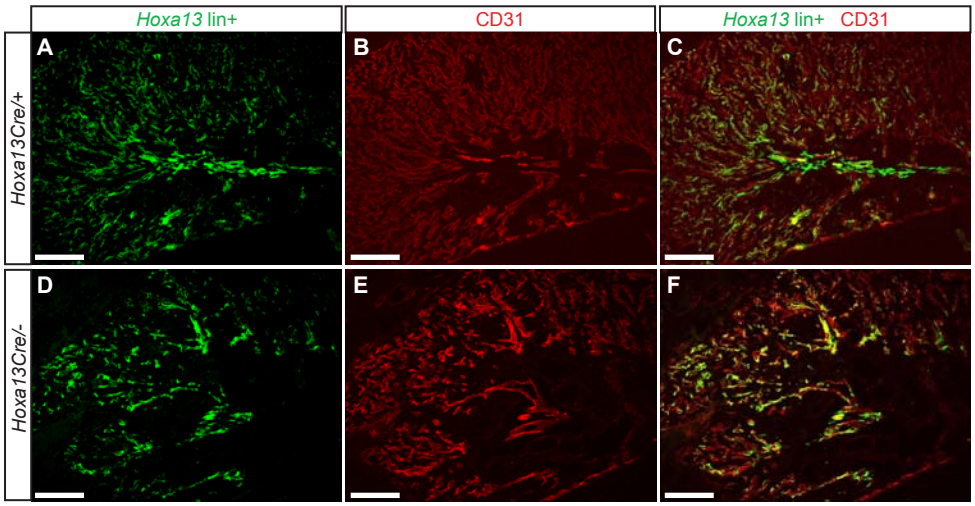

Figure S 2.4 *Hoxa13* function is dispensable for endothelial cell differentiation.

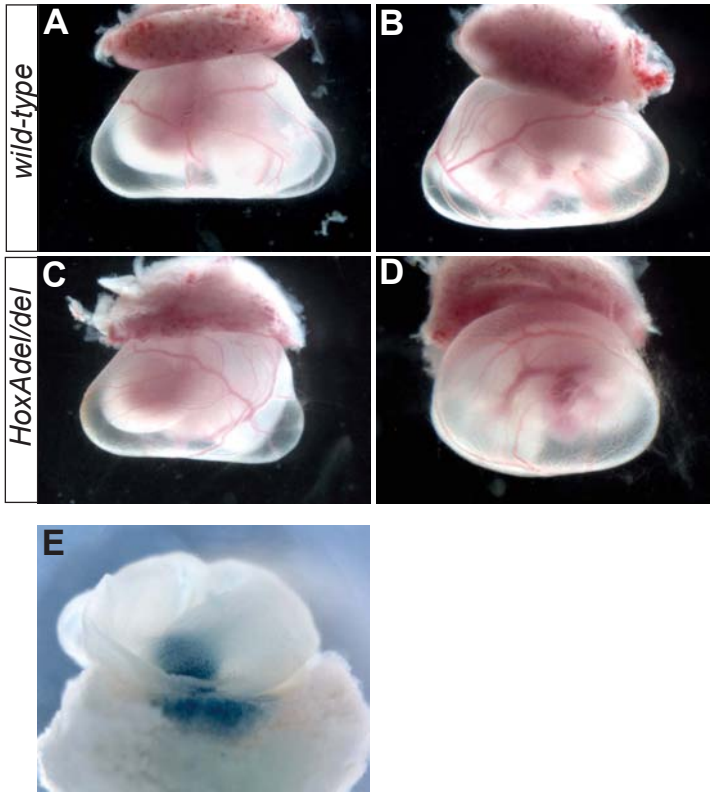

Figure S 2.5 The yolk sac from *HoxAdel/del* mutant is indistinguishable from wild-type yolk sac.

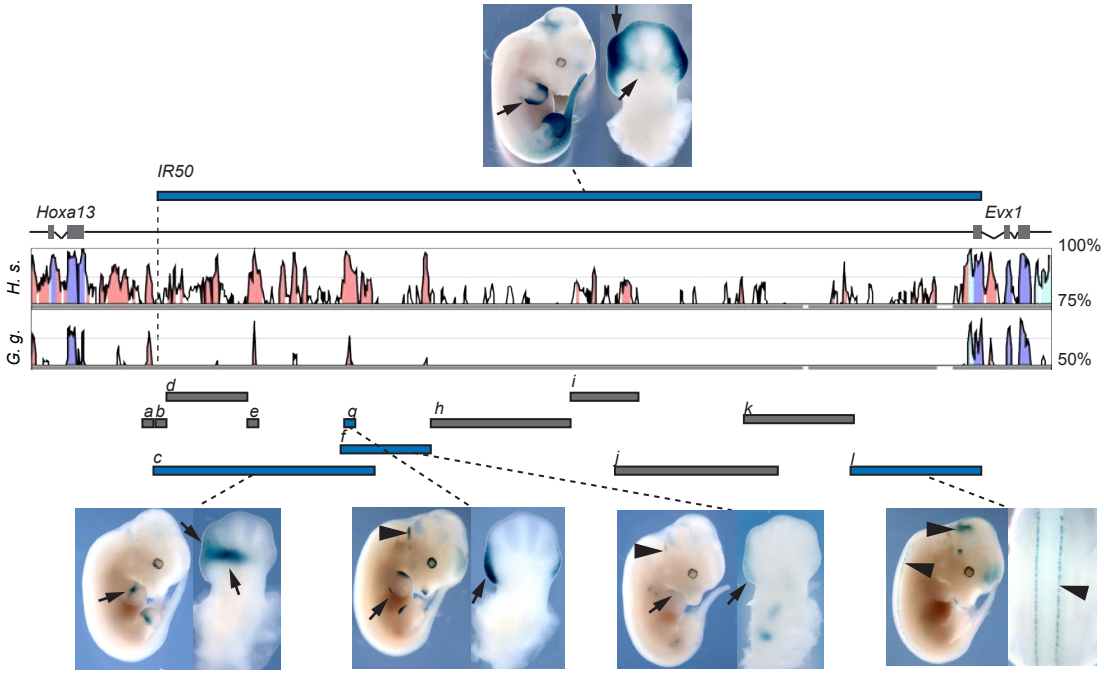

Figure S 2.6 Loss of allantois expression upon subdivision of the *Hoxa13-evx1* intergenic region.

Tg name	Start position	End position	E8.5 Tg/total	E8.5 Expressing/Tg (allantois)	E8.5 Expressing/Tg (tail bud)	E12.5 Tg/total	E12.5 Expressing/Tg (limb)	E12.5 Expressing/Tg (tail)
a	6:52214326	6:52215187	8/43	0/8	0/8	12/45	0/12	0/12
b	6:52215554	6:52216314	7/25	0/7	0/7	10/36	0/10	0/10
d	6:52216243	6:52220703	9/45	0/9	0/9	4/33	0/4	0/4
e	6:52220683	6:52221080	7/68	0/7	0/7	13/52	0/13	0/13
g	6:52226204	6:52226809	13/42	0/13	0/13	10/44	7/10	0/10
f	6:52225971	6:52231612	7/23	0/7	0/7	9/34	4/9	0/9
c	6:52215337	6:52227090	7/45	0/7	0/7	4/54	4/4	0/4
h	6:52231584	6:52240112	5/29	0/5	0/5	6/50	0/50	0/50
i	6:52240064	6:52243437	15/53	0/15	0/15	7/31	0/7	0/7
j	6:52241134	6:52251078	8/37	0/8	0/8	10/47	0/10	0/10
k	6:52250154	6:52258385	6/38	0/6	0/6	3/38	0/3	0/3
l	6:52258283	6:52264475	9/68	0/9	0/9	4/72	0/4	0/4

Table S 2.1 Transgenic analysis of the intergenic region between *Hoxa13* and *Evx1*

Chapter 3

Hoxa13 fate mapping reveals a major contribution of *Hoxa13* expressing cells and their descendants to the limb musculature.

Martina Scotti, Mark Cwajna and Marie Kmita *

Laboratory of Genetics and Development, Institut de Recherches Cliniques de Montréal (IRCM), 110 avenue des Pins Ouest, H2W1R7, Université de Montréal, Montréal Québec, Canada.

At the time of the submission of this thesis, the manuscript is in preparation for submission to Developmental Dynamics.

* Corresponding author: Marie Kmita

3.1 Author contribution:

I performed all the experiments described in this study and made all figures. Mark Cwajna performed preliminary experiments and some experiments not included in this version of the manuscript. Dr. Marie Kmita and I are collaborating very closely to write the manuscript.

3.2 Abstract:

Gene expression pattern in the developing embryo provides important information on tissue(s)/organ(s) where the gene is expected to be functional. Yet, such correlation is less obvious when expression occurring prior cell fate specification. In addition, it should be taken into account that the phenotypic outcome of a gene function can be sometimes detectable only after the gene is silenced. To circumvent this issue, genetic fate mapping using the loxP-Cre recombination system has proven invaluable. Here, we use genetic fate mapping to establish the tissues and organs originating from *Hoxa13*-expressing cells. Our results show that cells expressing *Hoxa13* in developing limb buds contribute to all bones of the forelimb autopod and validate *Hoxa13* as a distal limb marker as far as the skeleton is concerned. The situation is different in limb muscles, where in addition to autopod muscles, *Hoxa13*-expressing cells give rise to almost all muscular masses of the zeugopod and few masses of the stylopod. Together with previous expression data, our results demonstrate that the contribution of *Hoxa13*-expressing cells along the limb proximo-distal axis is significantly different depending on the limb tissue. Importantly, the contribution of these cells to only a subset of limb muscles is, to our knowledge, the first example of a genetic marker specific for a defined subgroup of limb muscles. This result raises the possibility of *Hoxa13* being involved in establishing specific features of these muscles. Finally, the *Hoxa13Cre* line used in this study should be a valuable tool to study musculo-skeletal development and diseases.

3.3 Introduction:

The Hox family of transcription factors plays a key role in the establishment of the body architecture (Iimura and Pourquie, 2007; Kmita and Duboule, 2003; Young and Deschamps, 2009). This function is conserved throughout the animal kingdom and relies on the differential combination of Hox proteins along the anterior-posterior axis of the developing embryo. Besides their ancestral role in patterning of the primary body axis, *Hox* genes have been repetitively recruited to achieve novel functions during evolution, such as the morphogenesis of vertebrate limbs (Zakany and Duboule, 2007). In mammals, there are 39 *Hox* genes organized in four clusters, referred to as *HoxA, B, C* and *D*. Each *Hox* cluster contains a series of 9 to 11 contiguous genes transcribed from the same DNA strand, thus defining a 5' to 3' polarity to the cluster. Due to the common origin of these clusters, genes located at the same relative position on different clusters (referred to as paralogous genes) share more sequence similarities than genes located on the same cluster (Krumlauf, 1994). Genes belonging to group 1 are located on the 3'-end of the clusters and are the first to be expressed. Moreover, group 1 genes are expressed in the anterior-most domains of the embryo compared to genes located in the 5'-end of the clusters (Kmita and Duboule, 2003).

Hoxa13 is the most 5' member of the *HoxA* cluster. In the mouse, its expression is first detected at embryonic day (e) 7.5 in the allantois, an extra-embryonic epiblast derivative located in the exocoelom (Scotti and Kmita, 2012). However, this expression is transient, and by e9.5, *Hoxa13* expression is restricted to embryonic structures (Scotti and

Kmita, 2012). At e9.5, *Hoxa13* mRNA is observed in the tail bud, and by e10 in the distal posterior region of the developing forelimb bud mesenchyme (Haack and Gruss, 1993). At e11, a similar expression pattern is detected in the hindlimb. Between e11 and e13, *Hoxa13* expression domain in the limb encompasses the mesenchyme of the entire presumptive autopod (hand/foot) and becomes restricted to peridigital tissue and interarticular condensations of digits by e14 (Stadler et al., 2001). Faint *Hoxa13* expression is also detected in the zeugopod and stylopod (forearm and arm) of the developing limb, in a domain corresponding to the developing musculature (Yamamoto and Kuroiwa, 2003). Moreover, *Hoxa13* mRNA is observed in the genital bud starting from e11.5, and at e14 in the urogenital system and gastrointestinal tract (Warot et al., 1997).

In mouse, loss of function of *Hoxa13* results in embryonic lethality at mid-gestation due to impaired development of the vasculature within the placental labyrinth (Fromental-Ramain et al., 1996b; Shaut et al., 2008). Mutant embryos display a severely defective urogenital system, characterized by hypoplasia of the urogenital sinus, absence of bladder and abnormal localization of ureters extremities (Warot et al., 1997). In the limb, inactivation of *Hoxa13* causes defects in the autopod. These include lack of digit 1, shortening and malformation of the other digits, fusion of the interdigital tissue and absence of pre-cartilaginous condensation for carpal and tarsal elements (Fromental-Ramain et al., 1996b). The autopod phenotype of *Hoxa13*-/- mutants is, at least in part, due to cell adhesion defects in cartilage condensations and reduced apoptosis in the interdigital tissue (Knosp et al., 2004; Salsi and Zappavigna, 2006; Stadler et al., 2001). However, the simple

Hoxa13 inactivation provides only partial information on *Hoxa13* functional properties. For instance, the simultaneous inactivation of *Hoxa13* and *Hoxd13* often results in a significantly more severe phenotype than the addition of individual gene loss-of-function phenotypes as a consequence of functional redundancy and synergism (Fromental-Ramain et al., 1996b; Warot et al., 1997). In addition, *Hoxa13*-/- mutants have defects in tissues/organs where *Hoxa13* expression is not detected but instead is associated with expression in progenitor cells, as reported for *Hoxa13* function in the development of the placental labyrinth (Scotti and Kmita, 2012).

To establish the tissues and organs originating from *Hoxa13*-expressing cells, we generated a novel *Hoxa13* allele to genetically mark *Hoxa13*-expressing cells and their descendants. The resulting fate-map allowed us to identify all organs and tissues derived from *Hoxa13*-expressing cells. In particular, our analysis demonstrates that *Hoxa13* expressing cells contribute exclusively to skeletal elements of the autopod, thereby confirming that *Hoxa13* can be used as a specific marker for distal skeletal elements. Our fate-map also shows that autopod, zeugopod and stylopod muscles stem in part from *Hoxa13*-expressing cells. Thus, while this study demonstrates that *Hoxa13* can be used as a distal marker as far as the skeleton is concerned, starting at e12 its expression cannot be used as a marker specific for cells committed to distal fate. Importantly, our analysis shows that the contribution of *Hoxa13*-expressing cells and their descendants (Hoxa13lin+) to the limb musculature is restricted to muscle fibers of a specific subset of muscles. Moreover,

the proportion of Hoxa13lin+ cells varies between these muscles, as well as between fibers of a given muscles suggesting a molecular heterogeneity of the myocytes.

3.4 Results:

3.4.1 Generation and validation of the *Hoxa13Cre* mice.

To map the fate of *Hoxa13*-expressing cells in the developing embryo, we targeted a *Cre:Ires:Venus* cassette into the *Hoxa13* start codon via homologous recombination in ES cells (Fig. 3.1A). After neomycin selection, recombinant clones were screened by Southern blot analysis. Successful targeting was confirmed by a restriction fragment length polymorphism detectable with the external probe, and absence of additional random insertion was verified using the internal probe (Fig. 3.1B, C). Two targeted clones were injected in mouse blastocysts to generate chimeras. Following germline transmission of the *Hoxa13Cre*$^{neo+}$ allele, the neomycin selection cassette was eliminated *in vivo* by crossing *Hoxa13Cre*$^{neo+}$/+ mice with *FLPeR* partners (Farley et al., 2000) (Fig. 3.1D). *Hoxa13Cre*$^{neo-}$/+ animals (named *Hoxa13Cre*/+ hereafter) are fully viable and fertile but *Hoxa13Cre* homozygous mutants die embryonically of placental defects (Scotti and Kmita, 2012), which is consistent with other *Hoxa13*-null mutant previously reported (Shaut et al., 2008) (Stadler et al., 2001) (Fromental-Ramain et al., 1996b).

Venus reporter expression was never detected either by direct fluorescence analysis or using immunostaining on sections (not shown). Therefore, in our studies, we were not able to use the Venus reporter to monitor real-time *Hoxa13* expression.

To verify that the Cre cassette works properly in our *Hoxa13Cre* allele, we crossed *Hoxa13Cre*/+ males with homozygous females from the Cre reporter strain Rosa26R (Soriano, 1999). X-gal staining performed on e10.5 *Hoxa13Cre*/+*; Rosa26R*/+ embryos showed that *Cre* reporter expression is comparable to *Hoxa13* expression pattern at this early stage, indicating that our *Hoxa13Cre* allele is functional and can be used to establish the fate map of *Hoxa13*-expressing cells (Fig. 3.2D, E).

3.4.2 *Hoxa13* fate-mapping analysis in the developing embryo.

To explore the fate of *Hoxa13* expressing cells in the developing embryo, we crossed *Hoxa13Cre*/+ males with the *Rosa26R* Cre reporter strain and compared the reporter activity with *Hoxa13* mRNA distribution. In *Hoxa13Cre*/+*; Rosa26R*/+ mutants, a transcriptional stop cassette is excised in presence of the *Cre* recombinase, irreversibly activating the β-gal reporter expression in all *Hoxa13* expressing cells and their descendants, hereafter referred to as Hoxa13lin+ cells. As previously reported, *Hoxa13* expression in the developing forelimb starts at e10.0 in the distal bud (Fig. 3.2A, arrow). However, whole mount X-gal staining of *Hoxa13Cre*/+*; Rosa26R*/+ embryos showed that the Cre reporter activity is only detectable in the forelimb bud starting from e10.75 (Fig.

3.2B, E), consistent with the delay between Cre transcriptional activation and synthesis of the β-gal reporter protein (Scotti and Kmita, 2012). Subsequently, we found that mesenchymal cells within the entire presumptive autopod region are Hoxa13lin+ (Fig. 3.2H, K, N), a fate map reminiscent of *Hoxa13* expression profile (Fig. 3.2G, J, M). From e11.5 onwards, Hoxa13lin+ cells are no longer restricted to the presumptive autopod and are found in more proximal regions of the developing limb. In contrast, *Hoxa13* expression in the proximal limb domain is barely detectable by whole-mount *in situ* hybridization.

Hoxa13 is also expressed in the developing hindlimb, with a pattern similar to the one observed in the forelimb (Fig. 3.2D, G, J, M). In contrast, Hoxa13lin+ cells are found throughout the hindlimb from early bud stage onwards, though with a primary contribution to the autopod domain (Fig. 3.2B, E). Such difference between *Hoxa13* expression in hindlimbs and the distribution of Hoxa13lin+ cells suggests that early and proximal Cre reporter activity is the consequence of *Hoxa13* expression in the lateral plate mesoderm, from which limb mesenchymal cells originate.

During development, *Hoxa13* is initially activated in the extra-embryonic compartment marking cells of the allantois, the precursor of the umbilical cord (Scotti and Kmita, 2012). By e9.0, *Hoxa13* is expressed in the tail bud (Fig. 3.2A, D arrowhead) and accordingly, X-gal staining is observed in the tail bud of *Hoxa13Cre*/+*; Rosa26R*/+ embryos starting from e10.0 (Fig. 3.2B, C). Subsequently, X-gal positive cells are located in the posterior mesoderm and neural tube, the X-gal staining being more posteriorly restricted in the mesoderm (Fig. 3.2F, I, L). Hoxa13lin+ cells are also detected in the

umbilical cord and developing genitals of *Hoxa13Cre/+; Rosa26R/+* embryos (Fig. 3.2C, F, L, O), consistent with *Hoxa13* expression in these structures (Warot et al., 1997). *Hoxa13* expression has been previously reported in the distal part of the urogenital and gastrointestinal tracts (Warot et al., 1997). Accordingly, we found Hoxa13lin+ cells in the developing ureters, bladder, caudal portions of the Müllerian and Wolffian ducts (Fig. 3.2Q). In addition, we observed a strong contribution of Hoxa13lin+ cells to the rectum and colon, as well as a modest contribution to the developing cecum (Fig. 3.2R).

3.4.3 *Hoxa13*-expressing cells and their descendants mark a subpopulation of myogenic progenitors in the developing forelimb pre-muscular masses.

Although *Hoxa13* is predominantly expressed in the presumptive autopod region, *Hoxa13* expressing cells have been identified in limb myogenic precursors of avian embryos and limb muscles of avian and mice limbs (Dolle et al., 1989; Haack and Gruss, 1993; Perez et al., 2010; Yamamoto et al., 1998; Yamamoto and Kuroiwa, 2003). By e12.0, Hoxa13lin+ cells are found in the proximal forelimb, with a spatial distribution that looks similar to the localization of developing muscles. To better define and characterize the fate of *Hoxa13*-expressing cells in the proximal region of the developing forelimb, we performed X-gal staining on *Hoxa13Cre/+; Rosa26R/+* forelimbs starting from early bud stage. To achieve a more precise staging of our samples, somites of the embryos were

counted. We found that, starting from 45-somite stage, few scattered X-gal positive cells are present within the proximal region of the forelimb (Fig. 3.3D arrow) and by 53-somite stage there is a distinct "patch" of Hoxa13lin+ cells in the presumptive zeugopod-stylopod region (Fig. 3.3F arrow).

Limb muscles derive from *Pax3*-expressing myogenic progenitors that delaminate from the hypaxial dermomyotome and migrate in the limb bud (Chevallier et al., 1977) (Daston et al., 1996; Williams and Ordahl, 1994). Based on whole-mount X-gal staining, proximal Hoxa13lin+ cells are either overlapping with myogenic precursors or located in their vicinity. To confirm the identity of Hoxa13lin+ cells, we performed double immunostaining for the Cre-reporter protein and Pax3 on transverse cryosections. The Pax3 antibody requires antigen retrieval treatment to recognize the protein epitope, however, the anti-βgal antibody, used to detect X-gal positive cells, does not work properly under these experimental conditions. Thus, for our analysis on sections, we used samples derived from the *mT/mG* Cre reporter strain that produces a green fluorescent protein (GFP) after Cre-mediated recombination (Muzumdar et al., 2007). In *Hoxa13Cre/+; mT/mG* embryos a green fluorescent membrane-targeted protein (mG) is expressed in cells where Cre-mediated recombination has occurred, while a red fluorescent membrane-targeted protein (mT) is expressed in the other cells. At all stages analyzed, *Hoxa13Cre* mediated recombination was detected in the limb mesenchymal cells and not in the limb ectoderm, (Fig. 3.4). At 47-somite stage, Pax3+ cells form two distinct ventral and dorsal pre-muscular masses in forelimb buds (red nuclear signal in Fig. 3.4B). These masses extend

distally into the limb (Fig. 3.4C) and few scattered GFP+/Pax3+ double positive cells are found in the central and distal regions of the ventral and dorsal pre-muscular masses (Fig. 3.4C dotted box). By 53-somite stage, the GPF+/Pax3+ double positive cell population has drastically increased and is located within the entire pre-muscular masses (Fig. 3.4F and dotted boxes).

3.4.4 Hoxa13lin+ cells form muscular fibers of a subset of limb muscles.

Pax3-expressing cells, which form the pre-muscular masses of the limb, activate a myogenic transcriptional program triggering differentiation into myoblasts in a proximal-to-distal manner (reviewed in (Christ and Brand-Saberi, 2002)). Myoblasts subsequently fuse into multinucleate myotubes and assemble to generate muscle fibers (reviewed in (Francis-West et al., 2003)). To follow the fate of Pax3+/Hoxa13lin+ myogenic progenitors during forelimb muscular development, we performed whole mount X-gal staining on *Hoxa13Cre*/+*; Rosa26R*/+ specimens at successive stages (Fig. 3.5 A-E). By e12.5, additional domains of X-gal staining are observed in the presumptive zeugopod and the posterior domains appear more proximal than the anterior ones (Fig. 3.5A). Later on, Hoxa13lin+ cells are detected in almost all dorsal muscles of the zeugopod (Fig. 3.5 B-E). The developing stylopod musculature contains much less Hoxa13lin+ cells, which are restricted to part of the forming triceps (Fig. 3.5E). We next performed a more detailed

analysis by immunostaining on cryosections of *Hoxa13Cre/+; mT/mG* forelimbs. Hoxa13lin+ cells were visualized by direct detection of GFP fluorescence from the *mT/mG* Cre reporter allele, while muscles fibers were labeled by immunostaining for the Myosin Heavy Chain. Tendons were identified on the basis of their morphology and anatomical position. In the autopod of *Hoxa13Cre/+; mT/mG* forelimbs, we found that all muscles, tendons and ligaments are GFP positive (Fig. 3.6 and not shown).

To follow the fate of *Hoxa13* expressing cells and their descendant and highlight possible variations in the Hoxa13lin+ cells contribution at different stages of muscle development, we analyzed transverse sections of the zeugopod and stylopod at e14.5 and e18.5. At all stages analyzed, Hoxa13lin+ cells are only localized in the muscle fibers, and excluded from the connective compartment of the muscle, as well as from tendons and ligaments (Fig. 3.7A, C and Fig. 3.8A, C arrowhead and not shown). At e14.5, Hoxa13lin+ cells are observed in all distal muscles of the zeugopod, but there are apparent differences in the level of GFP fluorescence between the various muscle masses (Fig. 3.7A-C). GFP fluorescence is also detected in muscular masses of the proximal zeugopod, but not all muscles were labeled (Fig. 3.7D-E). The most anterior muscle in the proximal-ventral part of the zeugopod (extensor carpi radialis longus #11 in Fig. 3.7D) is completely deprived of Hoxa13lin+ cells (Fig. 3.7D-F). In the e14.5 stylopod, Hoxa13lin+ cells contribute to the formation of the triceps (triceps brachii radialis and lateralis #19 and 18, Fig. 3.7G, L). No Hoxa13lin+ cells are detectable in the other stylopod muscles (Fig. 3.7I).

The distribution of Hoxa13lin+ cells in e18.5 zeugopod appears very similar to e14.5, with stronger GFP fluorescence in distal muscles and less GFP-positive fibers in more proximal masses (Fig. 3.8A-F). In the stylopod, Hoxa13lin+ cells are found exclusively in the triceps, with a predominant contribution to the radialis and lateralis and a minor contribution to the dorsal portion of the triceps longus (Fig. 3.8G-L). Interestingly, at all stages analyzed, fibers within the same muscle are also characterized by different GFP fluorescence intensity, and fibers with similar intensity are often clustered in the same region of the muscle (Fig. 3.8D, G #10, 14, 15, 12, 9).

3.4.5 Hoxa13lin+ cells contribution to the limb skeleton is restricted to the autopod.

To determine Hoxa13lin+ cells contribution to the limb skeletal elements we performed sagittal sections at the autopod/zeugopod junction of e18.5 specimens. We found that the entire skeleton of the autopod is composed of Hoxa13lin+ cells (Fig. 3.6A,G). Moreover, each bone element of the autopod is completely formed by Hoxa13lin+ cells, with the exception of the most proximal carpal elements (ulnare, radiale and intermedium), in which some lineage negative cells are found (Fig. 3.6D-F). In contrast, no Hoxa13lin+ cell was detected in the radius, and we could only differentiate few Hoxa13lin+ in the ulnar head, (Fig. 3.6D) suggesting that *Hoxa13*-expressing cells and their descendants establish a boundary between autopod and zeugopod bones (Fig. 3.6A).

3.5 Discussion.

To define tissues and organs deriving from *Hoxa13*-expressing cells during development, we generated the *Hoxa13Cre* allele aimed at inducing permanent reporter expression in *Hoxa13*-expressing cells and their descendants (Hoxa13lin+) to establish the fate of *Hoxa13*-expressing cells. As anticipated from expression data, Hoxa13lin+ cells are detected in limbs, posterior trunk, urogenital system and gastrointestinal tract. Genetic fate mapping in the limb demonstrated that *Hoxa13*-expressing cells give rise to the entire autopod, except blood vessels and ectoderm, and to a specific subset of muscles in the zeugopod and stylopod. Moreover, our fate map uncovered the specific contribution of *Hoxa13* expressing cells and their descendants to muscular fibers within limb muscles. Finally, we found that the contribution of *Hoxa13*-expressing cells and their descendents to the different limb muscles is not identical.

3.5.1 *Hoxa13* is a distal marker for the limb skeleton.

Starting from e10.0, *Hoxa13* is robustly expressed in the distal posterior region of the forelimb and by e11 its transcripts are located in the entire presumptive autopod (Dolle et al., 1989; Haack and Gruss, 1993). Based on these expression data, *Hoxa13* has been used as a marker of the distal limb. Yet, to date there was no evidence that the fate of *Hoxa13*-expressing cells is restricted to distal elements of the limb skeleton. The fate map

of *Hoxa13* expressing cells reported here demonstrates that skeletal progenitors expressing *Hoxa13* and their descendants remain distally restricted. Moreover we found that, with the exception of the most proximal carpal elements, all skeletal elements of the autopod are exclusively formed by Hoxa13lin+ cells. Together, these data demonstrate that *Hoxa13* is a *bona fide* marker of distal skeleton precursors.

3.5.2 Hoxa13lin+ cells are part of the limb musculature.

Limb muscles consist of two different components: somite-derived muscle tissue and connective tissue originating from the limb mesenchyme. The latter includes the different tendons and three layers of connective tissue that surround the muscular mass (Borg and Caulfield, 1980). Muscular tissue stems from myogenic progenitors, which are highly proliferating cells that differentiate into myoblasts. These myoblasts ultimately fuse together to generate the muscle fiber, a multinucleated cell forming the functional unit of the muscle (reviewed in e.g. (Biressi et al., 2007)). Expression analyses performed in avian and mouse embryos demonstrated that *Hoxa13* expression in developing limbs is not restricted to the autopod domain, but is also detected in a subgroup of developing muscles of the zeugopod and the stylopod. In chick embryos, it has been reported that a subpopulation of limb myogenic progenitors of the dorsal and ventral pre-muscular masses starts expressing *Hoxa13* once it has entered the limb bud territory (Yamamoto et al., 1998). At later stages, both in mouse and chick, *Hoxa13* mRNA is detected in a subset of

muscular masses of the zeugopod and stylopod (Yamamoto and Kuroiwa, 2003). However, the resolution of the *in situ* hybridization did not allow the exact localization of *Hoxa13* RNA within the muscle, and the contribution of *Hoxa13* expressing cells to either the muscular or the connective compartment of the muscle was not clear. Consistent with previous studies, the fate map of *Hoxa13*-expressing cells shows that Hoxa13lin+ cells are present also outside the presumptive autopod domain. We detected these cells in mouse limb buds starting from 47-somite stage and identified them as Pax3+ myogenic progenitors within the limb pre-muscular masses. At later stages, co-immunostaining studies demonstrate that, in the zeugopod and stylopod, *Hoxa13*-expressing cells and their descendants contribute exclusively to muscle fibers and not to the associated connective tissue. Strikingly, GFP fluorescence intensity from the Cre reporter varies within individual muscles. Careful observation reveals distinct GFP fluorescence between fibers. Since these fibers stem from the fusion of myoblasts and are thus multinucleated, it is likely that differences in fluorescence intensity reflects the ratio of Hoxa13lin+/Hoxa13lin- myoblasts that contributed to the formation of individual fibers. In this view, the intensity of the GFP fluorescence of each muscular fiber would be directly proportional to the number of Hoxa13lin+ myobasts contributing to a given fiber. Alternatively, differences in fluorescence intensity could reflect a differential timing of *Hoxa13* expression in the developing muscle. However, since the heterogeneity of the fluorescence does not change significantly over time, we favor the existence of a variable ratio of Hoxa13lin+/Hoxa13lin-

nuclei forming individual fibers of each muscle. It will be interesting to investigate whether such ratio has any impact on muscle function/identity.

3.5.3 *Hoxa13* function in the limb musculature.

Although the molecular mechanisms that control skeletal patterning have been extensively studied, patterning and morphogenesis of limb muscles and other soft tissues, essential for a functional limb, are still poorly understood. Recent studies have reported that limb muscle patterning and differentiation are in part determined by extrinsic signals derived from the muscular connective tissue (Hasson et al., 2010; Kardon et al., 2003; Mathew et al., 2011). However, data obtained from non-limb myoblasts, suggest that intrinsic *Hox*-dependent cues could also play a role in muscle patterning (Alvares et al., 2003). *Hox* genes are key regulators of patterning and specification in many different tissues, including the limb skeleton and motor neurons that innervate the limb (reviewed in (Dasen and Jessell, 2009; Zakany and Duboule, 2007)). In addition to *Hoxa13*, other *Hox* transcripts, such as *Hoxa10* and *Hoxa11*, have been detected in both developing and adult limb muscles (Haack and Gruss, 1993; Yamamoto et al., 1998) (Benson et al., 1995; Houghton and Rosenthal, 1999). Yet, simple and compound *Hox* mutants have not been extensively analyzed for the presence of patterning or functional abnormalities of the limb musculature. While preliminary studies on *Hoxa13*-/- animals suggest patterning defects in limb muscles (Yamamoto and Kuroiwa, 2003), embryonic lethality associated with *Hoxa13*

inactivation has limited further analysis (Fromental-Ramain et al., 1996b). In addition, as the muscular and skeletal development is intimately linked and influences each other (Hasson, 2011), it is difficult to determine the specific role(s) of *Hox* genes in muscles formation and/or function using ubiquitous null alleles. Consistent with a potential role for *Hoxa13* in the patterning of the limb musculature, our fate mapping analysis uncovered a differential contribution of Hoxa13lin+ cells to the different muscular masses within the limb. Yet, specific inactivation of *Hoxa13* in myogenic precursors will be necessary to establish whether it plays a role in patterning the limb musculature.

A functional limb requires the proper organization of muscles and bones and also correct muscle innervation (reviewed in (Bonanomi and Pfaff, 2010)). The identity of molecules implicated in nerve-muscle matching is still largely unknown. Previous experiments showed that in the limb, in absence of targets muscles, the main nerve branches still form, but smaller nerve branches that, in a normal limb, would lead to specific muscles fail to develop (Lewis et al., 1981; Phelan and Hollyday, 1990, 1991). These observations suggest the limb mesenchyme produces instructive cues to guide motor axons along different axes of the limb, but muscles as well are involved in the establishment of synaptic connectivity. The Eph receptor tyrosine kinases and their ephrin ligands form a large family of signaling molecules involved in patterning, morphogenesis and cell guidance in many different tissues (reviewed in (Klein, 2004; Palmer and Klein, 2003)). Eph and ephrins are not only expressed in motor neurons and their axon, but also in limb muscles, being involved in specific matching between motor axons and muscle

fibers (Chadaram et al., 2007; Feng et al., 2000; Lampa et al., 2004). Interestingly, *Hox* genes can regulate ephrin receptor expression in different tissues (Shaut et al., 2007; Studer et al., 1998). In particular, *Hoxa13* has been shown to directly regulate the expression of the ephrin receptor EphA7 in limb mesenchymal condensations (Salsi and Zappavigna, 2006; Stadler et al., 2001). Our fate-map provides evidence for a differential contribution of Hoxa13Lin+ cells between different muscular masses but also between fibers within the same muscle, which could result in differential expression of Eph/ephrins. In addition, fibers with similar Hoxa13lin+ contribution are often clustered in the same region of the muscle (Fig. 8D, G #10, 14, 15, 12, 9). As nerve-muscle connectivity occurs in determined regions of the muscle, clustering of muscle fibers with similar Hoxa13lin+ contribution is consistent with *Hoxa13* being potentially involved in establishing specific synaptic connectivity between motor neurons and target fibers.

3.5.4 Conclusion.

Our data demonstrate that skeletal elements deriving from *Hoxa13*-expressing cells are restricted to the autopod. Yet, consistent with previous expression analysis, our study also points out a significant contribution of *Hoxa13*-expressing cells to the most proximal muscles of the limb thereby revealing that *Hoxa13* is not a bona fide distal limb marker. The differential contribution of *Hoxa13*-expressing cells in the limb muscles is consistent with a potential role of *Hoxa13* in muscle patterning or determination of muscle identity.

Moreover, differences in the distribution of Hoxa13lin+ cells within fibers of the same muscle suggest that *Hoxa13* function could contribute to the establishment and/or refinement of specific neuromuscular synaptic connections. Importantly, based on the fate map reported here, our *Hoxa13Cre* line will be valuable to investigate the molecular signature of the various muscles and the mechanisms underlying the patterning of the limb musculature and the function of limb muscles.

3.6 Materials and Methods.

3.6.1 Targeting and generation of the *Hoxa13Cre* mice.

To generate the targeting vector, a 5.2 Kb MfeI-HindIII DNA fragment containing *Hoxa13* exon 1 and a 2.5 Kb HindIII DNA fragment containing the exon 2 were ligated and inserted into a modified pBluescript SK+ vector. A Cre:Ires:Venus cassette (modified from the Venus/PCS2 vector obtained from Atsushi Miyawaki) was inserted at the *Hoxa13* ATG using the Recombineering technique (Copeland et al., 2001) and replaces the entire exon 1. The SV40 666bp sequence and neomycin cassette flanked by two *Frt* sites and a *loxP* site (from the PL451 plasmid obtained from N. Copeland, NCI Frederick) were added to the 3' of the Cre:Ires:Venus cassette. The vector backbone was eliminated by PacI digest prior to electroporation into R1 ES cells. Following selection with G418, approximately 400

individual ES cell colonies were analyzed by Southern blot for homologous recombination. Two independent clones were injected into blastocysts obtained from C57BL/6J mice, subsequently implanted into pseudopregnant females. Germ-line transmission the *Hoxa13Cre* allele was obtained for both clones and the F1 offspring were intercrossed with homozygous FLPeR mice (Farley et al., 2000) to delete the neomycin cassette.

3.6.2 Genotyping and mating schemes.

Genotyping from ES cell, tail biopsies and yolk sacs was performed by Southern blot analysis. A scheme with restriction sites and probes used for ES cell genotyping is presented in Fig. 3.1. *Hoxa13Cre* mice were genotyped using the internal probe described in Fig. 1 and EcoRI digest. The *Cre* recombinase reporter lines were genotyped by PCR using the following primers: Rosa26R (Soriano, 1999) (5'-GCG AAG AGT TTG TCC TCA ACC-3'; -5'GGA GCG GGA GAA ATG GAT ATG-3'; 5'-AAA GTC GCT CTG AGT TGT TAT-3'; wild-type 550 bp amplicon, mutant 300 bp amplicon), *mT/mG* (Muzumdar et al., 2007) (CTCTGCTGCCTCCTGGCTTCT; CGAGGCGGATCACAAGCAATA; TCAATGGGCGGGGGTCGTT; wild-type 330 bp amplicon, mutant 250 bp amplicon). For fate mapping, we crossed *Hoxa13Cre*/+ males with Rosa26R or *mT/mG* homozygous females and used double heterozygous embryos and new borns.

3.6.3 Whole mount *in situ* hybridization, X-gal staining and imaging.

Whole mount *in situ* hybridizations were performed as previously described (Kondo et al., 1998a). *Hoxa13* probe was previously described (Warot et al., 1997). Whole mount X-gal staining was performed using standard protocols (Zakany et al., 1988). After staining, embryos and new born specimens were washed 3 times for one hour in PBS and stored in 4% PFA at 4°C. All specimens were imaged using the Leica DFC320 camera. X-gal staining was performed on a minimum of five samples per stage.

3.6.4 Immunostaining.

Whole embryos and limbs were dissected in ice cold PBS and fixed 1-2 hrs in 4% PFA on ice, rinsed three times ten minutes in PBS an then placed in 30% sucrose in PBS overnight. Specimens were then embedded in a 1:1 mix of 30% sucrose in PBS and Cryomatrix (Thermo Shandon). Immunostaining for with anti Pax3 (1:250, concentrate, Developmental Studies Hybridoma Bank) and anti GFP antibodies (1:100, Molecular Probes) was performed on 12 μm cryo-sections as previously described (Relaix et al., 2003). Immunostaining for my-32 (1:750, Sigma) was performed using the M.O.M kit (Vector) as in (Warot et al., 1997; Watson et al., 2009). Secondary antibodies were conjugated with Alexa 488 or 649 (1:500 Jackson Immunoresearch). All images were

captured using a ZEISS LSM710 confocal microscope. At least three sample per stage and 10 sections per sample were analyzed.

3.6.5 Muscle nomenclature.

The nomenclature for the forelimb muscle in table 1 was derived from the Mouse Limb Anatomy Atlas (Delaurier et al., 2008) and from (Watson et al., 2009).

3.7 Legends to figures.

Figure 3.1: Generation of the *Hoxa13Cre* mouse line.

(**A**) *Hoxa13* wild type locus (top). The targeting vector is shown below and dotted lines indicate sequence identity of homologous arms. Targeted locus after homologous recombination in ES cells (middle). Position of the internal (IP) and external probes (EP), restriction sites and size of the DNA fragments used for Southern blot genotyping are indicated. Bottom: targeted locus after the FLP mediated removal of the PGK-neo selection cassette. (**B**) Southern blot analysis of ES cells clones with the external probe to detect the targeted allele (2), and (**C**) with the internal probe to confirm the absence of additional incorporation of the targeting construct into the genome. (**D**) Southern blot analysis of *Hoxa13CreΔNeo*/+ offspring after Flp recombinase mediated excision of the PGK-Neo cassette (2).

Figure 3.2: Comparison between *Hoxa13* expression and Hoxa13lin+ cells distribution at different stages of embryonic development.

Whole mount *in situ* hybridization of wild-type embryos with *Hoxa13* probe at different stages of embryonic development (**A, D, G, J, M, P**). Whole mount X-gal staining of *Hoxa13Cre/+; Rosa26R/+* embryos (**B, C, E, F, H, I, K, L, N, O, Q, R**). (**B**) Dotted line demarcates the forelimb, where, at e10, *Hoxa13*lin+ cells are not yet detected. (**Q**) X-gal staining of urogenital apparatus and (**R**, upper section) gastrointestinal tract dissected out of the embryo before staining. (**R**, lower section) Magnification of the cecum. Arrow in (**A**) points to the forelimb. Arrowheads in **A** and **D** point to the tailbud.

FL: forelimb, TB: tail bud, UC: umbilical cord, US: urogenital sinus, NT: neural tube, GT: genital tubercle, a: adrenal gland, g: gonad, k: kidney, u: urether, b: bladder, MD: Mullerian duct, WD: Wolffian duct, s: stomach, ce: cecum, co: colon, re: rectum.

Figure 3.3: Hoxa13lin+ cells in the forelimb bud and early forelimb are not restricted to the presumptive autopod domain.

(A-F) Whole mount X-gal staining on *Hoxa13Cre/+; Rosa26R/+* forelimbs. The number of somites for each embryo is reported in the bottom-left corner. (**A**) Hoxa13lin+ cells are not detected in the developing limb at 36-somite stage. After 38-somite stage, some positive cells are detected in the posterior and distal part of the bud, which progressively becomes entirely Hoxa13lin+ (**B, C, D, E, F** arrowheads). (**D**) After 45-somite stage some Hoxa13lin+ cells are detected in the proximal region of the limb (**D, E, F**, arrows).

Figure 3.4: Myogenic progenitors within the developing ventral and dorsal muscular masses of the forelimb are also Hoxa13lin+.

(A-F) Immunostaining on *Hoxa13Cre/+; mTmG* forelimb bud cryosection of 47- (**A-C**) and 53- somite embryos (**D-F**) with anti-GFP (green signal targeted to the cell membrane) and anti-Pax3 (red nuclear signal). At 47-somite stage, some myogenic progenitors of the developing ventral and dorsal muscular masses are also Hoxa13lin+ (**C**, arrow and magnification in the dotted box). Note the increasing proportion of Pax3+/Hoxa13lin+ double positive cells at 53-somite stage (**F**, see magnification in the

dotted boxes). Nuclei are stained with DAPI (blue signal). d, dorsal; v, ventral. Scale bar 140 μm.

Figure 3.5: At later stages of development, the distribution of Hoxa13lin+ cells in the forelimb has a pattern reminiscent of the forming musculature.

(**A-E**) Whole mount X-gal staining on *Hoxa13Cre/+; Rosa26R/+* forelimbs at different stages of development, dorsal view. X-gal signal is detected in muscular masses of the zeugopod and stylopod.

Figure 3.6: The distribution of Hoxa13lin+ cells in the limb skeleton marks the transition between autopod and zeugopod.

(**A-C**) Immunostaining on longitudinal *Hoxa13Cre/+; mTmG* forelimb cryosections at e18.5. (**A-C**) Sections at the autopod-zeugopod junction (autopod on the bottom) are shown. Hoxa13lin+ cells express the endogenous green reporter. Myosin- positive muscular fibers are labeled in red. Arrowheads in **A** point to Hoxa13lin+ tendons in the autopod. (**D-F**) Magnification of the carpal-ulnar junction and (**G-I**) magnification of a

digit falanx in forelimb e18.5. In all panels, nuclei are stained with DAPI (blue signal). Scale bars 200 μm. U: ulna, R: radius, ul: ulnare, ra: radiale, i: intermedium, fa: falanx.

Figure 3.7: Hoxa13lin+ contribution to muscular masses of the zeugopod and stylopod at e14.5.

(**A-L**) Immunostaining on transversal cryosection of *Hoxa13Cre/+; mTmG* forelimb at e14.5. In all panels Hoxa13lin+ cells express the green endogenous reporter targeted to the cell membrane and muscles are stained with anti-myosin antibody (red signal). (**A-C**) Transversal section in the distal zeugopod. Arrowheads point to tendons, which are Hoxa13lin-. (**D-F**) transversal section in the proximal zeugopod. (**G-I**) Transversal section in the stylopod. (**J-L**) magnification of the boxed area in G. Numbers in **B**, **E**, **H** and **K** identify muscles in supplementary table 1. R: radius, U: ulna, H: humerus. Scale bar 150 μm. a: anterior; p: posterior; d: dorsal; v; ventral.

Figure 3.8: Hoxa13lin+ contribution to muscular masses of the zeugopod and stylopod at e18.5.

(**A-M**) Immunostaining on transversal cryosection of *Hoxa13Cre/+; mTmG* forelimb at e18.5. In all panels Hoxa13lin+ cells express the green endogenous reporter targeted to the cell membrane and muscles are stained with anti-myosin antibody (red

signal). (**A-C**) Transversal section in the distal zeugopod. Arrowheads point to tendons, which are Hoxa13lin-. (**D-F**) Transversal section in the proximal zeugopod. (**G-I**) Transversal section in the stylopod. (**J-L**) magnification of the boxed area in G. Numbers in **B**, **E**, and **H** identify muscles in supplementary table 1. R: radius, U: ulna, H: humerus. Scale bar 360 μm. a: anterior; p: posterior; d: dorsal; v; ventral.

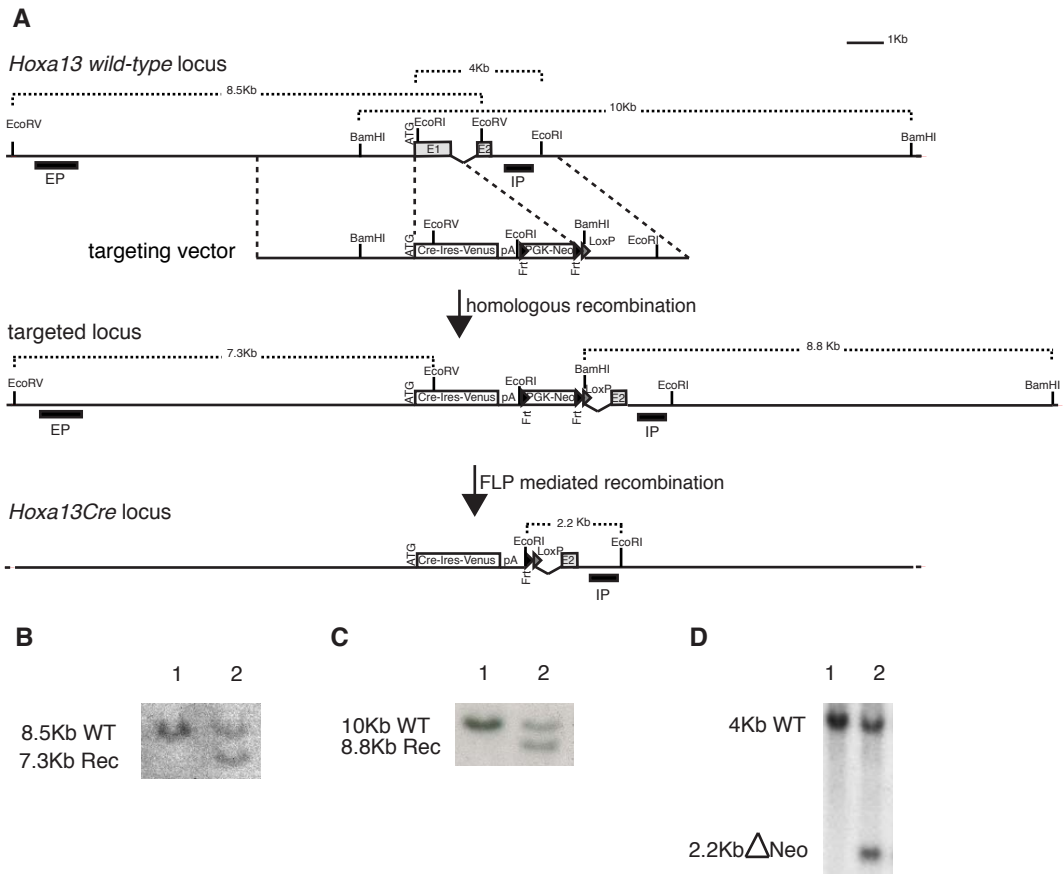

Figure 3.1 Generation of the Hoxa13Cre mouse line

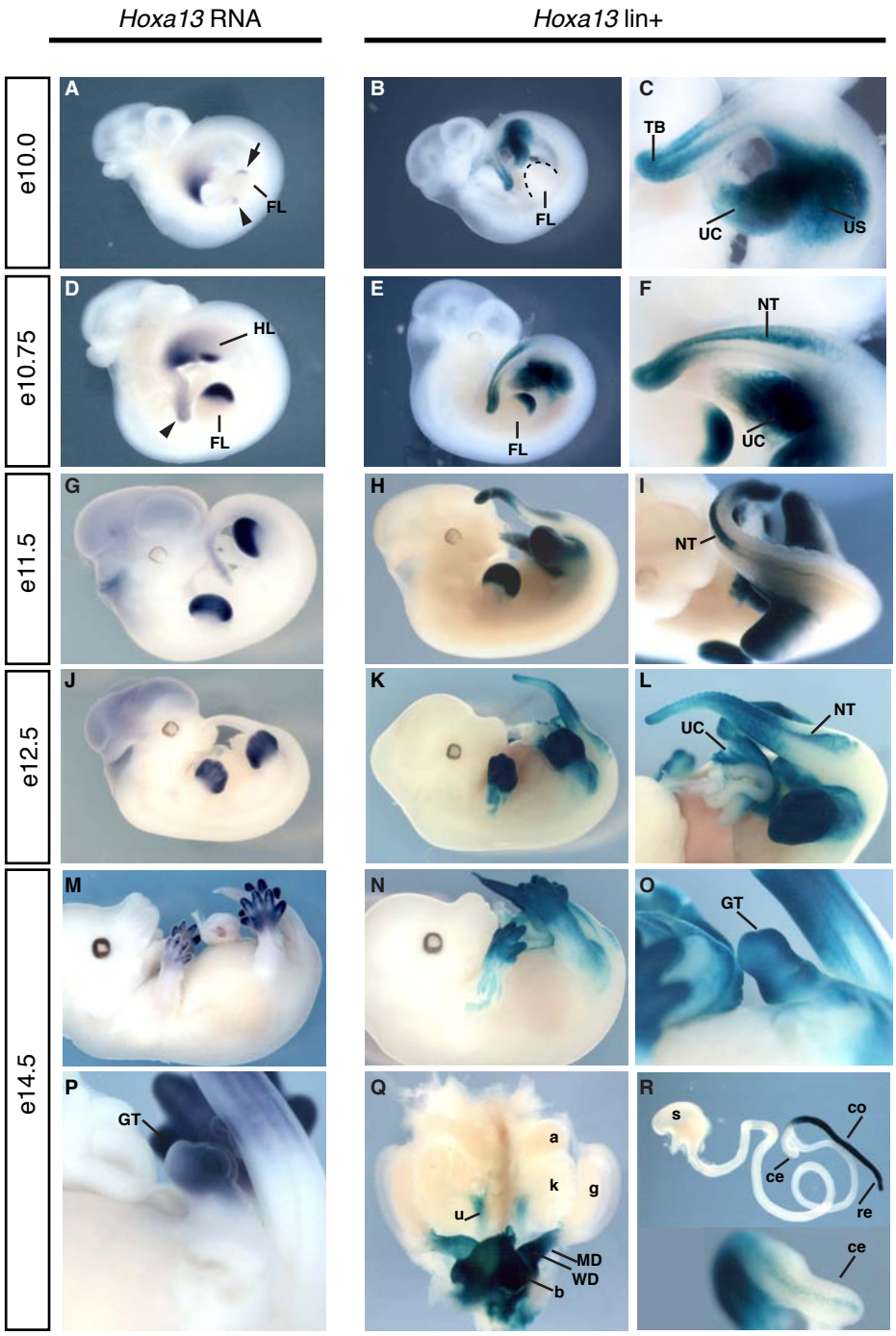

Figure 3.2 Comparison between *Hoxa13* expression and Hoxa13lin+ cells distribution at different stages of embryonic development

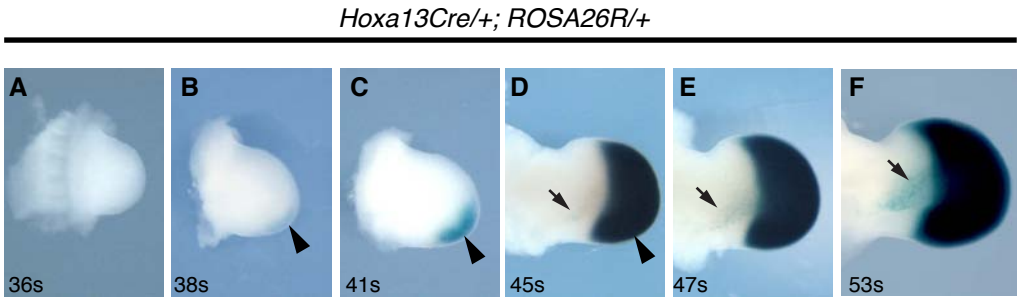

Figure 3.3 Hoxa13lin+ cells in the forelimb bud and early forelimb are not restricted to the presumptive autopod domain. .

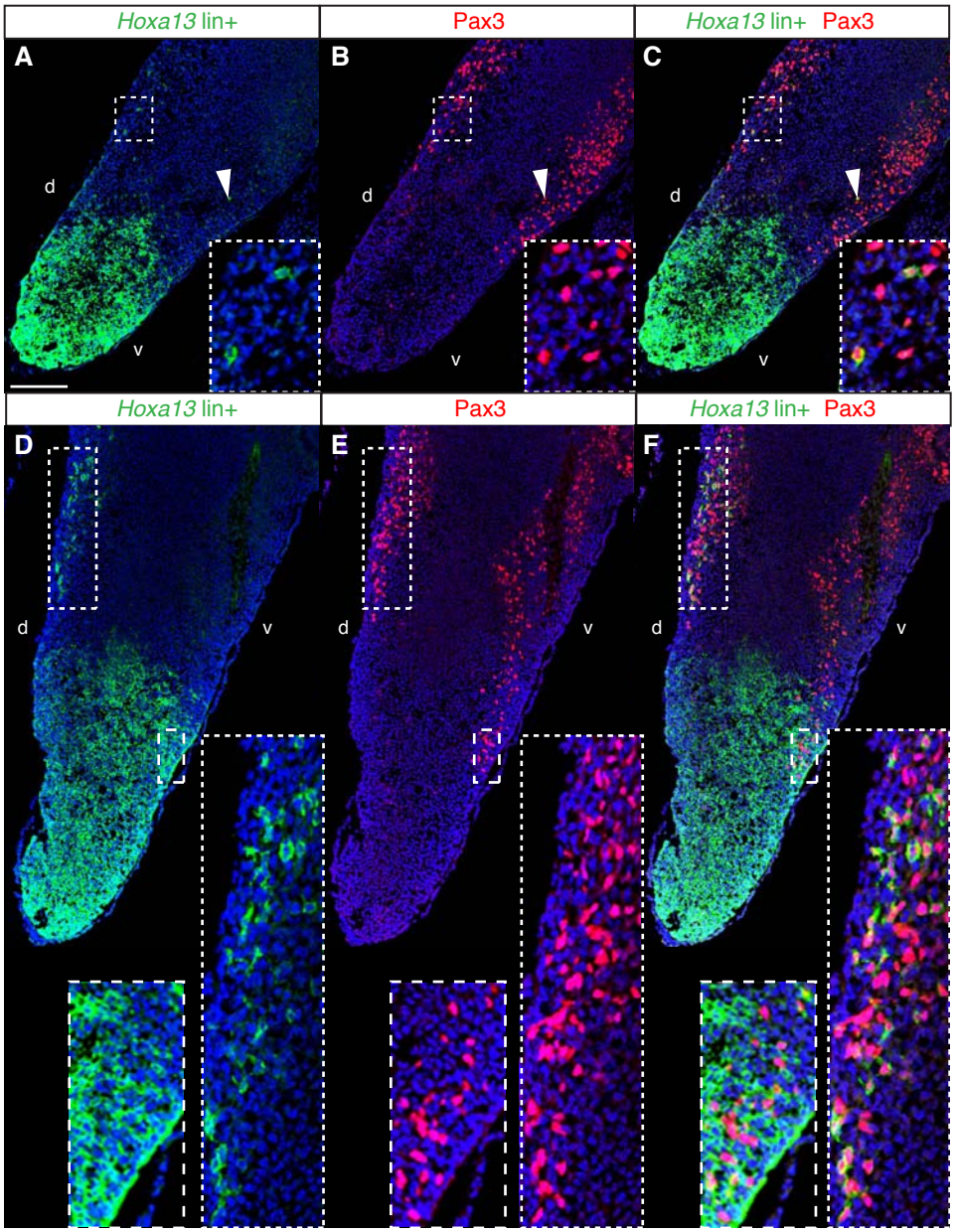

Fig. 3.4 Myogenic progenitors within the developing ventral and dorsal muscular masses of the forelimb are also Hoxa13lin+.

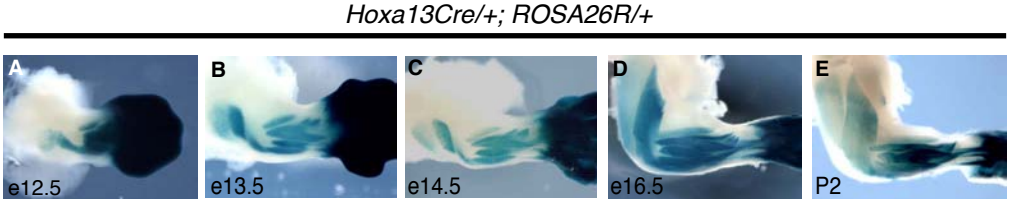

Fig. 3.5 At later stages of development, the distribution of Hoxa13lin+ cells in the forelimb has a pattern reminiscent of the forming musculature.

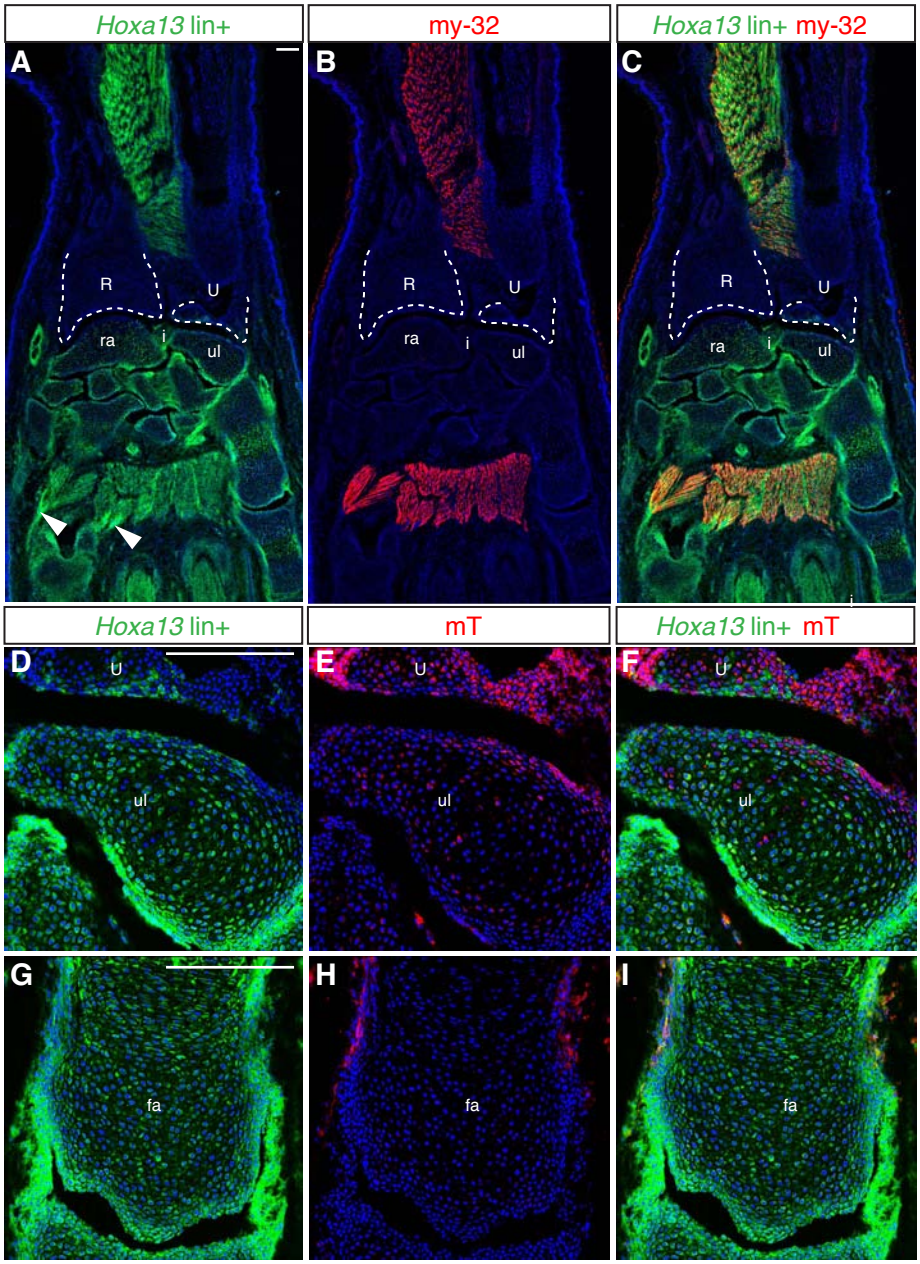

Fig. 3.6 The distribution of Hoxa13lin+ cells in the limb skeleton marks the transition between autopod and zeugopod.

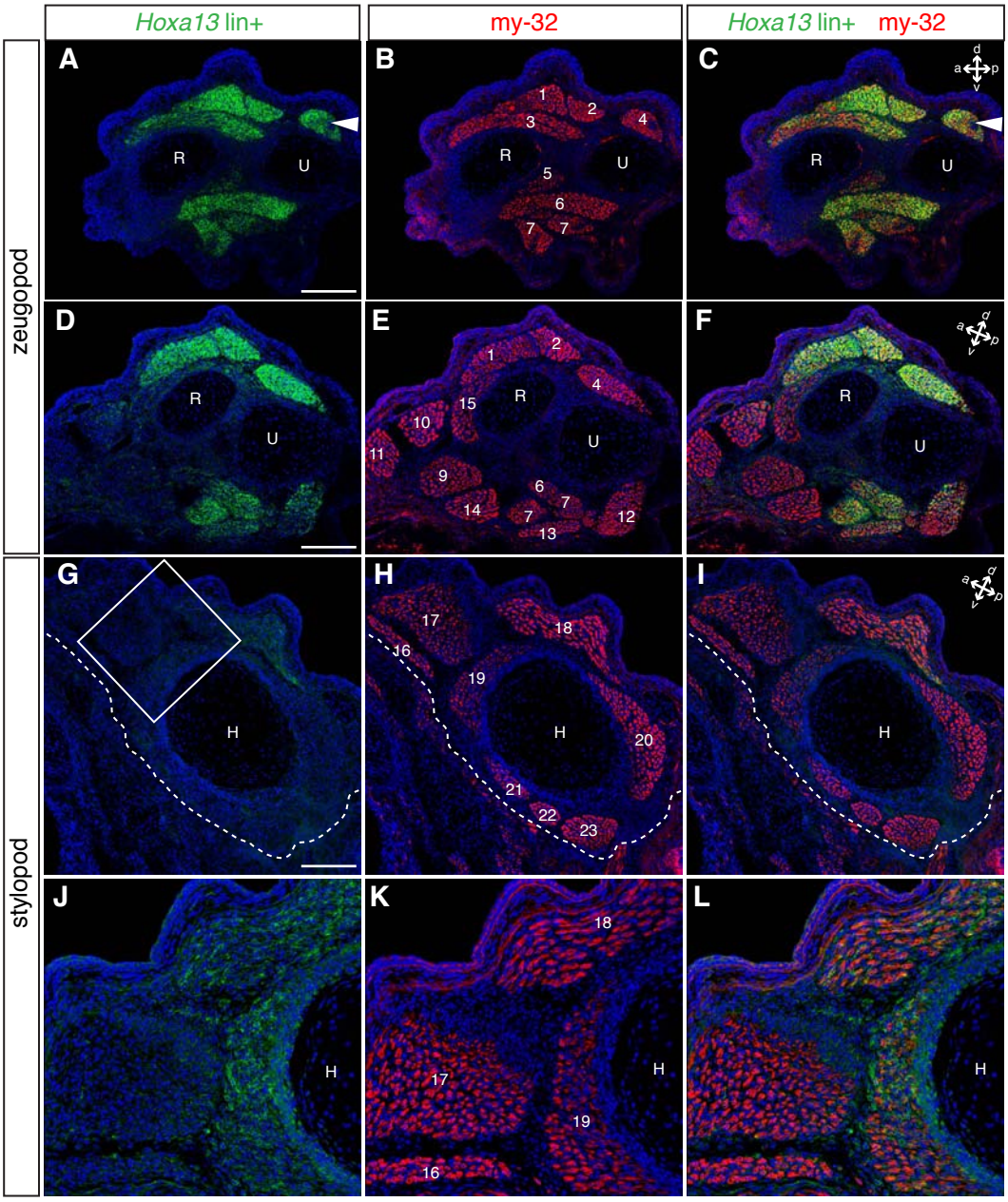

Fig. 3.7 Hoxa13lin+ contribution to muscular masses of the zeugopod and stylopod at e14.5.

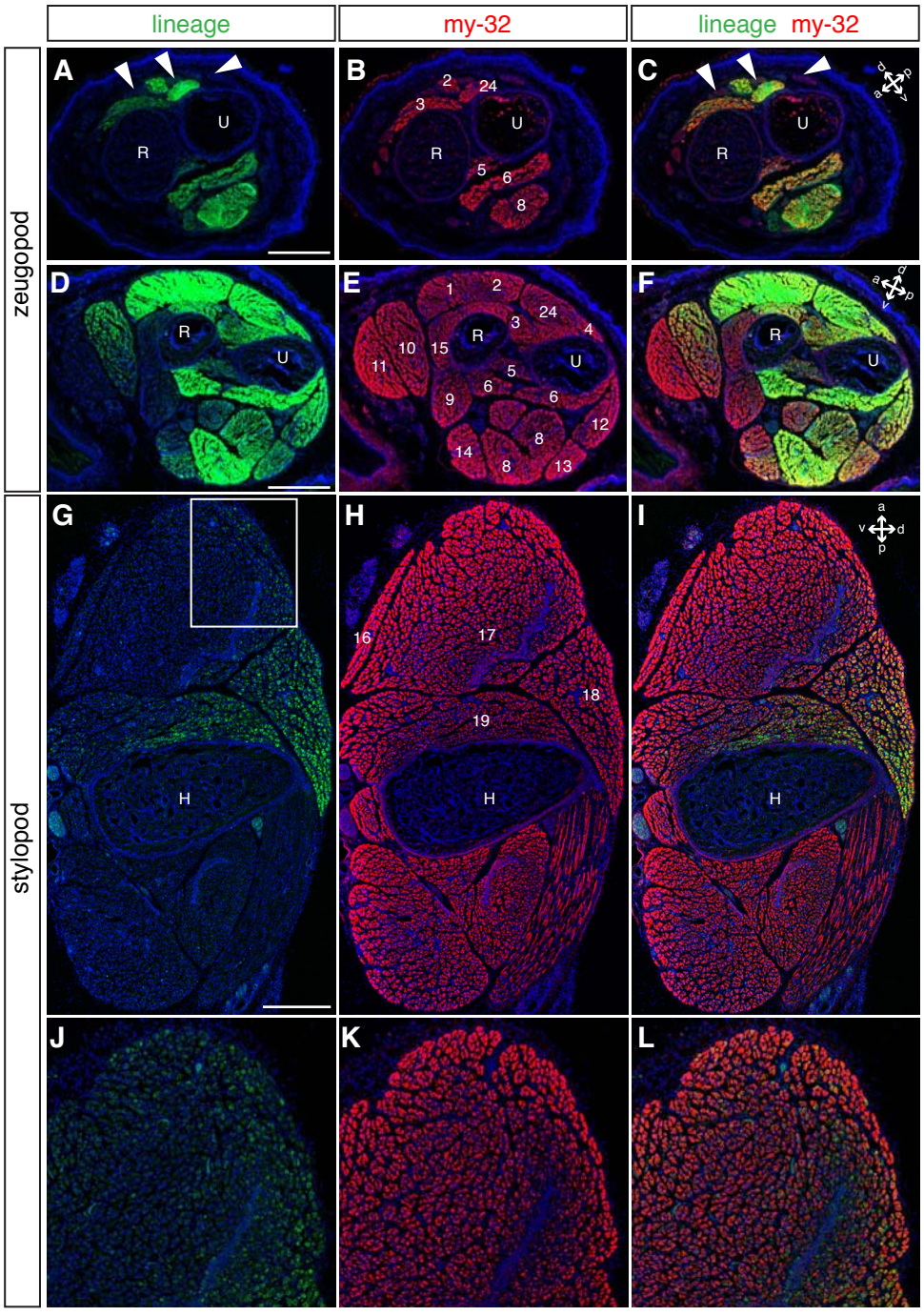

Fig. 3.8 Hoxa13lin+ contribution to muscular masses of the zeugopod and stylopod at e18.5.

Muscle #	Muscle name
1	Extensor digitorum communis
2	Extensor digitorum lateralis
3	Extensor pollicis
4	Extensor carpi ulnaris
5	Pronator quadratus
6	Flexor digitorum profundis
7	Flexor digitorum superficialis
8	Flexor digitorum sublimis
9	Supinator
10	Extensor carpi radialis brevis
11	Extensor carpi radialis longus
12	Flexor carpi ulnaris
13	Palmaris longus
14	Flexor carpi radialis
15	Pronator teres
16	Dorsoepitrachlearis brachii
17	Triceps brachii longus
18	Triceps brachii lateralis
19	Triceps brachii medialis
20	Brachialis
21	Coracobrachialis
22	Biceps brachii brevis
23	Biceps brachii longus
24	Extensor indicis propius

Table 3.1 Limb muscle nomenclature

Chapter 4: Discussion

4.1 *Hoxa* gene regulation in the extra-embryonic compartment.

In chapter 2, we established that, in the mouse, *Hoxa10*, *Hoxa11* and *Hoxa13* are expressed in the allantois, a hallmark of amniote vertebrates. When these 5' *Hoxa* genes are inactivated, embryos do not survive after e12 due to impaired development of the fetal vasculature within the placental labyrinth.

We generated deletion and genomic rearrangements inside and outside the *HoxA* cluster and used transgenic approaches to gain insights into the mechanisms underlying 5' *Hoxa* gene expression in the allantois. We found that *5'Hoxa* gene expression in this structure relies on an enhancer-sharing mechanism and not on the specificity of the 5' *Hoxa* promoters. We next determined that deletion of the entire *HoxA* cluster does not result in loss of expression of a reporter gene located on the 5' of the cluster in the allantois, suggesting that enhancer sequence(s) located outside the cluster are sufficient to drive expression in this structure. We found that the 50 kb intergenic region between *Hoxa13* and *Evx1* can trigger expression of a reporter gene in the allantois. However, the deletion of this region does not result in loss of *5'Hoxa* gene expression in the allantois, suggesting the existence of additional enhancer element(s).

Altogether, our studies provide preliminary insights into *Hoxa* gene regulation in the extra-embryonic compartment, however many important questions remain to be addressed.

4.1.1 Identification of *cis*-regulatory elements for *Hoxa* genes active in the allantois.

In some instances, *Hox* gene expression relies on local enhancers, however growing evidence suggests that *cis*-regulatory elements can be located far from their target promoters, as shown for *Hoxd* regulation in the limbs (Spitz et al., 2003; Spitz et al., 2005; Tschopp and Duboule, 2011). Various techniques have been employed to locate these regulatory sequences. Tagged BAC transgenes were used to scan the regulatory potential of the gene desert 5' to the *HoxD* cluster. This approach was combined with sequence conservation analysis between different species to map the enhancer regions more precisely, as enhancer elements often show a higher degree of inter-species conservation (reviewed in (Levine, 2010)). These techniques allowed the identification of two regions (GCR and Prox), located respectively 180 kb and 40 kb 5' to *Hoxd13,* in the gene desert. These regions are able to drive reporter gene expression in presumptive digits (Gonzalez et al., 2007; Spitz et al., 2003). While these regulatory sequences appear to be good candidates for the transcriptional control of *Hoxd* expression, the above experiments do not prove that *Hoxd* promoters are the actual targets of these regulatory elements. Moreover, it remains unclear whether additional enhancer elements are necessary to recapitulate the endogenous *Hoxd* gene expression in the digits.

Recent advances in sequencing technologies and molecular techniques have helped in the identification of transcriptional regulatory sequences (reviewed in (Levine, 2010)). It

was discovered that specific histone variants and histone modifications are associated with active enhancers (Ong and Corces, 2011). In addition, mapping of transcriptional co-activators binding (such as p300) was demonstrated to be a valuable tool to identify active enhancers (Blow et al., 2010; Visel et al., 2009). Distant enhancer-promoter interaction requires the formation of chromatin loops to physically trigger the association of distant DNA sequences within the cell nucleus (Engel and Tanimoto, 2000; Sexton et al., 2009). Various techniques have been recently developed to identify these contacts. For example, chromosome conformation capture (3C)- based techniques can be used to determine the interaction frequency of a specific promoter with regulatory regions located on the same chromosome, or even on different chromosomes (Gavrilov et al., 2009). Thus, the combined analysis of chromatin marks and chromatin conformation can be instrumental to identify enhancers active at different genomic loci.

Very recently, work from the Duboule lab has demonstrated that these techniques are valid tools to identify limb enhancers for *Hoxd* genes (Montavon et al., 2011). Using 3C, Montavon and collaborators confirmed for the first time the physical interaction *in vivo* between previously identified limb enhancers (GCR and Prox) and 5'*Hoxd* gene promoters. Moreover, analysis by chromosome conformation capture in the limb suggested the presence of additional limb enhancers located in a more remote location in the gene desert located on the centromeric side of the *HoxD* cluster. The further characterization of chromatin marks associated with active enhancers was used to verify that these sequences are likely limb enhancers. Transgenic analysis confirmed that some of these sequences are

able to drive expression of a reporter transgene in the limb. However, other elements cannot activate reporter transcription by themselves, and are probably required at the structural level, to generate a specific 3D chromatin conformation suitable for transcription. In fact, enhancer-promoter interaction, in some instances, may not be mediated by a single and direct chromatin loop, but could require a more complex 3D conformation, which would be favoured by the contacts of enhancers and promoter with other DNA sequences. Only the deletion of the entire 800 kb gene desert containing all these *cis*-regulatory elements results in the complete abrogation of 5' *Hoxd* genes in the limb (Montavon et al., 2011). Altogether, these data suggest that regulatory landscapes underlying *Hox* gene expression in embryonic tissues can be extremely complex, containing multiple and redundant enhancers active in the same tissues, some of which are very distant from the target gene promoters. Thus, the presence of multiple sequences driving expression of the same genes in a determined tissue could confer robustness to the system, making the expression of these genes particularly resilient to genetic mutations.

We have previously shown that the 50 kb intergenic region between *Hoxa13* and *Evx1* is able to drive reporter expression in the allantois. Our results, however, also demonstrate that other sequences are involved in 5' *Hoxa* gene regulation in this tissue. To identify these other *cis*-regulatory elements, a similar approach, as previously employed to locate enhancers of 5'*Hoxd* gene in the limb, could be used. 3C-based experiments combined with analysis of chromatin marks associated with active enhancers could be performed on allantois DNA. Chromatin marks associated with active enhancers and

binding sites for transcription co-activators, such as p300, could be measured using Chromatin Immunoprecipitation (ChIP), followed by high-throughput sequencing (ChIP-seq), in order to precisely map these regions (Park, 2009). Candidate regions could be subsequently tested by 3C for contacts with 5'*Hoxa* gene promoters. DNA sequences identified with these two techniques can be further tested by classical transgenesis. This unbiased approach will help to determine the position of other allantois enhancers, even if they are at a large distance in the chromosome. As in the case of the limbs, it is possible that some elements will be able to drive reporter gene expression in the allantois, while other sequences will be required to mediate the interaction of enhancers with target gene promoters, generating a specific 3D chromatin conformation suitable for transcription. It was previously shown that limb enhancers do not only contact *Hoxd* gene promoters, but also establish mutual interactions (Gonzalez et al., 2007; Montavon et al., 2011). To test whether a specific DNA element is essential in the allantois to maintain a 3D chromatin conformation permitting enhancer-promoter interactions, the sequential deletion of each previously identified region could be performed. Alternatively, as is the case for *Hoxd* genes in the limbs, it may be that only the deletion of the entire set of enhancers will result in the complete loss of 5'*Hoxa* gene expression in the allantois, suggesting that these regulatory elements are functionally redundant. Moreover, the establishment of the precise location of 5'*Hoxa* gene enhancer sequences in the allantois would also be crucial to predict binding sites for upstream regulators for 5'*Hoxa* genes.

4.1.2 Loss of enhancer activity upon fragmentation of the *IR50* transgene.

We have previously shown that the 50 kb intergenic region between *Hoxa13* and *Evx1* is able to drive reporter gene expression in the allantois. In an attempt to map more precisely the DNA sequence responsible for this activity, we subcloned the 50 kb fragment (*IR50*) into twelve smaller DNA regions and tested whether any of these smaller fragments could drive reporter gene expression in the allantois. Interestingly, none of the smaller transgenes was able to drive reporter gene expression in the allantois in our assay. Several possibilities could account for this result. As previously mentioned, enhancer elements are often, but not always, conserved among species. Thus, our experimental design, even if preserved the integrity of conservation sequences, could have simply led to the split of the enhancer(s) element(s) between two different transgenes. Alternatively, it is possible that the inability to trigger expression using our transgenic approach reflects an important role of the 3D organization of the *Hoxa13-Evx1* intergenic region in transcriptional control. In fact, it is possible that different regions within the *IR50* fragment need to physically interact in order to trigger expression of the reporter in the allantois. In this view, the synergism between two or more regions, any of which are unable, alone, to activate transcription, would be required to activate 5'*Hoxa* gene expression. Thus analysis of the DNA-DNA contacts in allantois cells between 5'*Hoxa* gene promoters and the 50 kb intergenic region will be instrumental to identify the putative enhancer(s). The candidate sequences could be further tested in transgenic assays to determine whether they can drive expression of a reporter gene. The identified regions could be tested in transgenic assays on their own, or

two or more identified regions could be combined together in the same transgene, to test if the interaction among these different elements is required for transcription.

We have shown that the *Hoxa13-Evx1* intergenic region is also able to drive reporter gene expression in the trunk (Fig. S 2.6). However, none of the smaller transgenes we generated was able to recapitulate this expression pattern, raising the possibility that the expression pattern in both trunk and in allantois could rely on the same regulatory sequences. Thus, the expression of *5'Hoxa* genes in the allantois could be the result of the subsequent functional co-option of the trunk enhancer, and not associated to the appearance of a novel cis-regulatory element. However, differences in 5' *Hoxa* gene activation in trunk and allantois would suggest that 5' *Hoxa* gene transcription relies on different mechanisms in these two regions. First, our genetic fate-mapping analysis of *Hoxa13*-expressing cells showed that only a subpopulation of mesenchymal cells of the allantois starts expressing *Hoxa13*, in contrast to the trunk. Furthermore, in the trunk, *Hoxa* genes are progressively activated in a sequential manner, *Hoxa1* being the first to be expressed and *Hoxa13* the last. In contrast, in the allantois, *Hoxa1* to *Hoxa9* are never expressed, and we coulnd't detect any differences in the timing of activation of *Hoxa10, Hoxa11* and *Hoxa13*.

To determine whether the expression of 5'*Hoxa* genes in the allantois was generated by co-option of trunk enhancer(s) or by evolutionarily novel regulatory elements, the DNA-DNA contacts established by 5'*Hoxa* gene promoters with DNA sequences within the 50

kb intergenic region in both allantois and trunk tissue could be determined. This analysis, combined with transgenic assays, will indicate whether the same region(s) within the 50 kb intergenic fragment contact 5'*Hoxa* gene promoters in both tissues or not.

4.1.3 *Hoxa* gene expression in the allantois is restricted to 5'*Hoxa* genes.

Another interesting question concerns the mechanisms by which *Hoxa* gene expression in the allantois is restricted to *Hoxa10, Hoxa11*, and *Hoxa13*. Our experiments suggest the presence of long distance enhancer element(s) necessary for 5'*Hoxa* gene expression in the allantois. However, the action of this/these enhancer(s) is specifically targeted to 5'*Hoxa* gene promoters, while the adjacent *Hoxa9* gene, as well as other 3'*Hoxa* genes, are not expressed in the allantois. It would be of interest to determine how this interaction between remote enhancer(s) is selectively restricted to this subset of *Hoxa* genes of the cluster. Interestingly, *Hoxa* gene expression in presumptive digits is also restricted to *Hoxa10*, *Hoxa11* and *Hoxa13* and involves an enhancer sharing mechanism. In fact, a reporter targeted to the 5' of *Hoxa13* is also expressed in the digits (not shown). Previous studies suggested that the regulation of 5'*Hoxa* genes in the limbs also relies on distant enhancers located on the 5' of *Hoxa13* (Lehoczky and Innis, 2008). We also found that the deletion of the 50 kb *Hoxa13-Evx1* intergenic region does not result in loss of 5'*Hoxa* gene expression in the limbs (not shown) suggesting that digit enhancer(s) are located at a remote position. Yet, only a subset of *Hoxa* genes is activated by this/these enhancer(s). One possibility is that an insulator element is involved in generating a transcription

boundary between *Hoxa9* and *Hoxa10*. Insulators are DNA sequences that preclude interaction between two DNA domains. Two different types of insulators have been identified. The first are enhancer-blocking insulators, which protect from activation by enhancers. Secondly, barrier insulators are involved in protecting DNA regions from heterochromatin-mediated silencing, and may be required to maintain heterochromatin organization (reviewed in (Gaszner and Felsenfeld, 2006)). The existence of both types of insulator elements has been described at the *β-globin* locus (Chung et al., 1993; Hebbes et al., 1994). Moreover, the presence of insulator sequences has been reported within the *Drosophila Hox* cluster (Akbari et al., 2006), and targeted rearrangements within mouse *Hox* clusters suggest that these sequences are also likely to be involved in the regulation of *Hox* gene expression in vertebrates (Kmita et al., 2000a; Kmita et al., 2002b).

Another possibility is that the exclusive expression of 5' *Hoxa* genes relies on the presence of promoter-proximal tethering elements in the vicinity of *Hoxa10, Hoxa11* and *Hoxa13* promoter (s). These elements have been identified in *Drosophila* and are required to mediate specific promoter-enhancer interaction within the *Antennapedia* complex (Calhoun et al., 2002; Ho et al., 2011), however, the presence of promoter-proximal tethering elements in vertebrate genomes has not yet been demonstrated.

To gather insights into the mechanism leading to the exclusive activation of specific 5'*Hoxa* genes in the allantois and in the limb, different deletions within the *HoxA* cluster could be generated, in order to delete putative insulators or promoter-proximal tethering elements. For example, if the deletion of the *Hoxa10-Hoxa13* region leads to the ectopic

activation of *Hoxa9*, it would suggest that promoter-proximal tethering elements are present in the *Hoxa10-Hoxa13* DNA fragment. If this deletion does not cause ectopic expression of *Hoxa9*, it would be more likely that an insulator element is located in the intergenic region between *Hoxa10* and *Hoxa9*. This last hypothesis could be challenged by generating a targeted deletion of the *Hoxa9-Hoxa10* intergenic region and by testing whether this configuration results in ectopic expression of *3'Hoxa* genes. Interestingly, a highly conserved DNA fragment is present just upstream of *Hoxa10*, and could be a good candidate insulator element. Preliminary experiments to test the ability of this DNA sequence to block enhancer activity could be performed *in vitro* as in (Lunyak et al., 2007)

4.1.4 Conclusion.

Altogether, the results presented in this thesis demonstrate that 5'*Hoxa* gene function in the allantois is required for embryonic survival. Moreover, we found that the regulatory mechanism underlying the expression of these genes in the extra-embryonic compartment is complex, suggesting that multiple *cis*-regulatory sequences are at work. Combined sequencing technologies and molecular techniques will be helpful to gain further understanding of 5'*Hoxa* gene transcriptional regulation in the allantois. Moreover, the generation of different deletions and rearrangements within the *HoxA* locus will allow a better understanding of *Hoxa* gene transcriptional control in the allantois and in other tissues/organs.

4.2 *Hoxa* gene function in the muscles.

In chapter 2, we showed that *Hoxa13* function in the extra-embryonic compartment is required for the proper development of foetal vasculature in the placental labyrinth. Our gene expression studies however, demonstrate that *Hoxa13* expression occurs transiently in the allantois, the structure from which the labyrinthine vasculature originates, and is not maintained in the labyrinth. In some instances therefore, *Hoxa13* function is important in domains in which its expression is not detected. Genetic fate-mapping experiments allow us to establish the ultimate fate of cells that express a gene of interest. Mapping all the organs and structures that originate from these cells is highly informative with respect to gene function. In chapter 3, to better characterize the role of *Hoxa13* and to identify potential novel aspects of its function, we generated a new *Hoxa13* allele to permanently label *Hoxa13*-expressing cells and their descendants (referred to as Hoxa13lin+). In the developing limbs, our lineage-tracing experiment demonstrated that Hoxa13lin+ cells contribute to all structures of the autopod. Moreover Hoxa13lin+ cells give rise to a specific subset of limb muscles within the zeugopod and stylopod, where they form muscular fibers. We found that *Hoxa13* expressing cells and their descendants are not equally distributed among the different muscular masses. Within a given muscle, fibers with similar Hoxa13lin+ cells contribution often cluster together. Altogether, our data and previous expression analyses suggest a function for Hoxa13 in the determination of muscle identity and/or in the biology of these muscles.

4.2.1 The *Hoxa13Cre* line is a tool to explore molecular identities of limb muscles.

Molecular differences have been identified among skeletal muscles committed to different tasks (Porter et al., 2001). However, whether muscles within the same anatomical structure, such as the limb, are characterized by an identical molecular profile remains unknown. Interestingly, we found that Hoxa13lin+ contribution to the different muscular masses of the limb is not the same, and muscles characterized by high GFP fluorescence emanating from the Cre reporter allele and muscle almost or completely deprived of GFP+ fibers can be distinguished. Thus, our *Hoxa13Cre* line could be a valuable tool to explore potential molecular differences between muscles characterized by different Hoxa13lin+ contributions. Specifically, GFP positive and negative fibers in each muscle could be easily separated using fluorescent activated-cell sorting from *Hoxa13Cre/+; mT/mG* animals. Subsequent expression profiling of the GFP+ population of one muscle could be compared to the GFP- of the other muscle using the RNA-seq technique to reveal differences in gene expression between the two cell populations (Wang et al., 2009). Moreover, the differential contribution of Hoxa13lin+ cells to the limb muscles raises the possibility that *Hoxa13* could be involved in establishing specific features of different muscles groups. To determine whether potential molecular differences between these two cell populations are a result of *Hoxa13* expression, the expression profile of the GFP+ population in

Hoxa13Cre/+; mT/mG could be compared to the GFP+ population of mice lacking *Hoxa13* function (*Hoxa13Cre/HoxaAflox*; *mT/mG* mutants, see next paragraph). This comparison could also help identify putative *Hoxa13* target genes in muscle.

Our genetic fate mapping in limbs demonstrated that Hoxa13lin+ cells differentially contribute to muscular fibers, in which differences in the Cre reporter GFP fluorescence can be detected. This heterogeneity could be explained either by a variable proportion of Hoxa13lin+/Hoxa13lin- myoblasts that fuse together to generate fibers, or by differences in the subsequent expression of *Hoxa13* after the fiber is formed. In the first case, the contribution of Hoxa13lin+ cells to the musculature would be established before myoblast fusion, while in the second case *Hoxa13* would also be expressed after fusion. To test these two hypotheses, a genetic approach could be used. The fusion of Hoxa13lin+ myoblasts could be blocked through the conditional inactivation of the small G-protein Rac1, which is essential for myoblast fusion in the mouse (Vasyutina et al., 2009). For this purpose, *Hoxa13Cre/+; Rac1flox/flox; mT/mG* embryos could be generated. In this mutant context, the fate of Hoxa13lin+ cells could be easily monitored using the Cre fluorescent reporter. Two scenarios are possible. In the first case, the Hoxa13lin+/GFP+ cell population could give rise only to mononucleated fibers, while multinucleated fibers will be mainly Hoxa13lin-/GFP-. This result would suggest that *Hoxa13* is only activated in myogenic progenitors before they fuse into the fiber, and Hoxa13lin- cells do not express *Hoxa13* after fusion. In contrast, if a significant percentage of multinucleated cells is

Hoxa13lin+/GFP+ it would indicate that, in these nuclei, *Hoxa13* activation occurred after myoblast fusion. In this case, the final Hoxa13lin+ contribution to each fiber would be established only at later stages.

4.2.2 The *Hoxa13Cre* line is a tool to explore *Hoxa13* function in limb muscles at later stages of development.

Hoxa13 homozygous mutants are embryonic lethal and do not survive after e15, precluding the analysis of potential mutant phenotypes in limb muscles at later stages of embryonic development and in adults. Our *Hoxa13Cre* allele is also a loss of function of *Hoxa13* due to the targeting of the Cre coding sequence at the first exon of the *Hoxa13* gene. Thus, in *Hoxa13Cre/HoxAflox* mutants, *Hoxa13* inactivation occurs in all cells that normally express *Hoxa13*. However, the time required for Cre mediated deletion of the *HoxA* cluster generates a slight delay in *Hoxa13* inactivation. This delay is sufficient to rescue the placental phenotype associated with *Hoxa13* loss-of-function, and *Hoxa13Cre/HoxAflox* mutants are fully viable and display a vasculature within the labyrinth comparable to wild-type specimens (Scotti and Kmita, 2012). However, these mice exhibit limb defects reminiscent of the phenotype associated with complete *Hoxa13* inactivation, including absence of digit 1, shortening and malformation of the other digits and fusion of the interdigital tissue (Fig. 2.5 in chapter 2). In fact, *Hoxa13* expression in the extra-embryonic tissues is only transient, while it is detected in the limbs over several days. Thus, *Hoxa13Cre/HoxAflox* mutant can be used to explore the role of *Hoxa13* at later

stages of development and may be a useful tool to investigate Hoxa13 function in the limb muscles. Moreover, our lineage fate-mapping analysis demonstrated that in the zeugopod and stylopod, *Hoxa13* expressing cells and their descendants only give rise to the muscles and not to skeletal elements. Thus, potential defects observed in the zeugopod and stylopod muscles of *Hoxa13Cre/HoxAflox* mutants would be a direct consequence of *Hoxa13* loss-of-function in this tissue, and not a secondary effect of *Hoxa13* inactivation in the skeleton.

In the mouse limb, the process of muscle formation starts soon after the onset of somitogenesis and continues after birth, throughout the entire life of the animal (reviewed in (Murphy and Kardon, 2011)). During muscle development, different phases of myogenesis can be identified (reviewed in (Biressi et al., 2007; Murphy and Kardon, 2011)). During embryonic myogenesis, which in the limbs begins around e10.5, the establishment of the basic muscular pattern takes place. Later on, during fetal and neonatal myogenesis (from e14.5 to P0 and from P0 to P21 respectively) muscles undergo a process of growth and maturation. Adult myogenesis promotes growth and repair of the damaged muscle tissue. During embryogenesis, primary fibers form from the fusion of embryonic myoblasts, and secondary fibers from fetal myoblasts (Kelly and Zacks, 1969). In the adult, muscle fibers can be classified on be basis of their speed of contraction (Wigmore and Evans, 2002).

Preliminary analysis performed on e14.5 *Hoxa13*-/- mutants reported the presence of defects in both shape and size of a subset of limb muscles, such as the flexor carpi radialis, the peroneus longus and brevis and the quadratus plantae (Yamamoto and Kuroiwa, 2003). However, analyses at later stages have been precluded by the embryonic lethality associated with *Hoxa13* inactivation. Expression analyses demonstrated that *Hoxa13* mRNA is still detectable in the limb muscles after e14.5 and in the adult tissue (Perez et al., 2010; Yamamoto and Kuroiwa, 2003). Thus, it is possible that *Hoxa13* function is required at later stages of muscle development for growth of the muscular masses and/or the determination of final morphology. To investigate this aspect, it would be of interest to perform analysis of *Hoxa13Cre*/*HoxAflox* limb muscles at late developmental stages, as many defects would be detectable only after e14.5. For this purpose, classical histology and immunohistochemistry on sections could be used to visualize muscular masses and to determine their size, organization and relative positions (Watson et al., 2009). Moreover, the different muscular masses could be analyzed for their fiber number and identity (primary/secondary, fast and slow), and the size of the fibers could be assessed. In fact, *Hoxa13* function could be required during embryonic or fetal myogenesis to form primary or secondary fibers respectively. In that case, the ratio between the primary and secondary fibers would be affected in *Hoxa13Cre*/*HoxAflox* mutants. An overall reduction in fiber number, without modification in the proportion of primary and secondary fibers, would suggest that *Hoxa13* function is required at both stages of myogenic differentiation.

After birth, the neonatal and adult muscle progenitors are mononucleated cells located between the cell membrane and the basal lamina of adult myofibers and are thus named satellite cells (Mauro, 1961). These cells proliferate and differentiate into myoblasts to complete the postnatal myogenic process and are reactivated in response to injury or damage to achieve muscle repair (Charge and Rudnicki, 2004). Previous *in vitro* experiments demonstrated that *Hoxa13* overexpression is able to downregulate the levels of the myogenic transcription factor *MyoD* in myoblast cells (Yamamoto and Kuroiwa, 2003). Thus, these results suggest that *Hoxa13* could be involved in the repression of *MyoD* and the myogenic differentiation program of a subset of muscle progenitors. It would be of interest to determine if satellite cells are also part of Hoxa13lin+ cell population. If this is the case, it could be established whether *Hoxa13* loss of function alters the number and/or the characteristics of satellite cells during normal postnatal muscle growth or after injury.

Neuromuscular junctions (NMJs) are synapses between motor neurons and the motor end plate. These form in specific region of the muscle, and expression of muscle-derived factors in these regions before innervation is essential for NMJ formation (neuromuscular pre-patterning) (Lin et al., 2001; Yang et al., 2001). Synapses form in excess and subsequently undergo refinement, in which supernumerary synapses are eliminated (Favero et al., 2009; Redfern, 1970). Hoxa13lin+ cells differentially contribute

to the various fibers within a specific muscle, and fibers characterized by similar GFP fluorescence are often clustered in the same region of the muscle. Thus, it is possible that *Hoxa13* could be involved in the establishment of neuromuscular connectivity, by controlling the expression of muscle-derived factors important for muscle pre-patterning in specific region of the muscle. To determine if *Hoxa13* function plays a role in muscle pre-patterning and/or NMJ formation or refinement, *Hoxa13Cre/HoxAflox* animals could be analyzed at different stages of development. At e14.5, before neuromuscular connections are established, the distribution of acetylcholine receptor and muscle-specific kinase, proteins involved in the neuromuscular pre-patterning process, can be tested by whole mount immunostaining (Chen et al., 2011). At later stages, the number, position, shape and functionality of the neuromuscular junctions could be assessed using immunostaining and electrophysiology techniques on dissected muscles (Chen et al., 2011; Noakes et al., 1995).

4.2.3 *Hoxa* gene function in muscle development.

The analyses of *Hoxa13Cre/HoxAflox* mutants will be informative to determine whether *Hoxa13* inactivation is associated with muscular defects. However, in many instances, the function of a specific *Hox* gene in a determined tissue cannot be assessed by the analysis of single loss-of-function allele because of functional redundancy among various *Hox* genes (see e.g. (Davis and Capecchi, 1996; Fromental-Ramain et al., 1996a; Fromental-Ramain et al., 1996b; Wellik and Capecchi, 2003)). In fact, the function of paralogous and/or non-paralogous genes in the same tissue can, in many cases, compensate

for the inactivation of the gene of interest. Thus, the simultaneous inactivation of more than one paralogous gene, or of different genes of the same cluster, can result in the appearance of novel mutant phenotypes, which are not present in single gene loss-of-function phenotype (Di-Poi et al., 2010a; Magnusson et al., 2007; Warot et al., 1997).

The expression of other *Hoxa* genes has been previously reported in limb muscles (Benson et al., 1995; Haack and Gruss, 1993; Houghton and Rosenthal, 1999; Yamamoto et al., 1998) raising the possibility that other *Hoxa* genes could be functional in this tissue. To assess their overall role in developing and adult muscles, *Hoxa* genes could be conditionally inactivated in all myogenic progenitors of the limb. The conditional inactivation could be achieved using a the *HoxAflox* allele and the *Pax3Cre* or *Lbx1Cre* deleter strains, which are expressed in all muscle progenitors of the body or all migrating myogenic cells in limb, tongue and diaphragm respectively (Engleka et al., 2005; Vasyutina et al., 2007). The limb muscles of *HoxAflox/flox; Pax3Cre* or *HoxAflox/flox; Lbx1Cre* embryos and mice could be analyzed at different stages of development as previously described for *Hoxa13Cre/HoxAflox* mutants.

In many instances, functional redundancy and synergism exist between *Hoxd* and *Hoxa* genes in developing limbs, and the inactivation of both clusters results in a limb phenotype much more severe than single cluster inactivation (Kmita et al., 2005). Moreover, preliminary results from Ashby and collaborators suggest that *Hoxd* genes are

also expressed in the developing limb muscles and *HoxD*-/- mutants present patterning defects in a subset of limb muscles (Ashby et al., 2002). Thus, the analysis of limb muscles from *Hoxa13Cre/HoxAflox*; *HoxD*-/- and *HoxAflox/flox; Pax3Cre; HoxD*-/- mutants could uncover novel phenotypes, or exacerbate defects already existent in single cluster inactivation.

4.2.4 Conclusion.

Altogether, our lineage fate-mapping experiments and previous expression analysis suggest that *Hoxa13* might be functional during limb muscle development. Importantly, the genetic tool we generated allow us to overcome the embryonic lethality associated to *Hoxa13* inactivation, and will be instrumental to explore *Hoxa13* function at later stages of muscle development. Moreover, our data provide support to previous evidence suggesting that *Hoxa and Hoxd* function during limb development might not be confined solely to the skeletal compartment. The analysis of *Hox* conditional inactivation in the different limb tissues will be critical in understanding the different roles of these genes in bone and muscle development.

Bibliography

Ahn, D., and Ho, R.K. (2008). Tri-phasic expression of posterior Hox genes during development of pectoral fins in zebrafish: implications for the evolution of vertebrate paired appendages. Dev Biol *322*, 220-233.

Akam, M. (1987). The molecular basis for metameric pattern in the Drosophila embryo. Development *101*, 1-22.

Akasaka, T., Kanno, M., Balling, R., Mieza, M.A., Taniguchi, M., and Koseki, H. (1996). A role for mel-18, a Polycomb group-related vertebrate gene, during theanteroposterior specification of the axial skeleton. Development *122*, 1513-1522.

Akbari, O.S., Bousum, A., Bae, E., and Drewell, R.A. (2006). Unraveling cis-regulatory mechanisms at the abdominal-A and Abdominal-B genes in the Drosophila bithorax complex. Dev Biol *293*, 294-304.

Alvares, L.E., Schubert, F.R., Thorpe, C., Mootoosamy, R.C., Cheng, L., Parkyn, G., Lumsden, A., and Dietrich, S. (2003). Intrinsic, Hox-dependent cues determine the fate of skeletal muscle precursors. Dev Cell *5*, 379-390.

Amemiya, C.T., Prohaska, S.J., Hill-Force, A., Cook, A., Wasserscheid, J., Ferrier, D.E., Pascual-Anaya, J., Garcia-Fernandez, J., Dewar, K., and Stadler, P.F. (2008). The amphioxus Hox cluster: characterization, comparative genomics, and evolution. J Exp Zool B Mol Dev Evol *310*, 465-477.

Amores, A., Force, A., Yan, Y.L., Joly, L., Amemiya, C., Fritz, A., Ho, R.K., Langeland, J., Prince, V., Wang, Y.L., *et al.* (1998). Zebrafish hox clusters and vertebrate genome evolution. Science *282*, 1711-1714.

Anson-Cartwright, L., Dawson, K., Holmyard, D., Fisher, S.J., Lazzarini, R.A., and Cross, J.C. (2000). The glial cells missing-1 protein is essential for branching morphogenesis in the chorioallantoic placenta. Nat Genet *25*, 311-314.

Ashby, P., Chinnah, T., Zakany, J., Duboule, D., and Tickle, C. (2002). 18 Muscle and tendon pattern is altered independently of skeletal pattern in HoxD mutant limbs. J Anat *201*, 422.

Aulehla, A., Wehrle, C., Brand-Saberi, B., Kemler, R., Gossler, A., Kanzler, B., and Herrmann, B.G. (2003). Wnt3a plays a major role in the segmentation clock controlling somitogenesis. Dev Cell *4*, 395-406.

Barrow, J.R., and Capecchi, M.R. (1996). Targeted disruption of the Hoxb-2 locus in mice interferes with expression of Hoxb-1 and Hoxb-4. Development *122*, 3817-3828.

Beck, F., Chawengsaksophak, K., Waring, P., Playford, R.J., and Furness, J.B. (1999). Reprogramming of intestinal differentiation and intercalary regeneration in Cdx2 mutant mice. Proc Natl Acad Sci U S A *96*, 7318-7323.

Beckers, J., and Duboule, D. (1998). Genetic analysis of a conserved sequence in the HoxD complex: regulatory redundancy or limitations of the transgenic approach? Dev Dyn *213*, 1-11.

Beddington, S.P. (1981). An autoradiographic analysis of the potency of embryonic ectoderm in the 8th day postimplantation mouse embryo. J Embryol Exp Morphol *64*, 87-104.

Bel-Vialar, S., Core, N., Terranova, R., Goudot, V., Boned, A., and Djabali, M. (2000). Altered retinoic acid sensitivity and temporal expression of Hox genes in polycomb-M33-deficient mice. Dev Biol *224*, 238-249.

Benson, G.V., Lim, H., Paria, B.C., Satokata, I., Dey, S.K., and Maas, R.L. (1996). Mechanisms of reduced fertility in Hoxa-10 mutant mice: uterine homeosis and loss of maternal Hoxa-10 expression. Development *122*, 2687-2696.

Benson, G.V., Nguyen, T.H., and Maas, R.L. (1995). The expression pattern of the murine Hoxa-10 gene and the sequence recognition of its homeodomain reveal specific properties of Abdominal B-like genes. Mol Cell Biol *15*, 1591-1601.

Biressi, S., Molinaro, M., and Cossu, G. (2007). Cellular heterogeneity during vertebrate skeletal muscle development. Dev Biol *308*, 281-293.

Blow, M.J., McCulley, D.J., Li, Z., Zhang, T., Akiyama, J.A., Holt, A., Plajzer-Frick, I., Shoukry, M., Wright, C., Chen, F., *et al.* (2010). ChIP-Seq identification of weakly conserved heart enhancers. Nat Genet *42*, 806-810.

Bonanomi, D., and Pfaff, S.L. (2010). Motor axon pathfinding. Cold Spring Harb Perspect Biol *2*, a001735.

Borg, T.K., and Caulfield, J.B. (1980). Morphology of connective tissue in skeletal muscle. Tissue Cell *12*, 197-207.

Branford, W.W., Benson, G.V., Ma, L., Maas, R.L., and Potter, S.S. (2000). Characterization of Hoxa-10/Hoxa-11 transheterozygotes reveals functional redundancy and regulatory interactions. Dev Biol *224*, 373-387.

Brooke, N.M., Garcia-Fernandez, J., and Holland, P.W. (1998). The ParaHox gene cluster is an evolutionary sister of the Hox gene cluster. Nature *392*, 920-922.

Brown, J.J., and Papaioannou, V.E. (1993). Ontogeny of hyaluronan secretion during early mouse development. Development *117*, 483-492.

Burke, A.C. (2000). Hox genes and the global patterning of the somitic mesoderm. Curr Top Dev Biol *47*, 155-181.

Burke, A.C., Nelson, C.E., Morgan, B.A., and Tabin, C. (1995). Hox genes and the evolution of vertebrate axial morphology. Development *121*, 333-346.

Byrd, K.N., and Shearn, A. (2003). ASH1, a Drosophila trithorax group protein, is required for methylation of lysine 4 residues on histone H3. Proc Natl Acad Sci U S A *100*, 11535-11540.

Calhoun, V.C., Stathopoulos, A., and Levine, M. (2002). Promoter-proximal tethering elements regulate enhancer-promoter specificity in the Drosophila Antennapedia complex. Proc Natl Acad Sci U S A *99*, 9243-9247.

Cao, R., and Zhang, Y. (2004). SUZ12 is required for both the histone methyltransferase activity and the silencing function of the EED-EZH2 complex. Mol Cell *15*, 57-67.

Carmeliet, P., Ferreira, V., Breier, G., Pollefeyt, S., Kieckens, L., Gertsenstein, M., Fahrig, M., Vandenhoeck, A., Harpal, K., Eberhardt, C., *et al.* (1996). Abnormal blood vessel development and lethality in embryos lacking a single VEGF allele. Nature *380*, 435-439.

Carpenter, E.M., Goddard, J.M., Chisaka, O., Manley, N.R., and Capecchi, M.R. (1993). Loss of Hox-A1 (Hox-1.6) function results in the reorganization of the murine hindbrain. Development *118*, 1063-1075.

Carroll, S.B. (1995). Homeotic genes and the evolution of arthropods and chordates. Nature *376*, 479-485.

Chadaram, S.R., Laskowski, M.B., and Madison, R.D. (2007). Topographic specificity within membranes of a single muscle detected in vitro. J Neurosci *27*, 13938-13948.

Chambeyron, S., and Bickmore, W.A. (2004). Chromatin decondensation and nuclear reorganization of the HoxB locus upon induction of transcription. Genes Dev *18*, 1119-1130.

Chambeyron, S., Da Silva, N.R., Lawson, K.A., and Bickmore, W.A. (2005). Nuclear re-organisation of the Hoxb complex during mouse embryonic development. Development *132*, 2215-2223.

Chang, H., Huylebroeck, D., Verschueren, K., Guo, Q., Matzuk, M.M., and Zwijsen, A. (1999). Smad5 knockout mice die at mid-gestation due to multiple embryonic and extraembryonic defects. Development *126*, 1631-1642.

Chapman, D.L., Garvey, N., Hancock, S., Alexiou, M., Agulnik, S.I., Gibson-Brown, J.J., Cebra-Thomas, J., Bollag, R.J., Silver, L.M., and Papaioannou, V.E. (1996). Expression of the T-box family genes, Tbx1-Tbx5, during early mouse development. Dev Dyn *206*, 379-390.

Charge, S.B., and Rudnicki, M.A. (2004). Cellular and molecular regulation of muscle regeneration. Physiol Rev *84*, 209-238.

Charite, J., de Graaff, W., Consten, D., Reijnen, M.J., Korving, J., and Deschamps, J. (1998). Transducing positional information to the Hox genes: critical interaction of cdx gene products with position-sensitive regulatory elements. Development *125*, 4349-4358.

Charite, J., de Graaff, W., and Deschamps, J. (1995). Specification of multiple vertebral identities by ectopically expressed Hoxb-8. Dev Dyn *204*, 13-21.

Chawengsaksophak, K., de Graaff, W., Rossant, J., Deschamps, J., and Beck, F. (2004). Cdx2 is essential for axial elongation in mouse development. Proc Natl Acad Sci U S A *101*, 7641-7645.

Chen, F., Greer, J., and Capecchi, M.R. (1998). Analysis of Hoxa7/Hoxb7 mutants suggests periodicity in the generation of the different sets of vertebrae. Mech Dev *77*, 49-57.

Chen, F., Liu, Y., Sugiura, Y., Allen, P.D., Gregg, R.G., and Lin, W. (2011). Neuromuscular synaptic patterning requires the function of skeletal muscle dihydropyridine receptors. Nat Neurosci *14*, 570-577.

Chevallier, A., Kieny, M., and Mauger, A. (1977). Limb-somite relationship: origin of the limb musculature. J Embryol Exp Morphol *41*, 245-258.

Chisaka, O., and Capecchi, M.R. (1991). Regionally restricted developmental defects resulting from targeted disruption of the mouse homeobox gene hox-1.5. Nature *350*, 473-479.

Chisaka, O., Musci, T.S., and Capecchi, M.R. (1992). Developmental defects of the ear, cranial nerves and hindbrain resulting from targeted disruption of the mouse homeobox gene Hox-1.6. Nature *355*, 516-520.

Cho, K.W., Morita, E.A., Wright, C.V., and De Robertis, E.M. (1991). Overexpression of a homeodomain protein confers axis-forming activity to uncommitted Xenopus embryonic cells. Cell *65*, 55-64.

Chourrout, D., Delsuc, F., Chourrout, P., Edvardsen, R.B., Rentzsch, F., Renfer, E., Jensen, M.F., Zhu, B., de Jong, P., Steele, R.E., *et al.* (2006). Minimal ProtoHox cluster inferred from bilaterian and cnidarian Hox complements. Nature *442*, 684-687.

Christ, B., and Brand-Saberi, B. (2002). Limb muscle development. Int J Dev Biol *46*, 905-914.

Chung, J.H., Whiteley, M., and Felsenfeld, G. (1993). A 5' element of the chicken beta-globin domain serves as an insulator in human erythroid cells and protects against position effect in Drosophila. Cell *74*, 505-514.

Ciruna, B., and Rossant, J. (2001). FGF signaling regulates mesoderm cell fate specification and morphogenetic movement at the primitive streak. Dev Cell *1*, 37-49.

Cockburn, K., and Rossant, J. (2010). Making the blastocyst: lessons from the mouse. J Clin Invest *120*, 995-1003.

Cohn, M.J., and Tickle, C. (1999). Developmental basis of limblessness and axial patterning in snakes. Nature *399*, 474-479.

Condie, B.G., and Capecchi, M.R. (1993). Mice homozygous for a targeted disruption of Hoxd-3 (Hox-4.1) exhibit anterior transformations of the first and second cervical vertebrae, the atlas and the axis. Development *119*, 579-595.

Copeland, N.G., Jenkins, N.A., and Court, D.L. (2001). Recombineering: a powerful new tool for mouse functional genomics. Nat Rev Genet *2*, 769-779.

Copp, A.J. (1995). Death before birth: clues from gene knockouts and mutations. Trends Genet *11*, 87-93.

Cordes, R., Schuster-Gossler, K., Serth, K., and Gossler, A. (2004). Specification of vertebral identity is coupled to Notch signalling and the segmentation clock. Development *131*, 1221-1233.

Core, N., Bel, S., Gaunt, S.J., Aurrand-Lions, M., Pearce, J., Fisher, A., and Djabali, M. (1997). Altered cellular proliferation and mesoderm patterning in Polycomb-M33-deficient mice. Development *124*, 721-729.

Cross, J.C., Nakano, H., Natale, D.R., Simmons, D.G., and Watson, E.D. (2006). Branching morphogenesis during development of placental villi. Differentiation *74*, 393-401.

Dasen, J.S., and Jessell, T.M. (2009). Hox networks and the origins of motor neuron diversity. Curr Top Dev Biol *88*, 169-200.

Daston, G., Lamar, E., Olivier, M., and Goulding, M. (1996). Pax-3 is necessary for migration but not differentiation of limb muscle precursors in the mouse. Development *122*, 1017-1027.

Davis, A.P., and Capecchi, M.R. (1994). Axial homeosis and appendicular skeleton defects in mice with a targeted disruption of hoxd-11. Development *120*, 2187-2198.

Davis, A.P., and Capecchi, M.R. (1996). A mutational analysis of the 5' HoxD genes: dissection of genetic interactions during limb development in the mouse. Development *122*, 1175-1185.

Davis, A.P., Witte, D.P., Hsieh-Li, H.M., Potter, S.S., and Capecchi, M.R. (1995). Absence of radius and ulna in mice lacking hoxa-11 and hoxd-11. Nature *375*, 791-795.

Davis, M.C., Dahn, R.D., and Shubin, N.H. (2007). An autopodial-like pattern of Hox expression in the fins of a basal actinopterygian fish. Nature *447*, 473-476.

de Rosa, R., Grenier, J.K., Andreeva, T., Cook, C.E., Adoutte, A., Akam, M., Carroll, S.B., and Balavoine, G. (1999). Hox genes in brachiopods and priapulids and protostome evolution. Nature *399*, 772-776.

Delaurier, A., Burton, N., Bennett, M., Baldock, R., Davidson, D., Mohun, T.J., and Logan, M.P. (2008). The Mouse Limb Anatomy Atlas: an interactive 3D tool for studying embryonic limb patterning. BMC Dev Biol *8*, 83.

Deschamps, J., van den Akker, E., Forlani, S., De Graaff, W., Oosterveen, T., Roelen, B., and Roelfsema, J. (1999). Initiation, establishment and maintenance of Hox gene expression patterns in the mouse. Int J Dev Biol *43*, 635-650.

Deschamps, J., and van Nes, J. (2005). Developmental regulation of the Hox genes during axial morphogenesis in the mouse. Development *132*, 2931-2942.

Deschamps, J., and Wijgerde, M. (1993). Two phases in the establishment of HOX expression domains. Dev Biol *156*, 473-480.

Di-Poi, N., Koch, U., Radtke, F., and Duboule, D. (2010a). Additive and global functions of HoxA cluster genes in mesoderm derivatives. Dev Biol *341*, 488-498.

Di-Poi, N., Montoya-Burgos, J.I., and Duboule, D. (2009). Atypical relaxation of structural constraints in Hox gene clusters of the green anole lizard. Genome Res *19*, 602-610.

Di-Poi, N., Montoya-Burgos, J.I., Miller, H., Pourquie, O., Milinkovitch, M.C., and Duboule, D. (2010b). Changes in Hox genes' structure and function during the evolution of the squamate body plan. Nature *464*, 99-103.

Ding, S., Wu, X., Li, G., Han, M., Zhuang, Y., and Xu, T. (2005). Efficient transposition of the piggyBac (PB) transposon in mammalian cells and mice. Cell *122*, 473-483.

Dolle, P., Dierich, A., LeMeur, M., Schimmang, T., Schuhbaur, B., Chambon, P., and Duboule, D. (1993). Disruption of the Hoxd-13 gene induces localized heterochrony leading to mice with neotenic limbs. Cell *75*, 431-441.

Dolle, P., and Duboule, D. (1989). Two gene members of the murine HOX-5 complex show regional and cell-type specific expression in developing limbs and gonads. EMBO J *8*, 1507-1515.

Dolle, P., Izpisua-Belmonte, J.C., Brown, J.M., Tickle, C., and Duboule, D. (1991). HOX-4 genes and the morphogenesis of mammalian genitalia. Genes Dev *5*, 1767-1767.

Dolle, P., Izpisua-Belmonte, J.C., Falkenstein, H., Renucci, A., and Duboule, D. (1989). Coordinate expression of the murine Hox-5 complex homoeobox-containing genes during limb pattern formation. Nature *342*, 767-772.

Donnenfeld, A.E., Schrager, D.S., and Corson, S.L. (1992). Update on a family with hand-foot-genital syndrome: hypospadias and urinary tract abnormalities in two boys from the fourth generation. Am J Med Genet *44*, 482-484.

Downs, K.M. (1998). The murine allantois. Curr Top Dev Biol *39*, 1-33.

Downs, K.M. (2009). The enigmatic primitive streak: prevailing notions and challenges concerning the body axis of mammals. Bioessays *31*, 892-902.

Downs, K.M., and Bertler, C. (2000). Growth in the pre-fusion murine allantois. Anat Embryol (Berl) *202*, 323-331.

Downs, K.M., and Davies, T. (1993). Staging of gastrulating mouse embryos by morphological landmarks in the dissecting microscope. Development *118*, 1255-1266.

Downs, K.M., and Gardner, R.L. (1995). An investigation into early placental ontogeny: allantoic attachment to the chorion is selective and developmentally regulated. Development *121*, 407-416.

Downs, K.M., Gifford, S., Blahnik, M., and Gardner, R.L. (1998). Vascularization in the murine allantois occurs by vasculogenesis without accompanying erythropoiesis. Development *125*, 4507-4520.

Downs, K.M., and Harmann, C. (1997). Developmental potency of the murine allantois. Development *124*, 2769-2780.

Downs, K.M., Hellman, E.R., McHugh, J., Barrickman, K., and Inman, K.E. (2004). Investigation into a role for the primitive streak in development of the murine allantois. Development *131*, 37-55.

Drake, C.J., and Fleming, P.A. (2000). Vasculogenesis in the day 6.5 to 9.5 mouse embryo. Blood *95*, 1671-1679.

Duarte, A., Hirashima, M., Benedito, R., Trindade, A., Diniz, P., Bekman, E., Costa, L., Henrique, D., and Rossant, J. (2004). Dosage-sensitive requirement for mouse Dll4 in artery development. Genes Dev *18*, 2474-2478.

Duboule, D. (1992). The vertebrate limb: a model system to study the Hox/HOM gene network during development and evolution. Bioessays *14*, 375-384.

Duboule, D. (1994). Temporal colinearity and the phylotypic progression: a basis for the stability of a vertebrate Bauplan and the evolution of morphologies through heterochrony. Dev Suppl, 135-142.

Duboule, D. (2007). The rise and fall of Hox gene clusters. Development *134*, 2549-2560.

Duboule, D., and Dolle, P. (1989). The structural and functional organization of the murine HOX gene family resembles that of Drosophila homeotic genes. EMBO J *8*, 1497-1505.

Duboule, D., and Morata, G. (1994). Colinearity and functional hierarchy among genes of the homeotic complexes. Trends Genet *10*, 358-364.

Dubrulle, J., McGrew, M.J., and Pourquie, O. (2001). FGF signaling controls somite boundary position and regulates segmentation clock control of spatiotemporal Hox gene activation. Cell *106*, 219-232.

Dubrulle, J., and Pourquie, O. (2004). fgf8 mRNA decay establishes a gradient that couples axial elongation to patterning in the vertebrate embryo. Nature *427*, 419-422.

Dumont, D.J., Fong, G.H., Puri, M.C., Gradwohl, G., Alitalo, K., and Breitman, M.L. (1995). Vascularization of the mouse embryo: a study of flk-1, tek, tie, and vascular endothelial growth factor expression during development. Dev Dyn *203*, 80-92.

Dupe, V., Davenne, M., Brocard, J., Dolle, P., Mark, M., Dierich, A., Chambon, P., and Rijli, F.M. (1997). In vivo functional analysis of the Hoxa-1 3' retinoic acid response element (3'RARE). Development *124*, 399-410.

Ekker, S.C., Jackson, D.G., von Kessler, D.P., Sun, B.I., Young, K.E., and Beachy, P.A. (1994). The degree of variation in DNA sequence recognition among four Drosophila homeotic proteins. EMBO J *13*, 3551-3560.

Engel, J.D., and Tanimoto, K. (2000). Looping, linking, and chromatin activity: new insights into beta-globin locus regulation. Cell *100*, 499-502.

Engleka, K.A., Gitler, A.D., Zhang, M., Zhou, D.D., High, F.A., and Epstein, J.A. (2005). Insertion of Cre into the Pax3 locus creates a new allele of Splotch and identifies unexpected Pax3 derivatives. Dev Biol *280*, 396-406.

Farley, F.W., Soriano, P., Steffen, L.S., and Dymecki, S.M. (2000). Widespread recombinase expression using FLPeR (flipper) mice. Genesis *28*, 106-110.

Favero, M., Massella, O., Cangiano, A., and Buffelli, M. (2009). On the mechanism of action of muscle fibre activity in synapse competition and elimination at the mammalian neuromuscular junction. Eur J Neurosci *29*, 2327-2334.

Favier, B., Le Meur, M., Chambon, P., and Dolle, P. (1995). Axial skeleton homeosis and forelimb malformations in Hoxd-11 mutant mice. Proc Natl Acad Sci U S A *92*, 310-314.

Favier, B., Rijli, F.M., Fromental-Ramain, C., Fraulob, V., Chambon, P., and Dolle, P. (1996). Functional cooperation between the non-paralogous genes Hoxa-10 and Hoxd-11 in the developing forelimb and axial skeleton. Development *122*, 449-460.

Feng, G., Laskowski, M.B., Feldheim, D.A., Wang, H., Lewis, R., Frisen, J., Flanagan, J.G., and Sanes, J.R. (2000). Roles for ephrins in positionally selective synaptogenesis between motor neurons and muscle fibers. Neuron *25*, 295-306.

Ferrara, N., Carver-Moore, K., Chen, H., Dowd, M., Lu, L., O'Shea, K.S., Powell-Braxton, L., Hillan, K.J., and Moore, M.W. (1996). Heterozygous embryonic lethality induced by targeted inactivation of the VEGF gene. Nature *380*, 439-442.

Ferrier, D.E., Minguillon, C., Holland, P.W., and Garcia-Fernandez, J. (2000). The amphioxus Hox cluster: deuterostome posterior flexibility and Hox14. Evol Dev *2*, 284-293.

Fischer, A., Schumacher, N., Maier, M., Sendtner, M., and Gessler, M. (2004). The Notch target genes Hey1 and Hey2 are required for embryonic vascular development. Genes Dev *18*, 901-911.

Fong, G.H., Rossant, J., Gertsenstein, M., and Breitman, M.L. (1995). Role of the Flt-1 receptor tyrosine kinase in regulating the assembly of vascular endothelium. Nature *376*, 66-70.

Force, A., Amores, A., and Postlethwait, J.H. (2002). Hox cluster organization in the jawless vertebrate Petromyzon marinus. J Exp Zool *294*, 30-46.

Forlani, S., Lawson, K.A., and Deschamps, J. (2003). Acquisition of Hox codes during gastrulation and axial elongation in the mouse embryo. Development *130*, 3807-3819.

Francis-West, P.H., Antoni, L., and Anakwe, K. (2003). Regulation of myogenic differentiation in the developing limb bud. J Anat *202*, 69-81.

Freitas, R., Zhang, G., and Cohn, M.J. (2007). Biphasic Hoxd gene expression in shark paired fins reveals an ancient origin of the distal limb domain. PLoS One *2*, e754.

Fried, C., Prohaska, S.J., and Stadler, P.F. (2004). Exclusion of repetitive DNA elements from gnathostome Hox clusters. J Exp Zool B Mol Dev Evol *302*, 165-173.

Frisen, L., Lagerstedt, K., Tapper-Persson, M., Kockum, I., and Nordenskjold, A. (2003). A novel duplication in the HOXA13 gene in a family with atypical hand-foot-genital syndrome. J Med Genet *40*, e49.

Fromental-Ramain, C., Warot, X., Lakkaraju, S., Favier, B., Haack, H., Birling, C., Dierich, A., Doll e, P., and Chambon, P. (1996a). Specific and redundant functions of the paralogous Hoxa-9 and Hoxd-9 genes in forelimb and axial skeleton patterning. Development *122*, 461-472.

Fromental-Ramain, C., Warot, X., Messadecq, N., LeMeur, M., Dolle, P., and Chambon, P. (1996b). Hoxa-13 and Hoxd-13 play a crucial role in the patterning of the limb autopod. Development *122*, 2997-3011.

Fujiwara, T., Dunn, N.R., and Hogan, B.L. (2001). Bone morphogenetic protein 4 in the extraembryonic mesoderm is required for allantois development and the localization and survival of primordial germ cells in the mouse. Proc Natl Acad Sci U S A *98*, 13739-13744.

Garcia-Fernandez, J. (2005). Hox, ParaHox, ProtoHox: facts and guesses. Heredity *94*, 145-152.

Garcia-Fernandez, J., and Holland, P.W. (1994). Archetypal organization of the amphioxus Hox gene cluster. Nature *370*, 563-566.

Gaszner, M., and Felsenfeld, G. (2006). Insulators: exploiting transcriptional and epigenetic mechanisms. Nat Rev Genet *7*, 703-713.

Gaunt, S.J. (1988). Mouse homeobox gene transcripts occupy different but overlapping domains in embryonic germ layers and organs: a comparison of Hox-3.1 and Hox-1.5. Development *103*, 135-144.

Gavalas, A., and Krumlauf, R. (2000). Retinoid signalling and hindbrain patterning. Curr Opin Genet Dev *10*, 380-386.

Gavrilov, A., Eivazova, E., Priozhkova, I., Lipinski, M., Razin, S., and Vassetzky, Y. (2009). Chromosome conformation capture (from 3C to 5C) and its ChIP-based modification. Methods Mol Biol *567*, 171-188.

Gendron, R.L., Paradis, H., Hsieh-Li, H.M., Lee, D.W., Potter, S.S., and Markoff, E. (1997). Abnormal uterine stromal and glandular function associated with maternal reproductive defects in Hoxa-11 null mice. Biol Reprod *56*, 1097-1105.

Gendron-Maguire, M., Mallo, M., Zhang, M., and Gridley, T. (1993). Hoxa-2 mutant mice exhibit homeotic transformation of skeletal elements derived from cranial neural crest. Cell *75*, 1317-1331.

Gerard, M., Duboule, D., and Zakany, J. (1993). Structure and activity of regulatory elements involved in the activation of the Hoxd-11 gene during late gastrulation. EMBO J *12*, 3539-3550.

Gluecksohn-Schoenheimer, S. (1944). The Development of Normal and Homozygous Brachy (T/T) Mouse Embryos in the Extraembryonic Coelom of the Chick. Proc Natl Acad Sci U S A *30*, 134-140.

Goddard, J.M., Rossel, M., Manley, N.R., and Capecchi, M.R. (1996). Mice with targeted disruption of Hoxb-1 fail to form the motor nucleus of the VIIth nerve. Development *122*, 3217-3228.

Gonzalez, F., Duboule, D., and Spitz, F. (2007). Transgenic analysis of Hoxd gene regulation during digit development. Dev Biol *306*, 847-859.

Goodman, F.R., Bacchelli, C., Brady, A.F., Brueton, L.A., Fryns, J.P., Mortlock, D.P., Innis, J.W., Holmes, L.B., Donnenfeld, A.E., Feingold, M.*, et al.* (2000). Novel HOXA13 mutations and the phenotypic spectrum of hand-foot-genital syndrome. Am J Hum Genet *67*, 197-202.

Gould, A. (1997). Functions of mammalian Polycomb group and trithorax group related genes. Curr Opin Genet Dev *7*, 488-494.

Gould, A., Morrison, A., Sproat, G., White, R.A., and Krumlauf, R. (1997). Positive cross-regulation and enhancer sharing: two mechanisms for specifying overlapping Hox expression patterns. Genes Dev *11*, 900-913.

Graham, A., Papalopulu, N., and Krumlauf, R. (1989). The murine and Drosophila homeobox gene complexes have common features of organization and expression. Cell *57*, 367-378.

Gregoire, D., and Kmita, M. (2008). Recombination between inverted loxP sites is cytotoxic for proliferating cells and provides a simple tool for conditional cell ablation. Proc Natl Acad Sci U S A *105*, 14492-14496.

Gurtner, G.C., Davis, V., Li, H., McCoy, M.J., Sharpe, A., and Cybulsky, M.I. (1995). Targeted disruption of the murine VCAM1 gene: essential role of VCAM-1 in chorioallantoic fusion and placentation. Genes Dev *9*, 1-14.

Haack, H., and Gruss, P. (1993). The establishment of murine Hox-1 expression domains during patterning of the limb. Dev Biol *157*, 410-422.

Halal, F. (1988). The hand-foot-genital (hand-foot-uterus) syndrome: family report and update. Am J Med Genet *30*, 793-803.

Hashimoto, K., Yokouchi, Y., Yamamoto, M., and Kuroiwa, A. (1999). Distinct signaling molecules control Hoxa-11 and Hoxa-13 expression in the muscle precursor and mesenchyme of the chick limb bud. Development *126*, 2771-2783.

Hasson, P. (2011). "Soft" tissue patterning: muscles and tendons of the limb take their form. Dev Dyn *240*, 1100-1107.

Hasson, P., DeLaurier, A., Bennett, M., Grigorieva, E., Naiche, L.A., Papaioannou, V.E., Mohun, T.J., and Logan, M.P. (2010). Tbx4 and tbx5 acting in connective tissue are required for limb muscle and tendon patterning. Dev Cell *18*, 148-156.

Hebbes, T.R., Clayton, A.L., Thorne, A.W., and Crane-Robinson, C. (1994). Core histone hyperacetylation co-maps with generalized DNase I sensitivity in the chicken beta-globin chromosomal domain. EMBO J *13*, 1823-1830.

Herault, Y., Beckers, J., Gerard, M., and Duboule, D. (1999). Hox gene expression in limbs: colinearity by opposite regulatory controls. Dev Biol *208*, 157-165.

Herault, Y., Fraudeau, N., Zakany, J., and Duboule, D. (1997). Ulnaless (Ul), a regulatory mutation inducing both loss-of-function and gain-of-function of posterior Hoxd genes. Development *124*, 3493-3500.

Herault, Y., Rassoulzadegan, M., Cuzin, F., and Duboule, D. (1998). Engineering chromosomes in mice through targeted meiotic recombination (TAMERE). Nat Genet *20*, 381-384.

Hiratsuka, S., Minowa, O., Kuno, J., Noda, T., and Shibuya, M. (1998). Flt-1 lacking the tyrosine kinase domain is sufficient for normal development and angiogenesis in mice. Proc Natl Acad Sci U S A *95*, 9349-9354.

Hiratsuka, S., Nakao, K., Nakamura, K., Katsuki, M., Maru, Y., and Shibuya, M. (2005). Membrane fixation of vascular endothelial growth factor receptor 1 ligand-binding domain is important for vasculogenesis and angiogenesis in mice. Mol Cell Biol *25*, 346-354.

Ho, M.C., Schiller, B.J., Akbari, O.S., Bae, E., and Drewell, R.A. (2011). Disruption of the abdominal-B promoter tethering element results in a loss of long-range enhancer-directed Hox gene expression in Drosophila. PLoS One *6*, e16283.

Hoey, T., and Levine, M. (1988). Divergent homeo box proteins recognize similar DNA sequences in Drosophila. Nature *332*, 858-861.

Hogan, B.L., Thaller, C., and Eichele, G. (1992). Evidence that Hensen's node is a site of retinoic acid synthesis. Nature *359*, 237-241.

Holland, P.W., and Garcia-Fernandez, J. (1996). Hox genes and chordate evolution. Dev Biol *173*, 382-395.

Horan, G.S., Kovacs, E.N., Behringer, R.R., and Featherstone, M.S. (1995a). Mutations in paralogous Hox genes result in overlapping homeotic transformations of the axial skeleton: evidence for unique and redundant function. Dev Biol *169*, 359-372.

Horan, G.S., Ramirez-Solis, R., Featherstone, M.S., Wolgemuth, D.J., Bradley, A., and Behringer, R.R. (1995b). Compound mutants for the paralogous hoxa-4, hoxb-4, and hoxd-4 genes show more complete homeotic transformations and a dose-dependent increase in the number of vertebrae transformed. Genes Dev *9*, 1667-1677.

Houghton, L., and Rosenthal, N. (1999). Regulation of a muscle-specific transgene by persistent expression of Hox genes in postnatal murine limb muscle. Dev Dyn *216*, 385-397.

Houle, M., Sylvestre, J.R., and Lohnes, D. (2003). Retinoic acid regulates a subset of Cdx1 function in vivo. Development *130*, 6555-6567.

Hsieh-Li, H.M., Witte, D.P., Weinstein, M., Branford, W., Li, H., Small, K., and Potter, S.S. (1995). Hoxa 11 structure, extensive antisense transcription, and function in male and female fertility. Development *121*, 1373-1385.

Hummel, K.P. (1970). Hypodactyly, a semidominant lethal mutation in mice. J Hered *61*, 219-220.

Iimura, T., and Pourquie, O. (2006). Collinear activation of Hoxb genes during gastrulation is linked to mesoderm cell ingression. Nature *442*, 568-571.

Iimura, T., and Pourquie, O. (2007). Hox genes in time and space during vertebrate body formation. Dev Growth Differ *49*, 265-275.

Inman, K.E., and Downs, K.M. (2006). Brachyury is required for elongation and vasculogenesis in the murine allantois. Development *133*, 2947-2959.

Inman, K.E., and Downs, K.M. (2007). The murine allantois: emerging paradigms in development of the mammalian umbilical cord and its relation to the fetus. Genesis *45*, 237-258.

Irvine, S.Q., Carr, J.L., Bailey, W.J., Kawasaki, K., Shimizu, N., Amemiya, C.T., and Ruddle, F.H. (2002). Genomic analysis of Hox clusters in the sea lamprey Petromyzon marinus. J Exp Zool *294*, 47-62.

Izpisua-Belmonte, J.C., Tickle, C., Dolle, P., Wolpert, L., and Duboule, D. (1991). Expression of the homeobox Hox-4 genes and the specification of position in chick wing development. Nature *350*, 585-589.

Jegalian, B.G., and De Robertis, E.M. (1992). Homeotic transformations in the mouse induced by overexpression of a human Hox3.3 transgene. Cell *71*, 901-910.

Johanson, Z., Joss, J., Boisvert, C.A., Ericsson, R., Sutija, M., and Ahlberg, P.E. (2007). Fish fingers: digit homologues in sarcopterygian fish fins. J Exp Zool B Mol Dev Evol *308*, 757-768.

Jorgensen, E.M., Ruman, J.I., Doherty, L., and Taylor, H.S. (2010). A novel mutation of HOXA13 in a family with hand-foot-genital syndrome and the role of polyalanine expansions in the spectrum of Mullerian fusion anomalies. Fertil Steril *94*, 1235-1238.

Kardon, G., Harfe, B.D., and Tabin, C.J. (2003). A Tcf4-positive mesodermal population provides a prepattern for vertebrate limb muscle patterning. Dev Cell *5*, 937-944.

Kaufman, T.C., Lewis, R., and Wakimoto, B. (1980). Cytogenetic Analysis of Chromosome 3 in DROSOPHILA MELANOGASTER: The Homoeotic Gene Complex in Polytene Chromosome Interval 84a-B. Genetics *94*, 115-133.

Kelly, A.M., and Zacks, S.I. (1969). The histogenesis of rat intercostal muscle. J Cell Biol *42*, 135-153.

Kessel, M., Balling, R., and Gruss, P. (1990). Variations of cervical vertebrae after expression of a Hox-1.1 transgene in mice. Cell *61*, 301-308.

Kessel, M., and Gruss, P. (1991). Homeotic transformations of murine vertebrae and concomitant alteration of Hox codes induced by retinoic acid. Cell *67*, 89-104.

Kinder, S.J., Tsang, T.E., Quinlan, G.A., Hadjantonakis, A.K., Nagy, A., and Tam, P.P. (1999). The orderly allocation of mesodermal cells to the extraembryonic structures and the anteroposterior axis during gastrulation of the mouse embryo. Development *126*, 4691-4701.

Kissinger, C.R., Liu, B.S., Martin-Blanco, E., Kornberg, T.B., and Pabo, C.O. (1990). Crystal structure of an engrailed homeodomain-DNA complex at 2.8 A resolution: a framework for understanding homeodomain-DNA interactions. Cell *63*, 579-590.

Klein, R. (2004). Eph/ephrin signaling in morphogenesis, neural development and plasticity. Curr Opin Cell Biol *16*, 580-589.

Kleinjan, D.A., Seawright, A., Schedl, A., Quinlan, R.A., Danes, S., and van Heyningen, V. (2001). Aniridia-associated translocations, DNase hypersensitivity, sequence comparison and transgenic analysis redefine the functional domain of PAX6. Hum Mol Genet *10*, 2049-2059.

Kmita, M., and Duboule, D. (2003). Organizing axes in time and space; 25 years of colinear tinkering. Science *301*, 331-333.

Kmita, M., Fraudeau, N., Herault, Y., and Duboule, D. (2002a). Serial deletions and duplications suggest a mechanism for the collinearity of Hoxd genes in limbs. Nature *420*, 145-150.

Kmita, M., Kondo, T., and Duboule, D. (2000a). Targeted inversion of a polar silencer within the HoxD complex re-allocates domains of enhancer sharing. Nat Genet *26*, 451-454.

Kmita, M., Tarchini, B., Duboule, D., and Herault, Y. (2002b). Evolutionary conserved sequences are required for the insulation of the vertebrate Hoxd complex in neural cells. Development *129*, 5521-5528.

Kmita, M., Tarchini, B., Zakany, J., Logan, M., Tabin, C.J., and Duboule, D. (2005). Early developmental arrest of mammalian limbs lacking HoxA/HoxD gene function. Nature *435*, 1113-1116.

Kmita, M., van Der Hoeven, F., Zakany, J., Krumlauf, R., and Duboule, D. (2000b). Mechanisms of Hox gene colinearity: transposition of the anterior Hoxb1 gene into the posterior HoxD complex. Genes Dev *14*, 198-211.

Knosp, W.M., Scott, V., Bachinger, H.P., and Stadler, H.S. (2004). HOXA13 regulates the expression of bone morphogenetic proteins 2 and 7 to control distal limb morphogenesis. Development *131*, 4581-4592.

Kondo, T., Dolle, P., Zakany, J., and Duboule, D. (1996). Function of posterior HoxD genes in the morphogenesis of the anal sphincter. Development *122*, 2651-2659.

Kondo, T., and Duboule, D. (1999). Breaking colinearity in the mouse HoxD complex. Cell *97*, 407-417.

Kondo, T., Herault, Y., Zakany, J., and Duboule, D. (1998a). Genetic control of murine limb morphogenesis: relationships with human syndromes and evolutionary relevance. Mol Cell Endocrinol *140*, 3-8.

Kondo, T., Zakany, J., and Duboule, D. (1998b). Control of colinearity in AbdB genes of the mouse HoxD complex. Mol Cell *1*, 289-300.

Kondo, T., Zakany, J., Innis, J.W., and Duboule, D. (1997). Of fingers, toes and penises. Nature *390*, 29.

Kostic, D., and Capecchi, M.R. (1994). Targeted disruptions of the murine Hoxa-4 and Hoxa-6 genes result in homeotic transformations of components of the vertebral column. Mech Dev *46*, 231-247.

Krebs, L.T., Xue, Y., Norton, C.R., Shutter, J.R., Maguire, M., Sundberg, J.P., Gallahan, D., Closson, V., Kitajewski, J., Callahan, R., *et al.* (2000). Notch signaling is essential for vascular morphogenesis in mice. Genes Dev *14*, 1343-1352.

Krumlauf, R. (1992). Evolution of the vertebrate Hox homeobox genes. Bioessays *14*, 245-252.

Krumlauf, R. (1994). Hox genes in vertebrate development. Cell *78*, 191-201.

Kwee, L., Baldwin, H.S., Shen, H.M., Stewart, C.L., Buck, C., Buck, C.A., and Labow, M.A. (1995). Defective development of the embryonic and extraembryonic circulatory systems in vascular cell adhesion molecule (VCAM-1) deficient mice. Development *121*, 489-503.

Lampa, S.J., Potluri, S., Norton, A.S., Fusco, W., and Laskowski, M.B. (2004). Ephrin-A5 overexpression degrades topographic specificity in the mouse gluteus maximus muscle. Brain Res Dev Brain Res *153*, 271-274.

Lawson, K.A. (1999). Fate mapping the mouse embryo. Int J Dev Biol *43*, 773-775.

Lawson, K.A., Dunn, N.R., Roelen, B.A., Zeinstra, L.M., Davis, A.M., Wright, C.V., Korving, J.P., and Hogan, B.L. (1999). Bmp4 is required for the generation of primordial germ cells in the mouse embryo. Genes Dev *13*, 424-436.

Lawson, K.A., Meneses, J.J., and Pedersen, R.A. (1991). Clonal analysis of epiblast fate during germ layer formation in the mouse embryo. Development *113*, 891-911.

Le Mouellic, H., Lallemand, Y., and Brulet, P. (1992). Homeosis in the mouse induced by a null mutation in the Hox-3.1 gene. Cell *69*, 251-264.

Lechleider, R.J., Ryan, J.L., Garrett, L., Eng, C., Deng, C., Wynshaw-Boris, A., and Roberts, A.B. (2001). Targeted mutagenesis of Smad1 reveals an essential role in chorioallantoic fusion. Dev Biol *240*, 157-167.

Lehoczky, J.A., and Innis, J.W. (2008). BAC transgenic analysis reveals enhancers sufficient for Hoxa13 and neighborhood gene expression in mouse embryonic distal limbs and genital bud. Evol Dev *10*, 421-432.

Lehoczky, J.A., Williams, M.E., and Innis, J.W. (2004). Conserved expression domains for genes upstream and within the HoxA and HoxD clusters suggests a long-range enhancer existed before cluster duplication. Evol Dev *6*, 423-430.

Lettice, L.A., Heaney, S.J., Purdie, L.A., Li, L., de Beer, P., Oostra, B.A., Goode, D., Elgar, G., Hill, R.E., and de Graaff, E. (2003). A long-range Shh enhancer regulates expression in the developing limb and fin and is associated with preaxial polydactyly. Hum Mol Genet *12*, 1725-1735.

Levine, M. (2010). Transcriptional enhancers in animal development and evolution. Curr Biol *20*, R754-763.

Lewis, E.B. (1978). A gene complex controlling segmentation in Drosophila. Nature *276*, 565-570.

Lewis, J., Chevallier, A., Kieny, M., and Wolpert, L. (1981). Muscle nerve branches do not develop in chick wings devoid of muscle. J Embryol Exp Morphol *64*, 211-232.

Lin, W., Burgess, R.W., Dominguez, B., Pfaff, S.L., Sanes, J.R., and Lee, K.F. (2001). Distinct roles of nerve and muscle in postsynaptic differentiation of the neuromuscular synapse. Nature *410*, 1057-1064.

Lohnes, D. (2003). The Cdx1 homeodomain protein: an integrator of posterior signaling in the mouse. Bioessays *25*, 971-980.

Lois, C., Hong, E.J., Pease, S., Brown, E.J., and Baltimore, D. (2002). Germline transmission and tissue-specific expression of transgenes delivered by lentiviral vectors. Science *295*, 868-872.

Lufkin, T., Dierich, A., LeMeur, M., Mark, M., and Chambon, P. (1991). Disruption of the Hox-1.6 homeobox gene results in defects in a region corresponding to its rostral domain of expression. Cell *66*, 1105-1119.

Lufkin, T., Mark, M., Hart, C.P., Dolle, P., LeMeur, M., and Chambon, P. (1992). Homeotic transformation of the occipital bones of the skull by ectopic expression of a homeobox gene. Nature *359*, 835-841.

Lumsden, A., and Krumlauf, R. (1996). Patterning the vertebrate neuraxis. Science *274*, 1109-1115.

Lunyak, V.V., Prefontaine, G.G., Nunez, E., Cramer, T., Ju, B.G., Ohgi, K.A., Hutt, K., Roy, R., Garcia-Diaz, A., Zhu, X., *et al.* (2007). Developmentally regulated activation of a SINE B2 repeat as a domain boundary in organogenesis. Science *317*, 248-251.

Macias, D., Ganan, Y., Sampath, T.K., Piedra, M.E., Ros, M.A., and Hurle, J.M. (1997). Role of BMP-2 and OP-1 (BMP-7) in programmed cell death and skeletogenesis during chick limb development. Development *124*, 1109-1117.

Maconochie, M.K., Nonchev, S., Studer, M., Chan, S.K., Popperl, H., Sham, M.H., Mann, R.S., and Krumlauf, R. (1997). Cross-regulation in the mouse HoxB complex: the expression of Hoxb2 in rhombomere 4 is regulated by Hoxb1. Genes Dev *11*, 1885-1895.

Maeda, R.K., and Karch, F. (2006). The ABC of the BX-C: the bithorax complex explained. Development *133*, 1413-1422.

Magnusson, M., Brun, A.C., Lawrence, H.J., and Karlsson, S. (2007). Hoxa9/hoxb3/hoxb4 compound null mice display severe hematopoietic defects. Exp Hematol *35*, 1421-1428.

Mahlapuu, M., Ormestad, M., Enerback, S., and Carlsson, P. (2001). The forkhead transcription factor Foxf1 is required for differentiation of extra-embryonic and lateral plate mesoderm. Development *128*, 155-166.

Mann, R.S., and Affolter, M. (1998). Hox proteins meet more partners. Curr Opin Genet Dev *8*, 423-429.

Mannaert, A., Amemiya, C.T., and Bossuyt, F. (2010). Comparative analyses of vertebrate posterior HoxD clusters reveal atypical cluster architecture in the caecilian Typhlonectes natans. BMC Genomics *11*, 658.

Manzanares, M., Bel-Vialar, S., Ariza-McNaughton, L., Ferretti, E., Marshall, H., Maconochie, M.M., Blasi, F., and Krumlauf, R. (2001). Independent regulation of initiation and maintenance phases of Hoxa3 expression in the vertebrate hindbrain involve auto- and cross-regulatory mechanisms. Development *128*, 3595-3607.

Manzanares, M., Cordes, S., Ariza-McNaughton, L., Sadl, V., Maruthainar, K., Barsh, G., and Krumlauf, R. (1999). Conserved and distinct roles of kreisler in regulation of the paralogous Hoxa3 and Hoxb3 genes. Development *126*, 759-769.

Manzanares, M., Cordes, S., Kwan, C.T., Sham, M.H., Barsh, G.S., and Krumlauf, R. (1997). Segmental regulation of Hoxb-3 by kreisler. Nature *387*, 191-195.

Manzanares, M., Nardelli, J., Gilardi-Hebenstreit, P., Marshall, H., Giudicelli, F., Martinez-Pastor, M.T., Krumlauf, R., and Charnay, P. (2002). Krox20 and kreisler co-operate in the transcriptional control of segmental expression of Hoxb3 in the developing hindbrain. EMBO J *21*, 365-376.

Marshall, H., Studer, M., Popperl, H., Aparicio, S., Kuroiwa, A., Brenner, S., and Krumlauf, R. (1994). A conserved retinoic acid response element required for early expression of the homeobox gene Hoxb-1. Nature *370*, 567-571.

Mates, L., Chuah, M.K., Belay, E., Jerchow, B., Manoj, N., Acosta-Sanchez, A., Grzela, D.P., Schmitt, A., Becker, K., Matrai, J., *et al.* (2009). Molecular evolution of a novel hyperactive Sleeping Beauty transposase enables robust stable gene transfer in vertebrates. Nat Genet *41*, 753-761.

Mathew, S.J., Hansen, J.M., Merrell, A.J., Murphy, M.M., Lawson, J.A., Hutcheson, D.A., Hansen, M.S., Angus-Hill, M., and Kardon, G. (2011). Connective tissue fibroblasts and Tcf4 regulate myogenesis. Development *138*, 371-384.

Mauro, A. (1961). Satellite cell of skeletal muscle fibers. J Biophys Biochem Cytol *9*, 493-495.

McCabe, C.D., and Innis, J.W. (2005). A genomic approach to the identification and characterization of HOXA13 functional binding elements. Nucleic Acids Res *33*, 6782-6794.

McClintock, J.M., Kheirbek, M.A., and Prince, V.E. (2002). Knockdown of duplicated zebrafish hoxb1 genes reveals distinct roles in hindbrain patterning and a novel mechanism of duplicate gene retention. Development *129*, 2339-2354.

McGinnis, W., and Krumlauf, R. (1992). Homeobox genes and axial patterning. Cell *68*, 283-302.

McIntyre, D.C., Rakshit, S., Yallowitz, A.R., Loken, L., Jeannotte, L., Capecchi, M.R., and Wellik, D.M. (2007). Hox patterning of the vertebrate rib cage. Development *134*, 2981-2989.

Medina-Martinez, O., Bradley, A., and Ramirez-Solis, R. (2000). A large targeted deletion of Hoxb1-Hoxb9 produces a series of single-segment anterior homeotic transformations. Dev Biol *222*, 71-83.

Merino, R., Ganan, Y., Macias, D., Economides, A.N., Sampath, K.T., and Hurle, J.M. (1998). Morphogenesis of digits in the avian limb is controlled by FGFs, TGFbetas, and noggin through BMP signaling. Dev Biol *200*, 35-45.

Moens, C.B., and Selleri, L. (2006). Hox cofactors in vertebrate development. Dev Biol *291*, 193-206.

Montavon, T., Le Garrec, J.F., Kerszberg, M., and Duboule, D. (2008). Modeling Hox gene regulation in digits: reverse collinearity and the molecular origin of thumbness. Genes Dev *22*, 346-359.

Montavon, T., Soshnikova, N., Mascrez, B., Joye, E., Thevenet, L., Splinter, E., de Laat, W., Spitz, F., and Duboule, D. (2011). A regulatory archipelago controls hox genes transcription in digits. Cell *147*, 1132-1145.

Morey, C., Da Silva, N.R., Perry, P., and Bickmore, W.A. (2007). Nuclear reorganisation and chromatin decondensation are conserved, but distinct, mechanisms linked to Hox gene activation. Development *134*, 909-919.

Morgan, E.A., Nguyen, S.B., Scott, V., and Stadler, H.S. (2003). Loss of Bmp7 and Fgf8 signaling in Hoxa13-mutant mice causes hypospadia. Development *130*, 3095-3109.

Mortlock, D.P., and Innis, J.W. (1997). Mutation of HOXA13 in hand-foot-genital syndrome. Nat Genet *15*, 179-180.

Mortlock, D.P., Post, L.C., and Innis, J.W. (1996). The molecular basis of hypodactyly (Hd): a deletion in Hoxa 13 leads to arrest of digital arch formation. Nat Genet *13*, 284-289.

Murphy, M., and Kardon, G. (2011). Origin of vertebrate limb muscle: the role of progenitor and myoblast populations. Curr Top Dev Biol *96*, 1-32.

Muzumdar, M.D., Tasic, B., Miyamichi, K., Li, L., and Luo, L. (2007). A global double-fluorescent Cre reporter mouse. Genesis *45*, 593-605.

Naiche, L.A., Arora, R., Kania, A., Lewandoski, M., and Papaioannou, V.E. (2011). Identity and fate of Tbx4-expressing cells reveal developmental cell fate decisions in the allantois, limb, and external genitalia. Dev Dyn *240*, 2290-2300.

Naiche, L.A., and Papaioannou, V.E. (2003). Loss of Tbx4 blocks hindlimb development and affects vascularization and fusion of the allantois. Development *130*, 2681-2693.

Nelson, C.E., Morgan, B.A., Burke, A.C., Laufer, E., DiMambro, E., Murtaugh, L.C., Gonzales, E., Tessarollo, L., Parada, L.F., and Tabin, C. (1996). Analysis of Hox gene expression in the chick limb bud. Development *122*, 1449-1466.

Nieto, M.A., Patel, K., and Wilkinson, D.G. (1996). In situ hybridization analysis of chick embryos in whole mount and tissue sections. Methods Cell Biol *51*, 219-235.

Noakes, P.G., Gautam, M., Mudd, J., Sanes, J.R., and Merlie, J.P. (1995). Aberrant differentiation of neuromuscular junctions in mice lacking s-laminin/laminin beta 2. Nature *374*, 258-262.

Nonchev, S., Maconochie, M., Vesque, C., Aparicio, S., Ariza-McNaughton, L., Manzanares, M., Maruthainar, K., Kuroiwa, A., Brenner, S., Charnay, P., *et al.* (1996). The conserved role of Krox-20 in directing Hox gene expression during vertebrate hindbrain segmentation. Proc Natl Acad Sci U S A *93*, 9339-9345.

Noordermeer, D., Leleu, M., Splinter, E., Rougemont, J., De Laat, W., and Duboule, D. (2011). The dynamic architecture of Hox gene clusters. Science *334*, 222-225.

Oefelein, M., Chin-Chance, C., and Bushman, W. (1996). Expression of the homeotic gene Hox-d13 in the developing and adult mouse prostate. J Urol *155*, 342-346.

Ong, C.T., and Corces, V.G. (2011). Enhancer function: new insights into the regulation of tissue-specific gene expression. Nat Rev Genet *12*, 283-293.

Otting, G., Qian, Y.Q., Billeter, M., Muller, M., Affolter, M., Gehring, W.J., and Wuthrich, K. (1990). Protein--DNA contacts in the structure of a homeodomain--DNA complex determined by nuclear magnetic resonance spectroscopy in solution. EMBO J *9*, 3085-3092.

Packer, A.I., Crotty, D.A., Elwell, V.A., and Wolgemuth, D.J. (1998). Expression of the murine Hoxa4 gene requires both autoregulation and a conserved retinoic acid response element. Development *125*, 1991-1998.

Palmer, A., and Klein, R. (2003). Multiple roles of ephrins in morphogenesis, neuronal networking, and brain function. Genes Dev *17*, 1429-1450.

Park, P.J. (2009). ChIP-seq: advantages and challenges of a maturing technology. Nat Rev Genet *10*, 669-680.

Pearson, J.C., Lemons, D., and McGinnis, W. (2005). Modulating Hox gene functions during animal body patterning. Nat Rev Genet *6*, 893-904.

Peichel, C.L., Prabhakaran, B., and Vogt, T.F. (1997). The mouse Ulnaless mutation deregulates posterior HoxD gene expression and alters appendicular patterning. Development *124*, 3481-3492.

Perez, W.D., Weller, C.R., Shou, S., and Stadler, H.S. (2010). Survival of Hoxa13 homozygous mutants reveals a novel role in digit patterning and appendicular skeletal development. Dev Dyn *239*, 446-457.

Phelan, K.A., and Hollyday, M. (1990). Axon guidance in muscleless chick wings: the role of muscle cells in motoneuronal pathway selection and muscle nerve formation. J Neurosci *10*, 2699-2716.

Phelan, K.A., and Hollyday, M. (1991). Embryonic development and survival of brachial motoneurons projecting to muscleless chick wings. J Comp Neurol *311*, 313-320.

Pierce, R.J., Wu, W., Hirai, H., Ivens, A., Murphy, L.D., Noel, C., Johnston, D.A., Artiguenave, F., Adams, M., Cornette, J.*, et al.* (2005). Evidence for a dispersed Hox gene cluster in the platyhelminth parasite Schistosoma mansoni. Mol Biol Evol *22*, 2491-2503.

Podlasek, C.A., Duboule, D., and Bushman, W. (1997). Male accessory sex organ morphogenesis is altered by loss of function of Hoxd-13. Dev Dyn *208*, 454-465.

Pollard, S.L., and Holland, P.W. (2000). Evidence for 14 homeobox gene clusters in human genome ancestry. Curr Biol *10*, 1059-1062.

Popperl, H., Bienz, M., Studer, M., Chan, S.K., Aparicio, S., Brenner, S., Mann, R.S., and Krumlauf, R. (1995). Segmental expression of Hoxb-1 is controlled by a highly conserved autoregulatory loop dependent upon exd/pbx. Cell *81*, 1031-1042.

Porter, J.D., Khanna, S., Kaminski, H.J., Rao, J.S., Merriam, A.P., Richmonds, C.R., Leahy, P., Li, J., and Andrade, F.H. (2001). Extraocular muscle is defined by a

fundamentally distinct gene expression profile. Proc Natl Acad Sci U S A *98*, 12062-12067.

Post, L.C., and Innis, J.W. (1999). Altered Hox expression and increased cell death distinguish Hypodactyly from Hoxa13 null mice. Int J Dev Biol *43*, 287-294.

Post, L.C., Margulies, E.H., Kuo, A., and Innis, J.W. (2000). Severe limb defects in Hypodactyly mice result from the expression of a novel, mutant HOXA13 protein. Dev Biol *217*, 290-300.

Poznanski, A.K., Kuhns, L.R., Lapides, J., and Stern, A.M. (1975). A new family with the hand-foot-genital syndrome--a wider spectrum of the hamd-foot-uterus syndrome. Birth Defects Orig Artic Ser *11*, 127-135.

Puschel, A.W., Balling, R., and Gruss, P. (1991). Separate elements cause lineage restriction and specify boundaries of Hox-1.1 expression. Development *112*, 279-287.

Ramirez-Solis, R., Zheng, H., Whiting, J., Krumlauf, R., and Bradley, A. (1993). Hoxb-4 (Hox-2.6) mutant mice show homeotic transformation of a cervical vertebra and defects in the closure of the sternal rudiments. Cell *73*, 279-294.

Rancourt, D.E., Tsuzuki, T., and Capecchi, M.R. (1995). Genetic interaction between hoxb-5 and hoxb-6 is revealed by nonallelic noncomplementation. Genes Dev *9*, 108-122.

Redfern, P.A. (1970). Neuromuscular transmission in new-born rats. J Physiol *209*, 701-709.

Relaix, F., Polimeni, M., Rocancourt, D., Ponzetto, C., Schafer, B.W., and Buckingham, M. (2003). The transcriptional activator PAX3-FKHR rescues the defects of Pax3 mutant mice but induces a myogenic gain-of-function phenotype with ligand-independent activation of Met signaling in vivo. Genes Dev *17*, 2950-2965.

Renucci, A., Zappavigna, V., Zakany, J., Izpisua-Belmonte, J.C., Burki, K., and Duboule, D. (1992). Comparison of mouse and human HOX-4 complexes defines conserved sequences involved in the regulation of Hox-4.4. EMBO J *11*, 1459-1468.

Rijli, F.M., Dolle, P., Fraulob, V., LeMeur, M., and Chambon, P. (1994). Insertion of a targeting construct in a Hoxd-10 allele can influence the control of Hoxd-9 expression. Dev Dyn *201*, 366-377.

Rijli, F.M., Mark, M., Lakkaraju, S., Dierich, A., Dolle, P., and Chambon, P. (1993). A homeotic transformation is generated in the rostral branchial region of the head by disruption of Hoxa-2, which acts as a selector gene. Cell *75*, 1333-1349.

Ringrose, L., and Paro, R. (2007). Polycomb/Trithorax response elements and epigenetic memory of cell identity. Development *134*, 223-232.

Rossant, J., and Cross, J.C. (2001). Placental development: lessons from mouse mutants. Nat Rev Genet *2*, 538-548.

Ryan, J.F., Mazza, M.E., Pang, K., Matus, D.Q., Baxevanis, A.D., Martindale, M.Q., and Finnerty, J.R. (2007). Pre-bilaterian origins of the Hox cluster and the Hox code: evidence from the sea anemone, Nematostella vectensis. PLoS One *2*, e153.

Saegusa, H., Takahashi, N., Noguchi, S., and Suemori, H. (1996). Targeted disruption in the mouse Hoxc-4 locus results in axial skeleton homeosis and malformation of the xiphoid process. Dev Biol *174*, 55-64.

Salsi, V., and Zappavigna, V. (2006). Hoxd13 and Hoxa13 directly control the expression of the EphA7 Ephrin tyrosine kinase receptor in developing limbs. J Biol Chem *281*, 1992-1999.

Sato, T.N., Tozawa, Y., Deutsch, U., Wolburg-Buchholz, K., Fujiwara, Y., Gendron-Maguire, M., Gridley, T., Wolburg, H., Risau, W., and Qin, Y. (1995). Distinct roles of the receptor tyrosine kinases Tie-1 and Tie-2 in blood vessel formation. Nature *376*, 70-74.

Satokata, I., Benson, G., and Maas, R. (1995). Sexually dimorphic sterility phenotypes in Hoxa10-deficient mice. Nature *374*, 460-463.

Scott, M.P. (1992). Vertebrate homeobox gene nomenclature. Cell *71*, 551-553.

Scott, M.P., and Weiner, A.J. (1984). Structural relationships among genes that control development: sequence homology between the Antennapedia, Ultrabithorax, and fushi tarazu loci of Drosophila. Proc Natl Acad Sci U S A *81*, 4115-4119.

Scotti, M., and Kmita, M. (2012). Recruitment of 5' Hoxa genes in the allantois is essential for proper extra-embryonic function in placental mammals. Development.

Seo, H.C., Edvardsen, R.B., Maeland, A.D., Bjordal, M., Jensen, M.F., Hansen, A., Flaat, M., Weissenbach, J., Lehrach, H., Wincker, P., *et al.* (2004). Hox cluster disintegration with persistent anteroposterior order of expression in Oikopleura dioica. Nature *431*, 67-71.

Sexton, T., Bantignies, F., and Cavalli, G. (2009). Genomic interactions: chromatin loops and gene meeting points in transcriptional regulation. Semin Cell Dev Biol *20*, 849-855.

Shalaby, F., Rossant, J., Yamaguchi, T.P., Gertsenstein, M., Wu, X.F., Breitman, M.L., and Schuh, A.C. (1995). Failure of blood-island formation and vasculogenesis in Flk-1-deficient mice. Nature *376*, 62-66.

Sham, M.H., Vesque, C., Nonchev, S., Marshall, H., Frain, M., Gupta, R.D., Whiting, J., Wilkinson, D., Charnay, P., and Krumlauf, R. (1993). The zinc finger gene Krox20 regulates HoxB2 (Hox2.8) during hindbrain segmentation. Cell *72*, 183-196.

Shaut, C.A., Keene, D.R., Sorensen, L.K., Li, D.Y., and Stadler, H.S. (2008). HOXA13 Is essential for placental vascular patterning and labyrinth endothelial specification. PLoS Genet *4*, e1000073.

Shaut, C.A., Saneyoshi, C., Morgan, E.A., Knosp, W.M., Sexton, D.R., and Stadler, H.S. (2007). HOXA13 directly regulates EphA6 and EphA7 expression in the genital tubercle vascular endothelia. Dev Dyn *236*, 951-960.

Simmons, D.G., and Cross, J.C. (2005). Determinants of trophoblast lineage and cell subtype specification in the mouse placenta. Dev Biol *284*, 12-24.

Small, K.M., and Potter, S.S. (1993). Homeotic transformations and limb defects in Hox A11 mutant mice. Genes Dev *7*, 2318-2328.

Sordino, P., van der Hoeven, F., and Duboule, D. (1995). Hox gene expression in teleost fins and the origin of vertebrate digits. Nature *375*, 678-681.

Soriano, P. (1999). Generalized lacZ expression with the ROSA26 Cre reporter strain. Nat Genet *21*, 70-71.

Soshnikova, N., and Duboule, D. (2009a). Epigenetic regulation of vertebrate Hox genes: a dynamic equilibrium. Epigenetics *4*, 537-540.

Soshnikova, N., and Duboule, D. (2009b). Epigenetic temporal control of mouse Hox genes in vivo. Science *324*, 1320-1323.

Spitz, F., and Duboule, D. (2008). Global control regions and regulatory landscapes in vertebrate development and evolution. Adv Genet *61*, 175-205.

Spitz, F., Gonzalez, F., and Duboule, D. (2003). A global control region defines a chromosomal regulatory landscape containing the HoxD cluster. Cell *113*, 405-417.

Spitz, F., Gonzalez, F., Peichel, C., Vogt, T.F., Duboule, D., and Zakany, J. (2001). Large scale transgenic and cluster deletion analysis of the HoxD complex separate an ancestral regulatory module from evolutionary innovations. Genes Dev *15*, 2209-2214.

Spitz, F., Herkenne, C., Morris, M.A., and Duboule, D. (2005). Inversion-induced disruption of the Hoxd cluster leads to the partition of regulatory landscapes. Nat Genet *37*, 889-893.

Sproul, D., Gilbert, N., and Bickmore, W.A. (2005). The role of chromatin structure in regulating the expression of clustered genes. Nat Rev Genet *6*, 775-781.

Stadler, H.S., Higgins, K.M., and Capecchi, M.R. (2001). Loss of Eph-receptor expression correlates with loss of cell adhesion and chondrogenic capacity in Hoxa13 mutant limbs. Development *128*, 4177-4188.

Stern, A.M., Gall, J.C., Jr., Perry, B.L., Stimson, C.W., Weitkamp, L.R., and Poznanski, A.K. (1970). The hand-food-uterus syndrome: a new hereditary disorder characterized by hand and foot dysplasia, dermatoglyphic abnormalities, and partial duplication of the female genital tract. J Pediatr *77*, 109-116.

Studer, M., Gavalas, A., Marshall, H., Ariza-McNaughton, L., Rijli, F.M., Chambon, P., and Krumlauf, R. (1998). Genetic interactions between Hoxa1 and Hoxb1 reveal new roles in regulation of early hindbrain patterning. Development *125*, 1025-1036.

Studer, M., Popperl, H., Marshall, H., Kuroiwa, A., and Krumlauf, R. (1994). Role of a conserved retinoic acid response element in rhombomere restriction of Hoxb-1. Science *265*, 1728-1732.

Subramanian, V., Meyer, B.I., and Gruss, P. (1995). Disruption of the murine homeobox gene Cdx1 affects axial skeletal identities by altering the mesodermal expression domains of Hox genes. Cell *83*, 641-653.

Suemori, H., and Noguchi, S. (2000). Hox C cluster genes are dispensable for overall body plan of mouse embryonic development. Dev Biol *220*, 333-342.

Tajbakhsh, S., and Buckingham, M. (2000). The birth of muscle progenitor cells in the mouse: spatiotemporal considerations. Curr Top Dev Biol *48*, 225-268.

Tallquist, M.D., and Soriano, P. (2000). Epiblast-restricted Cre expression in MORE mice: a tool to distinguish embryonic vs. extra-embryonic gene function. Genesis *26*, 113-115.

Tam, P.P., and Beddington, R.S. (1987). The formation of mesodermal tissues in the mouse embryo during gastrulation and early organogenesis. Development *99*, 109-126.

Tarchini, B., and Duboule, D. (2006). Control of Hoxd genes' collinearity during early limb development. Dev Cell *10*, 93-103.

Taylor, H.S., Vanden Heuvel, G.B., and Igarashi, P. (1997). A conserved Hox axis in the mouse and human female reproductive system: late establishment and persistent adult expression of the Hoxa cluster genes. Biol Reprod *57*, 1338-1345.

Tiret, L., Le Mouellic, H., Lallemand, Y., Maury, M., and Brulet, P. (1993). Altering the spatial determinations in the mouse embryos by manipulating the Hox genes. C R Acad Sci III *316*, 1009-1024.

Trainor, P.A., and Krumlauf, R. (2001). Hox genes, neural crest cells and branchial arch patterning. Curr Opin Cell Biol *13*, 698-705.

Tschopp, P., and Duboule, D. (2011). A genetic approach to the transcriptional regulation of hox gene clusters. Annu Rev Genet *45*, 145-166.

Tschopp, P., Tarchini, B., Spitz, F., Zakany, J., and Duboule, D. (2009). Uncoupling time and space in the collinear regulation of Hox genes. PLoS Genet *5*, e1000398.

Utsch, B., McCabe, C.D., Galbraith, K., Gonzalez, R., Born, M., Dotsch, J., Ludwig, M., Reutter, H., and Innis, J.W. (2007). Molecular characterization of HOXA13 polyalanine expansion proteins in hand-foot-genital syndrome. Am J Med Genet A *143A*, 3161-3168.

van den Akker, E., Forlani, S., Chawengsaksophak, K., de Graaff, W., Beck, F., Meyer, B.I., and Deschamps, J. (2002). Cdx1 and Cdx2 have overlapping functions in anteroposterior patterning and posterior axis elongation. Development *129*, 2181-2193.

van den Akker, E., Fromental-Ramain, C., de Graaff, W., Le Mouellic, H., Brulet, P., Chambon, P., and Deschamps, J. (2001). Axial skeletal patterning in mice lacking all paralogous group 8 Hox genes. Development *128*, 1911-1921.

van den Akker, E., Reijnen, M., Korving, J., Brouwer, A., Meijlink, F., and Deschamps, J. (1999). Targeted inactivation of Hoxb8 affects survival of a spinal ganglion and causes aberrant limb reflexes. Mech Dev *89*, 103-114.

van der Hoeven, F., Zakany, J., and Duboule, D. (1996). Gene transpositions in the HoxD complex reveal a hierarchy of regulatory controls. Cell *85*, 1025-1035.

van der Lugt, N.M., Alkema, M., Berns, A., and Deschamps, J. (1996). The Polycomb-group homolog Bmi-1 is a regulator of murine Hox gene expression. Mech Dev *58*, 153-164.

van der Lugt, N.M., Domen, J., Linders, K., van Roon, M., Robanus-Maandag, E., te Riele, H., van der Valk, M., Deschamps, J., Sofroniew, M., van Lohuizen, M.*, et al.* (1994). Posterior transformation, neurological abnormalities, and severe hematopoietic defects in mice with a targeted deletion of the bmi-1 proto-oncogene. Genes Dev *8*, 757-769.

van Meeteren, L.A., Ruurs, P., Stortelers, C., Bouwman, P., van Rooijen, M.A., Pradere, J.P., Pettit, T.R., Wakelam, M.J., Saulnier-Blache, J.S., Mummery, C.L.*, et al.* (2006). Autotaxin, a secreted lysophospholipase D, is essential for blood vessel formation during development. Mol Cell Biol *26*, 5015-5022.

van Nes, J., de Graaff, W., Lebrin, F., Gerhard, M., Beck, F., and Deschamps, J. (2006). The Cdx4 mutation affects axial development and reveals an essential role of Cdx genes in the ontogenesis of the placental labyrinth in mice. Development *133*, 419-428.

Vasyutina, E., Lenhard, D.C., Wende, H., Erdmann, B., Epstein, J.A., and Birchmeier, C. (2007). RBP-J (Rbpsuh) is essential to maintain muscle progenitor cells and to generate satellite cells. Proc Natl Acad Sci U S A *104*, 4443-4448.

Vasyutina, E., Martarelli, B., Brakebusch, C., Wende, H., and Birchmeier, C. (2009). The small G-proteins Rac1 and Cdc42 are essential for myoblast fusion in the mouse. Proc Natl Acad Sci U S A *106*, 8935-8940.

Visel, A., Blow, M.J., Li, Z., Zhang, T., Akiyama, J.A., Holt, A., Plajzer-Frick, I., Shoukry, M., Wright, C., Chen, F.*, et al.* (2009). ChIP-seq accurately predicts tissue-specific activity of enhancers. Nature *457*, 854-858.

Wagner, G.P., and Lynch, V.J. (2005). Molecular evolution of evolutionary novelties: the vagina and uterus of therian mammals. J Exp Zool B Mol Dev Evol *304*, 580-592.

Wang, B.B., Muller-Immergluck, M.M., Austin, J., Robinson, N.T., Chisholm, A., and Kenyon, C. (1993). A homeotic gene cluster patterns the anteroposterior body axis of C. elegans. Cell *74*, 29-42.

Wang, J., Mager, J., Schnedier, E., and Magnuson, T. (2002). The mouse PcG gene eed is required for Hox gene repression and extraembryonic development. Mamm Genome *13*, 493-503.

Wang, Z., Gerstein, M., and Snyder, M. (2009). RNA-Seq: a revolutionary tool for transcriptomics. Nat Rev Genet *10*, 57-63.

Warot, X., Fromental-Ramain, C., Fraulob, V., Chambon, P., and Dolle, P. (1997). Gene dosage-dependent effects of the Hoxa-13 and Hoxd-13 mutations on morphogenesis of the terminal parts of the digestive and urogenital tracts. Development *124*, 4781-4791.

Watson, E.D., and Cross, J.C. (2005). Development of structures and transport functions in the mouse placenta. Physiology (Bethesda) *20*, 180-193.

Watson, S.S., Riordan, T.J., Pryce, B.A., and Schweitzer, R. (2009). Tendons and muscles of the mouse forelimb during embryonic development. Dev Dyn *238*, 693-700.

Wellik, D.M., and Capecchi, M.R. (2003). Hox10 and Hox11 genes are required to globally pattern the mammalian skeleton. Science *301*, 363-367.

Whiting, J., Marshall, H., Cook, M., Krumlauf, R., Rigby, P.W., Stott, D., and Allemann, R.K. (1991). Multiple spatially specific enhancers are required to reconstruct the pattern of Hox-2.6 gene expression. Genes Dev *5*, 2048-2059.

Wigmore, P.M., and Evans, D.J. (2002). Molecular and cellular mechanisms involved in the generation of fiber diversity during myogenesis. Int Rev Cytol *216*, 175-232.

Williams, B.A., and Ordahl, C.P. (1994). Pax-3 expression in segmental mesoderm marks early stages in myogenic cell specification. Development *120*, 785-796.

Winnier, G., Blessing, M., Labosky, P.A., and Hogan, B.L. (1995). Bone morphogenetic protein-4 is required for mesoderm formation and patterning in the mouse. Genes Dev *9*, 2105-2116.

Woltering, J.M., and Duboule, D. (2010). The origin of digits: expression patterns versus regulatory mechanisms. Dev Cell *18*, 526-532.

Woltering, J.M., and Durston, A.J. (2006). The zebrafish hoxDb cluster has been reduced to a single microRNA. Nat Genet *38*, 601-602.

Yamada, G., Suzuki, K., Haraguchi, R., Miyagawa, S., Satoh, Y., Kamimura, M., Nakagata, N., Kataoka, H., Kuroiwa, A., and Chen, Y. (2006). Molecular genetic cascades for external genitalia formation: an emerging organogenesis program. Dev Dyn *235*, 1738-1752.

Yamamoto, M., Gotoh, Y., Tamura, K., Tanaka, M., Kawakami, A., Ide, H., and Kuroiwa, A. (1998). Coordinated expression of Hoxa-11 and Hoxa-13 during limb muscle patterning. Development *125*, 1325-1335.

Yamamoto, M., and Kuroiwa, A. (2003). Hoxa-11 and Hoxa-13 are involved in repression of MyoD during limb muscle development. Dev Growth Differ *45*, 485-498.

Yang, J.T., Rayburn, H., and Hynes, R.O. (1995). Cell adhesion events mediated by alpha 4 integrins are essential in placental and cardiac development. Development *121*, 549-560.

Yang, X., Arber, S., William, C., Li, L., Tanabe, Y., Jessell, T.M., Birchmeier, C., and Burden, S.J. (2001). Patterning of muscle acetylcholine receptor gene expression in the absence of motor innervation. Neuron *30*, 399-410.

Ying, Y., Liu, X.M., Marble, A., Lawson, K.A., and Zhao, G.Q. (2000). Requirement of Bmp8b for the generation of primordial germ cells in the mouse. Mol Endocrinol *14*, 1053-1063.

Ying, Y., and Zhao, G.Q. (2001). Cooperation of endoderm-derived BMP2 and extraembryonic ectoderm-derived BMP4 in primordial germ cell generation in the mouse. Dev Biol *232*, 484-492.

Yokouchi, Y., Nakazato, S., Yamamoto, M., Goto, Y., Kameda, T., Iba, H., and Kuroiwa, A. (1995). Misexpression of Hoxa-13 induces cartilage homeotic transformation and changes cell adhesiveness in chick limb buds. Genes Dev *9*, 2509-2522.

Yokouchi, Y., Sakiyama, J., Kameda, T., Iba, H., Suzuki, A., Ueno, N., and Kuroiwa, A. (1996). BMP-2/-4 mediate programmed cell death in chicken limb buds. Development *122*, 3725-3734.

Young, T., and Deschamps, J. (2009). Hox, Cdx, and anteroposterior patterning in the mouse embryo. Curr Top Dev Biol *88*, 235-255.

Young, T., Rowland, J.E., van de Ven, C., Bialecka, M., Novoa, A., Carapuco, M., van Nes, J., de Graaff, W., Duluc, I., Freund, J.N., *et al.* (2009). Cdx and Hox genes differentially regulate posterior axial growth in mammalian embryos. Dev Cell *17*, 516-526.

Yu, B.D., Hanson, R.D., Hess, J.L., Horning, S.E., and Korsmeyer, S.J. (1998). MLL, a mammalian trithorax-group gene, functions as a transcriptional maintenance factor in morphogenesis. Proc Natl Acad Sci U S A *95*, 10632-10636.

Yu, B.D., Hess, J.L., Horning, S.E., Brown, G.A., and Korsmeyer, S.J. (1995). Altered Hox expression and segmental identity in Mll-mutant mice. Nature *378*, 505-508.

Zakany, J., and Duboule, D. (2007). The role of Hox genes during vertebrate limb development. Curr Opin Genet Dev *17*, 359-366.

Zakany, J., Fromental-Ramain, C., Warot, X., and Duboule, D. (1997a). Regulation of number and size of digits by posterior Hox genes: a dose-dependent mechanism with potential evolutionary implications. Proc Natl Acad Sci U S A *94*, 13695-13700.

Zakany, J., Gerard, M., Favier, B., and Duboule, D. (1997b). Deletion of a HoxD enhancer induces transcriptional heterochrony leading to transposition of the sacrum. EMBO J *16*, 4393-4402.

Zakany, J., Kmita, M., Alarcon, P., de la Pompa, J.L., and Duboule, D. (2001). Localized and transient transcription of Hox genes suggests a link between patterning and the segmentation clock. Cell *106*, 207-217.

Zakany, J., Kmita, M., and Duboule, D. (2004). A dual role for Hox genes in limb anterior-posterior asymmetry. Science *304*, 1669-1672.

Zakany, J., Tuggle, C.K., Patel, M.D., and Nguyen-Huu, M.C. (1988). Spatial regulation of homeobox gene fusions in the embryonic central nervous system of transgenic mice. Neuron *1*, 679-691.

Zhadanov, A.B., Provance, D.W., Jr., Speer, C.A., Coffin, J.D., Goss, D., Blixt, J.A., Reichert, C.M., and Mercer, J.A. (1999). Absence of the tight junctional protein AF-6 disrupts epithelial cell-cell junctions and cell polarity during mouse development. Curr Biol *9*, 880-888.

Zhang, H., and Bradley, A. (1996). Mice deficient for BMP2 are nonviable and have defects in amnion/chorion and cardiac development. Development *122*, 2977-2986.

Zhang, M., Kim, H.J., Marshall, H., Gendron-Maguire, M., Lucas, D.A., Baron, A., Gudas, L.J., Gridley, T., Krumlauf, R., and Grippo, J.F. (1994). Ectopic Hoxa-1 induces rhombomere transformation in mouse hindbrain. Development *120*, 2431-2442.

Zou, H., Choe, K.M., Lu, Y., Massague, J., and Niswander, L. (1997). BMP signaling and vertebrate limb development. Cold Spring Harb Symp Quant Biol *62*, 269-272.

Zou, H., and Niswander, L. (1996). Requirement for BMP signaling in interdigital apoptosis and scale formation. Science *272*, 738-741.

Zuzarte-Luis, V., and Hurle, J.M. (2002). Programmed cell death in the developing limb. Int J Dev Biol *46*, 871-876.